DOCTOR OF PHILOSOPHY

The Neural Mechanisms of Planning and Executing Skilled Movement Sequences

Yewbrey, Rhys

Award date:
2024

Awarding institution:
Bangor University

PRIFYSGOL
BANGOR
UNIVERSITY

The Neural Mechanisms of Planning and Executing Skilled Movement Sequences

Rhys Yewbrey

Thesis submitted to the School of Psychology, Bangor University, in partial fulfilment of the requirements for the degree of Doctor of Philosophy

Declaration

Yr wyf drwy hyn yn datgan mai canlyniad fy ymchwil fy hun yw'r thesis hwn, ac eithrio lle nodir yn wahanol. Caiff ffynonellau eraill eu cydnabod gan droednodiadau yn rhoi cyfeiriadau eglur. Nid yw sylwedd y gwaith hwn wedi cael ei dderbyn o'r blaen ar gyfer unrhyw radd, ac nid yw'n cael ei gyflwyno ar yr un pryd mewn ymgeisiaeth am unrhyw radd oni bai ei fod, fel y cytunwyd gan y Brifysgol, am gymwysterau deuol cymeradwy.

Rwy'n cadarnhau fy mod yn cyflwyno'r gwaith hwn gyda chytundeb fy Ngoruchwyliwr (Goruchwylwyr)

I hereby declare that this thesis is the results of my own investigations, except where otherwise stated. All other sources are acknowledged by bibliographic references. This work has not previously been accepted in substance for any degree and is not being concurrently submitted in candidature for any degree unless, as agreed by the University, for approved dual awards.

I confirm that I am submitting this work with the agreement of my Supervisor(s).

Acknowledgements

This thesis has been a long journey of ups and downs, but I would not be where I am if it weren't for the support and guidance of those around me.

I would like to sincerely thank my supervisor, Dr. Katja Kornysheva, without whose unwavering guidance none of this would have been possible. From the sharing of thoughts and ideas to journal clubs to manuscript feedback, it has been a pleasure working with you through my master's and PhD projects.

Thank you also to the Bangor Sensorimotor group, especially Dr. Simon Watt and Dr. Kenneth Valyear, my second supervisor, who offered their enthusiastic thoughts and voices whenever we required feedback on some new off-beat idea. Also, to the Bangor Imaging Group, for giving me my first taste of a true neuroimaging forum and for giving us key feedback on the methodology of Chapter 1. Thank you to Prof. Kami Koldewyn, my committee chair, for your advice, reassurance, and guidance throughout my entire PhD – especially during the final stretch. And to David McKiernan, James Naunton-Morgan, and Elfyn Roberts, for your expertise when what felt like all of the technical issues in the world were bearing down on us.

From my time at Birmingham, thank you to all the post docs and PhD students who have reassured and given me guidance for the past two years, you welcomed me as one of your own. Especially office 110 et al. You made coming into the CHBH something I could look forward to.

To my friends from home and my friends from Bangor, thank you for distracting me when things were difficult and for celebrating with me when things were good. And Paige, for being right by my side for the last and most challenging two years. The support from all of you means more than you know.

And lastly, to my parents. Thank you for your unending support, encouragement, and for always offering your shoulders to lean on. For raising me and for building a support platform for me to thrive. This is all thanks to you.

Summary

To produce movement sequences is to interact meaningfully with the world around us. Large amounts of the human behavioural repertoire, such as typing on a keyboard, executing a dance routine, or playing a piece of music require the sequential execution of movements. Moreover, to execute sequences is to plan them. Without planning, execution is far more prone to failure. This thesis Investigates the cognitive and neural mechanisms which underly the planning and execution of movement sequences.

In *Chapter 1*, relevant research is described and summarised that elucidates how sequences are prepared, controlled, and implemented under a motor hierarchical framework. Evidence from neuroimaging and electrophysiology is integrated to provide an overarching account of how the brain plans movements and transitions into effective execution. However, how high- and low-level hierarchical sequence features map onto the planning and execution of movement sequences is unclear.

To investigate such mapping, *Chapter 2* assesses the presence of high-level order and timing, and low-level integration, in motor cortical regions throughout sequence planning and execution using multivariate analysis of functional magnetic resonance imaging (fMRI). A shift from the control of order and timing during planning, to integration with online timing control during execution was identified.

With a hierarchical shift identified in the cortex, *Chapter 3* investigates the presence of sequence features in subcortical regions which have been shown to play important roles in the generation of movement. The left hippocampus is shown to plan the order of movements in advance. Additionally, the basal ganglia, thalamus, and bilateral hippocampus show distinct activity patterns between planning and execution, supporting findings from electrophysiology which show that planning and execution occupy orthogonal subspaces.

Chapter 4 explores the role of inhibition of unused effectors in the resolution of competitive planning processes. Behavioural markers of competitive queueing were found in the hand to be used in the upcoming sequence; however, the contralateral hand displayed a mirrored gradient of inhibition which is thought to reflect interhemispheric transcallosal inhibition processes used to reduce the likelihood of incorrect movements.

The summary *Chapter 5* formulates a systems-level framework for the planning and execution of skilled movement sequences, integrating findings from both the literature and the previous empirical chapters. The hippocampus and parietal cortex are thought to plan the order of upcoming movements in extrinsic and intrinsic space respectively, after which a signal to move ascends through the thalamus and causes reorganisation of cortical and subcortical neural patterns, with the former shifting to low-level sequential integration with elements of online timing. The implications and future directions of such a model are discussed with respect to both research and clinical significance.

Disseminated Work

Chapter 2 is published in the Journal of Neuroscience as Yewbrey, R., Mantziara, M., & Kornysheva, K. (2023). Cortical patterns shift from sequence feature separation during planning to integration during motor execution. *Journal of Neuroscience*, *43*(10), 1742-1756.

Chapter 3 is in preparation for submission as Yewbrey, R., & Kornysheva, K. (2024). Hippocampus retrieves the order of skilled typing sequences during movement planning [Manuscript in preparation].

Chapter 4 is in preparation for submission as Yewbrey, R., Wright, H., Sadnicka, A., & Kornysheva, K. (2024). The hand contralateral to sequential movement execution shows a mirrored suppression gradient during planning [Manuscript in preparation].

Conference Presentations

Yewbrey, R. (2022, July 25-29). *Neocortical control and integration of movement order and timing during sequence planning and execution* [Poster presentation]. Society for the Neural Control of Movement, Dublin, Ireland.

Yewbrey, R. (2022, June 19-23). *Cortical integration of order and timing occurs during sequence execution, but not planning.* [Poster presentation]. Organisation for Human Brain Mapping, Glasgow, United Kingdom.

Yewbrey, R. (2022, May 24-25). *Cortical integration of order and timing occurs during sequence execution, but not planning.* [Blitz talk, Poster presentation]. British Association for Cognitive Neuroscience, Birmingham, United Kingdom.

Yewbrey, R. (2021, April 20-22). *Neocortical Control of Sequence Movement Order and Timing During Sequence Planning and Execution.* [Poster presentation]. Society for the Neural Control of Movement, Virtual.

Contents

Figures and Tables

Chapter 2

Chapter 3

Chapter 4

Chapter 1 - General Introduction

1.1 Neural control of movement sequences

Being able to produce several movements in quick succession is an ability that underpins many facets of the human experience. Whether it is playing a musical instrument, typing on a keyboard, or tying one's shoelaces, movement sequences are ubiquitous in daily life, and their accurate execution is a pre-requisite for success across many activities. Poor sequence performance might result in an unpleasant piece of music, typos throughout a professional piece of writing, or tripping on one's own shoelace. The neural control of movement sequences appears to not be simple or centralised, but rather involves several distinct mechanisms and anatomical regions across the human brain. Breakdowns are commonly observed across several distinct neurological disorders, each of which can serve to inform us of the mechanisms and anatomical brain regions required for successful movement sequence learning and execution. This, in turn, allows us to create better ways to treat and rehabilitate those individuals affected. Firstly, Developmental Coordination Disorder (commonly known as Dyspraxia) is characterised by deficits across several motor domains compared to same-age controls (Wilson et al., 2013), where impaired sequence execution (Biotteau et al., 2016) could be related to malfunctions in movement planning and the development of a forward model (Opitz et al., 2020). Task-specific Dystonia, however, results in a focal impairment to one form of skilled execution, such as a talented musician suddenly becoming unable to play a particular musical instrument, and is thought to be caused by extensive overtraining resulting in a loss of flexibility during action selection (Sadnicka et al., 2018). Moreover, Parkinson's disease results in impaired movement and cognition (Sveinbjornsdottir, 2016; Wilkinson et al., 2009) due to a loss of dopaminergic neurons in the substantia nigra which cause a resultant dysfunction of the basal ganglia (Rubin et al., 2012). The functional role of the basal ganglia has been debated between action selection (Frank, 2011; Gurney et al., 2001) and the specification and storage of movement kinematics (Dhawale et al., 2021; Harpaz et al., 2022), yet optogenetics shows that they are necessary to the execution of movement sequences nonetheless (Mizes et al., 2023a). Alzheimer's disease, closely associated with degeneration of the hippocampus (Dubois et al., 2016; Förstl & Kurz, 1999), results in reduced motor learning capacity (van

Halteren-van Tilborg et al., 2007). Furthermore, the cerebellum is closely associated with the definition of movement kinematics, best represented by eye blink conditioning (Christian & Thompson, 2003) and cerebellar ataxia (Diener & Dichgans, 1992).

In this chapter, I will summarise relevant cognitive and neuroscience research which further cements movement sequence production as a distributed system across several anatomical regions and mechanisms. Findings will further be interpreted and integrated under a hierarchical systems model, which will provide a rationale for the empirical research carried out as part of this thesis.

1.1.1 Motor hierarchy

Motor sequences have been described as hierarchical and found to be encoded in multiple representational layers (Grafton & Hamilton, 2007; Lashley, 1951; Rosenbaum et al., 1983; Yokoi & Diedrichsen, 2019a). According to the framework described by Diedrichsen & Kornysheva (2015), these consist of selection, intermediate, and execution layers. Motor primitives, or synergies, make up the execution layer as the lowest level in the hierarchy and control spatiotemporal patterns of muscle activity ranging from small movements such as individual finger contractions, to whole arm extension, flexion, grasping, and licking (Flash & Hochner, 2005; Graziano, Taylor, Moore, et al., 2002; Graziano, 2016; Overduin et al., 2012). Primitives can be involuntary evoked by stimulating the spinal cord (Zimmermann et al., 2011) or the primary motor cortex (Gentner et al., 2010; Graziano, Taylor, & Moore, 2002; Overduin et al., 2012), suggesting that these movements are stored in the motor system within stable populations of neuronal networks which directly project onto the peripheral nervous system (Diedrichsen & Kornysheva, 2015a). During early movement sequence learning, primitives belonging to the target sequence must be selected and executed serially (Verwey, 2023a; Verwey & Abrahamse, 2012). Selection is a time-consuming process and can be made longer when there are multiple choices (Hick, 1952), how similar choices are to one another (Rosenbaum et al., 1988), and when there are translations required between the cue and the target action (e.g., ‘A’ having to be translated to a forward reach; Goodman & Kelso, 1980; Haith & Bestmann, 2020). Given that movements within sequences typically need to be executed in rapid succession, such as playing piano keys in time with a fast melody, repeatedly performing the time-consuming selection process prior to each individual movement element might be inconvenient at best

and completely disrupt performance at worst. Thus, the motor system must find a way to avoid the costly process of repeated action selection. One possibility is that sequences themselves may become stored as entirely new primitives; that is, as a sequence becomes learned and practiced, primitives become inseparably bound together and form a new representation to be stored in neuronal populations belonging to the motor network (Lashley, 1951). Such a theory would explain how sequences can be executed in a rapid fashion with very short movement times (Abrahamse et al., 2013) as each movement would be directly functionally inseparable from the prior and following movements. While stimulating the motor cortex of musicians using transcranial magnetic stimulation (TMS) can elicit complex movements such as those from a musical instrument repertoire in musically trained humans (Gentner et al., 2010), or naturalistic behaviours from everyday life in monkeys (Overduin et al., 2012) that can even consist of multi-step movements such as grasping food and putting it to their mouths (Graziano, Taylor, & Moore, 2002), there is no evidence for stimulation eliciting entire movement sequences. This suggests that commonly used, naturalistic, complex movements can be stored as primitives, yet this is unlikely to be true for whole sequences. Moreover, by its nature a mechanism that stores whole sequences inflexibly would result in an individual being unable to continue executing a sequence should they be interrupted, instead having to start the sequence over which would be detrimental in many circumstances such as playing a long piece of music (Rosenbaum et al., 1983). This view also does not account for transposition errors, a common error seen during sequence execution where the order of two elements in a sequence is unintentionally switched (Lashley, 1951).

Providing further evidence against the storage of sequences as a single primitive, clear patterns emerge during sequence production where extended pauses surround periods of rapid movement execution, called ‘chunks’, which represent the second layer of the motor hierarchy (Diedrichsen & Kornysheva, 2015a; Sakai et al., 2003; Verwey & Eikelboom, 2003). These chunks are characterised by series of movements that are closely bound in temporal proximity, typically arise idiosyncratically (Sakai et al., 2003), and can be identified trial-by-trial using Bayesian modelling (Acuna et al., 2014). Much like the well-documented chunking system in working memory (Thalmann et al., 2019), storing short strings of movements as a chunk allows for greater computational efficiency compared to the serial storage, retrieval,

and execution of sequential movements (Ramkumar et al., 2016). Serial organisation of movements within chunks has been thought to employ state-dependent movement control, where the next movement to be executed is determined by the state of the system following execution of a prior movement (Diedrichsen et al., 2007; Kornysheva, 2016). As such, chunks allow for the execution of fast and accurate sequential movements and learnt chunks can often be applied to new sequences which contain a similar string of movements, facilitating learning (Diedrichsen & Kornysheva, 2015a). After extensive learning, sequence representations then call upon a number of these chunks to successfully execute a movement sequence with speed and accuracy.

Motor sequence learning therefore begins with manual selection of motor primitives in a slow and intensive process. As learning progresses, an 'intermediate' layer consisting of well-learnt chunks develops, allowing the nervous system to selectively activate strings of several movements which facilitates rapid production and allows for transferability when learning new sequences. However, this mechanism is not immune to breakdowns. Task-specific Dystonia is a disorder that causes highly skilled individuals to become unable to perform actions that they once could do with ease, such as a pianist being no longer able to play the piano (Albanese et al., 2013). Initial evidence from electrophysiology in monkeys suggests that overtraining rapid and repetitive grasping movements causes a breakdown of the somatotopic organisation in S1, causing overlap of the receptive fields belonging to relevant effectors such as the dorsal and palmer region of the hand, resulting in symptoms that are similar to task-specific dystonia (Byl et al., 1996). More recently, this model has been criticised as it can only account for the broad effects related to general dystonia rather than the task selectiveness observed in task specific dystonia, and the increased receptive fields were not observed in a cohort of human participants using functional Magnetic Resonance Imaging (fMRI; Sadnicka et al., 2023). Instead, a framework was proposed by Sadnicka, Kornysheva, and colleagues based on maladaptation of the motor hierarchy (Sadnicka et al., 2018). They suggested that in healthy skilled motor learning the intermediate layer allows for flexibility in applying learnt sequences to different contexts such as changing around certain notes in a piece of music, adjusting the rhythm of the piece (see 1.1.3 Movement timing), or changing the tool used to execute the sequence, such as an illustrator using a tablet and stylus instead of their usual easel and paintbrush. When a

highly skilled individual begins to overtrain a sequential movement in a repetitive way or strenuous way, such as preparing a musical piece for a concert by performing it repeatedly, Sadnicka, Kornysheva and colleagues propose that this intermediate architecture is lost to make the movement faster and more automatic. This however results in a lack of flexibility to changing task demands and that is prone to breakdowns when exposed to other risk factors. For example, when the individual must play the same piece on a new piano which may require a greater level of force to execute key presses, yet the individual is undergoing high levels of psychological stress, has some pain in the muscles of the arm, and has to execute a repetitive task requiring considerable force, the system is too rigid and the performance can no longer be executed, resulting in task-specific dystonia. This framework, however, also suggests task-specific dystonia can be prevented by avoiding the loss of intermediate architecture to maintain flexibility in the system. The authors suggest measures such as using a variety of different pianos, playing at different pitches or tempos, and avoiding highly repetitive training when learning.

Research has sought to further investigate the neural signatures of hierarchical layering. Yokoi and Diedrichsen (2019) presented a landmark study in which they identified the presence of each layer belonging to the motor hierarchy by training participants to execute movement sequences; by manipulating the constituent chunks to elicit predictable representational structures depending on the hierarchical level that a respective target region represents. For example, in a region that is responsible for intermediate chunking, sequences with matching chunks would be more similar than sequences with distinct chunks. This is also the case for whole sequences and the constituent finger movements, representing selection and execution layers respectively. Crucially, Yokoi and Diedrichsen imposed the chunking structure of sequences throughout learning, meaning that they could match sequences overall yet impose different chunking structures. After generating predicted representational structures for each layer of the hierarchy they fit these representational models back to the data using Pattern Component Modelling (PCM), a Bayesian method that predicts the likelihood of the data if the proposed model was true (Diedrichsen et al., 2018). Upon fitting the models, along with all possible model combinations, the primary motor cortex (M1) was found to primarily represent the first finger of the sequence. Premotor and parietal regions, however, encoded both sequences

and chunks with some degree of overlap in their anatomical location. This carefully controlled study provided evidence for the separation of hierarchical movement elements throughout the cortex in humans, with a key dichotomy established between the function of primary motor cortex and secondary motor cortices, with the former processing single finger movements and the latter chunks or whole sequences.

The first initial evidence for a primary-secondary motor cortex divide was shown as early as the mid-90s by Tanji and Shima (1994). They recorded activity from individual neurons in monkeys that were trained to execute sequences of push, pull, and turn movements, where neurons in the SMA showed an increase in spiking rate preceding certain movements, only when they were followed by another specific movement. For example, some neurons would fire before the execution of a turn movement, but only when the succeeding movement was pull. However, the same neuron did not fire when the first movement was still turn, but the second was instead push. Moreover, neurons in the primary motor cortex (M1) did not show such sensitivity to preceding movements and would increase their firing rate unselectively, thus suggesting that different roles of cortical regions as to how movements were tracked throughout sequences. More recently, findings by Churchland and colleagues (Russo et al., 2020) have shown strong support for this phenomenon using multi-unit recordings in monkeys that were trained to perform a cycling motion with their hand. This cycling motion served to move them through virtual space where they were instructed to stop at a target point on the path ahead of them. While performing this task, dimensionality reduction of neural population recordings showed that the SMA tracked the number of rotations that were executed by shifting the occupied subspace along the first principal component for each rotation of the cycle, tracking the movement's progression. M1, however, maintained a consistent overlapping trajectory throughout the movement, showing a lack of sensitivity to the progression of cycling rotations but rather tuning to the execution of each individual rotation. Additional research from human behavioural and neuroimaging methods provides further evidence for this divide, with the pre-SMA controlling the initiation of movement chunks within sequences (Kennerley et al., 2004), and primary motor cortex showing mostly control of individual finger movements (Berlot et al., 2020; Yokoi et al., 2018). Moreover, sequences appear to be held in extrinsic reference frames in dorsal premotor cortex in contrast to intrinsic frames in primary motor cortex,

suggesting that movement sequence elements are more abstract in secondary motor cortex compared to primary where each element is closely tied to the used effector (Wiestler et al., 2014).

Aside from regions that are directly involved in motor control, distinct hierarchical tuning during movement can be observed in other regions both cortical and subcortical. Rostrolateral prefrontal cortex, for example, shows ramping activation across the span of movement sequences that resets upon sequence completion, and perturbation of this region using TMS results in more mistakes towards the end of sequence execution, consistent with the region playing a role in tracking sequence progress (Desrochers et al., 2015). Furthermore, the basal ganglia have traditionally been associated with action selection through the inhibition and disinhibition of competing unwanted and target movement plans respectively, which would associate them with high-level selection processes (Benjamin et al., 2010; Frank, 2011; Gurney et al., 2001; Mink, 1996; Redgrave et al., 1999). Alternatively, Ölveczky and colleagues put forth contemporary findings suggesting that the dorsolateral striatum in rats (equivalent to the human putamen) may actually play a role in the storing of movement kinematics for over-trained sequences, thus controlling hierarchically low-level elements such as motor primitives (Dhawale et al., 2021; Harpaz et al., 2022). Mizes et al (Mizes et al., 2023a) from this group show that optogenetic perturbation of the dorsolateral striatum in rats who learnt to produce movement sequences lead to a deterioration in the performance of automatic sequences (over-trained sequences which required no cues to execute) but not in the performance of sequences that relied on working memory of following sensory cues. Based on this, the basal ganglia may be a potential candidate for the storage of entire movement sequence kinematics in the brain. However, the automatic sequences used in this task were executed through long bouts of repetition, a process which is unnaturalistic and lacks the known benefits of contextual interference during training, including better retention and skill transfer (Magill & Hall, 1990). A recent study by Ölveczky and colleagues suggested that executing previously automatic sequences in a context that requires flexibility, i.e. also producing other sequences in the same block and utilising the same primitives, in this case lever presses, across sequences, necessitates input from motor cortical regions, suggesting that not only

does the amount of practice impact the brain regions required to produce a sequence, but also the surrounding context within which the execution occurs (Mizes et al., 2023b).

1.1.2 Sequential movement order

The motor hierarchy serves as a systems-level framework to understand the organisation and function of the motor system. However, the exact mechanism that allows for the definition and implementation of movement order in the intermediate level remains unclear. The order of execution is vital to the success of movement sequences, for example when tying shoelaces, one must first go over under then make a bow to ensure success, so the motor system requires a consistent, reliable, and flexible way to do so. Initial theories proposed by Ebbinghaus in 1885, predominantly from the area of memory and learning, suggested that sequential elements may be recalled or executed serially based a cueing function provided by the end point of the prior element (Ebbinghaus, 2013). In the motor domain, this process, which would later be named the Reflex Chaining Theory (Clower, 1998), relied on the resultant sensory state of the system following a movement's production to prime the initiation of the following movement. Reflex Chaining Theory became prominent not only in the motor and memory domains, but also among behaviourists (Washburn, 1916; Watson, 1920) up until Lashley's seminal critique 'The problem of serial order in behavior' (Lashley, 1951). Lashley argued against the serial account due to its lack of flexibility, namely: transposition errors, where two items in a sequence are unintentionally switched, cannot be accounted for under the model; there would need to be a near infinite amount of chains to allow for the vast repertoire of skilled movements that humans produce in daily life; and in rapid sequences, there is unlikely to be enough time for sensory feedback to arrive from the periphery to drive the next movement. Given this criticism, Lashley proposed an opposing parallel theory that action plans are vital for sequential execution and each element must be simultaneously pre-activated. This theory of parallel pre-planning would later be developed into the Competitive Queueing (CQ) hypothesis (Houghton, 1990; Houghton & Hartley, 1995).

There are three layers to modern CQ theories: the parallel planning layer, competitive choice layer, and output layer (Bullock, 2004; Bullock & Rhodes, 2002). Nodes representing each element of a sequence are present in the parallel planning layer which develops throughout learning, with each node being activated to a varied extent depending on the

respective element's position in the sequence, e.g., the first element will receive the greatest activation and the final element the least. The competitive choice layer receives these activation inputs and subsequently selects the element with the greatest activation. In turn, there is lateral inhibition between competing elements within the competitive choice layer, allowing only one movement to pass through to the output layer and be subsequently executed by the downstream motor system. These dynamics result in a winner-takes-all model and after an element has won it proceeds to self-inhibit, allowing the node with the next greatest activation in the parallel planning layer to become the next winner. This process is repeated iteratively until the sequence is completed in its entirety, allowing for a parallel planning mechanism that facilitates serial execution.

CQ models make clear predictions of neural activation gradients, where neuronal populations should encode upcoming items of a sequence with weighted strengths depending on their ordinal position in the sequence - a CQ gradient. Transposition errors also have a clear basis under this theory, where noise in the system may cause the weighting of a subsequent sequence element to become greater than those that were supposed to precede it, resulting in competitive inhibition and unintended execution. Neural evidence for competitive queueing was first shown in primates by Averbeck et al (2002), who trained Rhesus Macaque monkeys to draw 2D shapes using a joystick while recording from 16 independent single cells in the prefrontal cortex contralateral to the moving effector. The shapes were separated into segments depending on the number of edges, for example a square consisted of four edges and a triangle of three, which were considered individual movement elements due to the required substantial changes in trajectory, including stops between movements. The authors then trained a linear discriminant analysis (LDA) decoder to discriminate between each segment during the production period based on single unit activity from 16 microelectrodes, which was subsequently used to categorise the probability of patterns belonging to each segment during the period preceding movement. They found that prior to movement onset, the first segment showed the highest pattern probability followed by subsequent elements, weighted by their ordinal position in the sequence. Additionally, neural patterns from trials with transposition errors showed greater classification accuracy on subsequent movements, suggesting that later elements may have unintentionally won the selection process leading

to unintended premature execution. Following on from this initial work by Averbeck & colleagues, contemporary research was able to identify a similar CQ gradient in the neural dynamics of human participants using magnetoencephalography (MEG) during a delayed sequence production (DSP) task (Kornysheva et al., 2019a). The researchers also used an LDA classifier to measure the pattern probability of each sequence element prior to movement based on MEG signal amplitude across the whole brain. The LDA was trained on 10ms windows prior to each movement during sequence execution, then tested on 10ms windows throughout the planning phase prior to movement. Much like Averbeck et al (2002), Kornysheva et al (2019) found a CQ gradient where the probability of upcoming movement elements was weighted depending on their ordinal position in the sequence. In addition, this effect was shown to be finger-independent, as classification was accurate both within- and across-sequences. The strength of the CQ gradient, i.e. how well-separated the sequence elements were prior to execution, was also found to be predictive of performance as it showed a negative correlation with error rate and temporal accuracy during execution, and median splits revealed that above-average performing participants had greater CQ gradients compared to below-average performing participants. Signals most closely related to this CQ gradient were localised using a searchlight analysis to parahippocampal regions and cerebellar lobules 5 and 8, suggesting these areas play a key role in the pre-ordering of sequential movement elements.

The hippocampus has historically been associated with memory formation (Knierim, 2015), memory consolidation (Peigneux et al., 2004), spatial navigation (Moser et al., 2015), and crucially the definition of non-motor sequence order (Davachi & DuBrow, 2015). Moreover, hippocampal and parahippocampal areas are recruited during several examples of movement sequence learning tasks (Schendan et al., 2003) with their activity levels correlating with the accuracy of movement execution (Steele & Penhune, 2010). Dolfen et al (2023), in preparation, used representational similarity analysis (RSA) of fMRI data in humans to investigate how the hippocampus represents sequential movements, finding that the unlike other motor cortical and subcortical regions the hippocampus binds movements to their ordinal position in a learned sequence but not when the same movements are arranged in a random order. Additional research from the same group has reinforced this, showing the involvement of the hippocampus in arranging movements in sequences (Albouy

et al., 2015; B. R. King et al., 2022). Further, lobules 5 and 8 of the cerebellum show finger-specific sensory and motor representations (Buckner, 2013; Wiestler et al., 2011), and are recruited during movement sequence tasks (M. King et al., 2019). Given their established functions, the hippocampus may define an abstract template for a movement sequence which is then assigned to effectors by circuits in the cerebellum (Kornysheva et al., 2019a) although these anatomical localisations of function require further investigation to clarify.

In addition to their neural predictions, CQ models also make clear predictions regarding the availability of behaviours. The pre-activation of the first movement in a sequence would not only suggest that its neural availability is highest but also its behavioural availability, as no other competing movements must be inhibited before the first movement can be executed. For the second movement, however, the system must inhibit the first movement prior to its execution and so on for further elements in a target sequence. To assess this hypothesis, Mantziara et al (2021) trained participants to produce movement sequences in a DSP task, where sequences were executed from memory based on an abstract cue that was shown for a short period prior to execution, similar to the MEG study … Kornysheva et al. 2019. On some trials, instead of prompting execution from memory, the Go cue would instead prompt a singular element of the sequence and the subsequent reaction time and error rate would be recorded under its respective position in the sequence that was initially cued. CQ models predict that earlier elements of the sequence would have lower reaction times and error rates as they would be more prepared and require less inhibition of prior movement elements. A behavioural CQ gradient was found between elements one through three within both reaction time and error differences, with the strength of this CQ gradient relating closely to the quality of execution much like findings from neural data had shown previously (Averbeck et al., 2002; Kornysheva et al., 2019a).

There are several variables in addition to the size of the CQ gradient that impact the quality of movement sequence execution, such as experience playing a musical instrument (Sobierajewicz et al., 2018). Trained musicians also show changes in neural anatomy (Gaser & Schlaug, 2003) and function, with a reduced motor cortical potential compared to untrained controls (Bianco et al., 2018; Wright et al., 2012a). What isn't clear, however, is whether musicians' improved performance on movement sequencing tasks is linked to a greater CQ gradient relative to non-musicians. This may also be the case with other forms of

expertise which require extensive motor capabilities such as dance (Teixeira-Machado et al., 2019), sports (Maudrich et al., 2021), and video gaming (Kowal et al., 2018).

Another finding from the study by Mantziara et al (2021) was that the timing structure of the upcoming sequence, i.e. the length of inter-press intervals, did not impact the measured CQ gradient. The researchers had initially hypothesised that if the CQ gradient represented timing structure, the difference in availability between two consecutive movements might modulate the length of the temporal interval between them, such that two movements with a large difference in availability would be produced with a large temporal interval due to the amount of respective suppression and activation required to transition from one element to the next. While this was not the case, other research has attempted to identify whether timing structures are an emergent or independent property, and how they are implemented in the motor system.

1.1.3 Movement timing

The existence of a dedicated system for the production of serial order has been widely accepted since Lashley's (1951) criticism of the reflex chaining account, but the order of movements is not the only aspect of a sequence's construction that is crucial for successful execution - rhythmic structure, or timing, can be just as important. Playing a piece of music on the piano or producing a tennis serve both require strict timing of constituent movements, else a sloppy tune or a mishit tennis ball result. However, whether the control of timing is an emergent property that comes as a by-product of the specification of serial order, or an independent process entirely, has been debated (Kornysheva, 2016). Early results from force adaptation experiments found that participants adapted well to a forcefield that depended on factors such as movement velocity, but not timing (Conditt & Mussa-Ivaldi, 1999; Karniel & Mussa-Ivaldi, 2003) although these results were later criticised for lacing external movement initiation cues (Kornysheva, 2016). Medina et al (2005) later provided evidence from smooth eye pursuit, suggesting that perturbations based on timing were indeed accounted for and could be flexibly combined with those involved in the processing of space. Furthermore, initial evidence from the serial reaction time task (SRTT) suggested that timing was inseparable from the ordinal movement structure it was paired to, as knowing the timing structure of a new sequence did not facilitate learning, when prior knowledge of the order did (O'Reilly et al., 2008; Shin & Ivry, 2002, 2003). However, Ullén

and Bengtsson (2003) claimed that the temporal structures of sequences in this experiment were modulated by participants' reaction times due to each stimulus onset interval being relative to the time of the last press, resulting in inconsistent timing structures. To investigate the flexibility of timing control further, Ullén & Bengtsson trained participants to produce three types of sequences: ordinal, which required different finger presses at an isochronous rhythm; temporal, which required a single repeating press with a defined timing structure; or combined, which required different finger presses with a defined timing structure. They found strong transfer effects, with the learning of a new combined sequence being facilitated if it had the same timing structure as a temporal sequence that participants were trained on.

Additional evidence for the independent control of timing comes from an alternate SRTT, where participants were trained to produced sequences with a specific order and timing structure, then exposed to repeated trials of sequences which either had the same order, timing, or both, compared to the trained sequence (Kornysheva et al., 2013). Evidence of facilitated performance was immediate for sequences with the same order or both, however sequences with only the same timing took three exposures to show performance benefits relative to unfamiliar control sequences. This suggests that the advantage of timing transfer only becomes applicable after the new order structure is known, and that timing is a flexible modular mechanism that can be transferred to aid in the learning of a new sequence. In an attempt to investigate the neural basis behind this independent mechanism, Kornysheva and Diedrichsen (2014) replicated the SRTT format of this study while also recording neural signals during movement sequence execution using fMRI. To localise the control of timing in the cortex, they trained an LDA to distinguish between timing structures when paired with certain orders, which they then tested to distinguish between the same timings when paired with different orders. Cortical regions in which the LDA shows above chance decoding accuracy are likely to possess neural patterns associated with independent and flexible timing control. A surface-based searchlight revealed such flexible timing control in the Supplementary Motor Area (SMA), and dorsal and ventral Premotor Cortex (PMd and PMv, respectively). Additionally, independent order control was identified using a complimentary analysis where an LDA was trained to distinguish between orders paired with different timings, revealing control in parietal, PMd, and SMA regions.

Finally, a third classifier was trained and tested to distinguish between all sequences once the mean activity patterns for individual timings and orders had been subtracted, akin to residual patterns following removal of transferrable timing and order control, which signified representations of non-transferrable spatio-temporal idiosyncrasies of each sequence. This integrated accuracy was found solely within contralateral primary motor cortex (M1). In sum, these findings demonstrate that order and timing are independently controlled by secondary motor regions and combined in M1, a key output region with direct projections onto the spinal cord.

The order and integration of movements investigated by Kornysheva & Diedrichsen (2014) have clear mappings onto the Motor Hierarchy (See 1.1.1 Motor hierarchy), constituting the selection or intermediate and execution layers respectively (Diedrichsen & Kornysheva, 2015a). However, it is less clear how an independent system for timing control might be implemented. One theory states that movement timing exists within the intermediate layer, that can be selected similarly to different orders and adjusts the temporal distance between serial movements in a multiplicative fashion (Kornysheva, 2016; Kornysheva & Diedrichsen, 2014). This theory suggests multiplicative rather than additive because knowledge of the sequential order is required for known timing to grant any benefit to performance (Kornysheva et al., 2013; Kornysheva & Diedrichsen, 2014). Moreover, the localisation of timing to premotor regions (SMA, PMd, PMv) aligns well with intermediate hierarchical layers that have been found in secondary motor regions (Yokoi & Diedrichsen, 2019a). In addition to those regions included above, other research has historically implicated the cerebellum and the striatum in the control and implementation of movement timing (Buhusi & Meck, 2005; Lewis & Miall, 2003) and, more recently, the hippocampus in encoding the timing of events into memory (Eichenbaum, 2014). However, given that these regions vary significantly in their anatomical structures, and several distinct yet viable mechanisms have been proposed that allow neural networks to process time (Paton & Buonomano, 2018), it is likely that they each function using different and perhaps complimentary neural mechanisms that depend on the behavioural context.

Neurophysiological studies have investigated the nature of temporal processing in the medial frontal cortex (MFC) in primates (equivalent to the SMA in humans). Wang et al (2018) trained Rhesus monkeys to produce specified timing intervals in a cue-set-go task,

where a visual context cue at the onset of each trial indicated the length of the upcoming target interval. Population recordings from MFC show temporal scaling when projected onto a low-dimensional space that depends on the length of the temporal interval being produced; activity became faster when producing a shorter interval, and slower when producing a longer interval. This effect was also observed in downstream caudate neurons but originated in MFC. Moreover, similar scaling mechanisms have been observed in parietal (Jazayeri & Shadlen, 2015; Schneider & Ghose, 2012) and premotor cortices (Zhou et al., 2020), with subcortical structures such as the striatum (Kunimatsu et al., 2018), hippocampus (Eichenbaum, 2014; Itskov et al., 2011), and cerebellum (Narain et al., 2018; Tanaka et al., 2021) showing activity which spikes at specific time points or interval durations. Additional distinctions can be made between cortical and subcortical processing of time as tasks involving explicit time processing typically result in greater recruitment in the SMA (Mondok & Wiener, 2023) compared to implicit time processing such as eye blink conditioning, which has historically been associated with the cerebellum (R. Ivry, 1997; Johansson et al., 2016; Mauk & Buonomano, 2004). Such a distributed network, including the motor cortico-basal ganglia-thalamo-cortical loop, is thought to protect against injury, disease, or degeneration from aging which might leave a system that relies on a singular timing hub vulnerable (Merchant, Harrington, et al., 2013).

As highlighted above, the order and timing are predominantly studied during execution. However, a growing body of research has begun to investigate the period preceding movement: motor planning.

1.2 Motor planning: evidence from behaviour, electrophysiology, and brain imaging

Motor planning, or motor preparation, is a term that has been used throughout the literature to refer generally to the period preceding movement that can range from as short as 150ms up to 700ms prior to movement onset (Haith & Bestmann, 2020). However, several processes are likely to be occurring during this period that may or may not be directly related to the execution of movement itself such as decision making, action selection, and specifying movement kinematics (Wong et al., 2015). For example, in tasks where there is some degree of translation required prior to movement, such as ‘F’ indicating a forward motion and ‘B’ indicating a backward motion, reaction times are significantly longer than when the target movement is spatially cued (Goodman & Kelso, 1980;

Rosenbaum, 1980). By the account of Haith and colleagues, movement preparation consists solely of processes that occur in just 50ms prior to movement initiation and some circumstances do not require planning whatsoever for movement initiation to occur (Haith et al., 2016). Moreover, the same group proposed a line of thinking which categorises motor planning processes into two key categories: 'What' to execute and 'How' to execute it (Wong et al., 2015). 'What' processes involve processes such as observation of the environment, object selection, and task application, which are used to determine motor goals, whereas 'How' processes specify how to achieve said motor goals through kinematics, action selection, and movement specification. Under an absolute account, all processes which determine 'What' to execute are not strictly motor but instead relate more to cognitive processing. Alternatively, these concepts may map onto the motor hierarchy (Diedrichsen & Kornysheva, 2015; see 1.1.1 Motor hierarchy). 'What' to execute would constitute the selection and intermediate layers of the motor hierarchy, i.e. higher level, whereas 'how' to execute a movement would constitute the execution layer and motor primitives. When studying motor planning and how planning transitions into movement, it is crucial to study whether and how populations of neurons plan upcoming movements at the fundamental level.

The neural investigation of motor planning of sequences was pioneered by researchers such as Tanji (Tanji & Evarts, 1976; Tanji & Shima, 1994) who studied single unit activity of neurons prior to movement onset. More recently, multivariate approaches and dimensionality reduction of electrophysiological recordings in non-human animals have allowed researchers a unique insight into the informational content of motor regions during the planning period preceding movement (Zimnik & Churchland, 2021a). This is also true for human neuroimaging methods, where researchers have employed approaches such as linear multivoxel decoding (Cox & Savoy, 2003; Haynes & Rees, 2006; Norman et al., 2006), representational similarity analyses (Kriegeskorte, 2008) and representational model fitting (Diedrichsen et al., 2011; Diedrichsen & Kriegeskorte, 2017), to analyse the informational content of non-invasive neural recordings such as fMRI and MEG. These multivariate analyses prove to be informative especially in the context of motor learning, where the responses of neuronal populations are not always related to a simple increase of activity as learning progresses (Berlot et al., 2020).

1.2.1 Planning as a distinct neural state to execution

Following the success of characterising the responses of neurons in the visual cortex (Hubel & Wiesel, 1962), researchers in the movement domain attempted to assess whether responses from neurons in the motor cortex correlated with task parameters. This was somewhat successful (Georgopoulos et al., 1982, 2007), yet responses were overall heterogenous and difficult to categorise, especially during the planning period prior to movement. Planning dynamics were revealed to be tuned to a variety of information about the upcoming movement such as velocity (Churchland et al., 2006), direction (Messier & Kalaska, 2000; Riehle & Requin, 1989), and movement order (Tanji & Shima, 1994). With such variance in tuning across the motor system, researchers hypothesised that preparation is a dynamical system which sets the initial state of the neuronal population, which initiation causes the motor system to cascade though a low-dimensional manifold producing movement (Shenoy et al., 2013; Vyas et al., 2020). In other terms, planning aligns certain conditions such that the target movement can occur naturally, much like a paper boat being sent down a stream. The amount of force that sends the boat forwards, the direction in which it is released, and the strength of the stream's current all contribute to the trajectory and the end state at which the boat arrives. The dynamical system does not state that perfect conditions are required for execution to begin, however, as evidence shows that the system can still execute movements even in absence of an extended delay period for planning (Ames et al., 2014). Further investigations show that planning states can be entered in remarkably little time, in some cases within around 40ms for single movements (Lara et al., 2018), and can even occur during ongoing movement (Zimnik & Churchland, 2021a).

However, the same neurons whose preparatory dynamics are informative of the upcoming movement often drive movement dynamics during execution (Green & Kalaska, 2011; Remington et al., 2018; Riehle & Requin, 1989; Wong et al., 2015), thus leaving unclear what mechanism allows the motor system to set an appropriate planning state without causing unintentional movement. One theory proposes that the neural activity patterns underpinning movement planning are identical to those during execution, albeit below the threshold required to initiate movement (Cisek & Kalaska, 2005; Duque & Ivry, 2009a). Activity is kept below the threshold required to initiate movement by inhibitory

corticospinal circuits, which allows for movements to be planned without readout to downstream neurons and resultantly muscles, causing unintentional movements before the intended point of initiation. Further, the role of inhibition in movement planning has been investigated using Transcranial Magnetic Stimulation (TMS) during reaction time tasks in order to elicit motor-evoked potentials (MEP) which are indicative of the level of active suppression in the system (Duque et al., 2017). When the target movement was a press with the left index finger, broad suppression was found across both hands including right index and little fingers which increased throughout the preparatory period, with the highest increase observed in the target effector (Duque et al., 2014; Klein et al., 2016). Inhibition was not observed in the leg suggesting that inhibition during movement preparation may be focal depending on the effector required. However, these results also suggest that there is an element of interhemispheric inhibition that occurs when a movement is prepared, i.e. the left hand shows greater inhibition relative to control regions (leg) when the right hand is prepared. Circuits in M1 are characterised by cross-callosal interhemispheric inhibition (Perez & Cohen, 2009). Inhibition in contralateral M1 can also be induced by stimulation of secondary motor regions (Fiori et al., 2017), suggesting that there is substantial interhemispheric inhibition occurring across cortical motor regions which may act to avoid unintentional movements. What is not clear, however, is the resolution of this effect; is the suppression of individual fingers modulated depending on the target movement? Although interhemispheric inhibition of individual fingers is not clear, execution-related representations of individual finger sequence elements has been found in the motor regions of the hemisphere ipsilateral to movement, suggesting that there is a mechanism to communicate information regarding individual finger elements across hemispheres (Diedrichsen et al., 2013).

Despite the evidence for a suppression system that prevents unintended movements during planning, findings showed that planning activity is not a below-threshold version of execution (Churchland et al., 2010). The null-space hypothesis, proposed by Kaufman et al (2014), suggests that movements are planned by activity shifts across populations of neurons in such a way that the overall output across the population remains constant. For example, in a theoretical population with just two excitatory neurons, a movement would be prepared by an increase in the firing rate of one neuron and a decrease in the firing rate

of another. While the activity pattern across the population has changed, a downstream region which receives input from both neurons would not be able to discern a noticeable change in its overall input and would hence not adjust its firing rate in response. This dimension along which population activity can change while maintaining the overall output is labelled the 'output-null' dimension. After a shift along this output-null dimension, activity then can shift orthogonally into an 'output-potent' dimension, resulting in an increase or decrease in population output and hence impacting on downstream receptive neurons. This allows the system to plan movements in advance by shifting the dimension of overall activity without requiring a gating system such as is seen in the oculomotor system (Evinger et al., 1982). Not only does a null-space gating mechanism offer an explanation for how the cortex can prepare movements without eliciting responses in the spinal cord, but the authors also found that this mechanism works to prevent unintentional communication between dorsal premotor and primary motor cortex during movement planning (Kaufman et al., 2014). This mechanism likely prevents contamination of movement-related processing across several motor-related regions and could potentially be a more generalised mechanism that applies to more regions and more behaviours than movement alone. This, however, remains to be seen.

When further investigating the null space phenomenon, Kaufman et al (2016) noticed that a significant portion of the multi-unit signal in M1 and PMd of monkeys during a delayed-reaching task reflected movement onset, as opposed to information about the movement, e.g. direction, found previously (Messier & Kalaska, 2000). This condition invariant signal was identified because, unlike tuned components, the dimensionality reduced signal did not seem to vary depending on the condition of the stimulus but would rather ramp its activity to the point of initiation. Further research expanded on these findings by using dimensionality reduction to identify three modes of neural activity in the mouse anterior lateral motor cortex (ALM; equivalent to premotor cortex in humans) that showed independent shifts during movement planning: the Delay mode, the Go mode, and the Response mode (Inagaki et al., 2018; Li et al., 2016). Neural activity during planning begins with the Delay mode which encodes details about the upcoming movement, specifically in the case of the research the direction of licks made by mice towards one of two targets. Activity in this mode separates until the go cue is observed, at which point it

becomes abolished as activity in the Go mode rapidly spikes, indiscriminate to the target condition and movement, and subsequently falls off in a short burst. Activity in the Response mode then increases, sensitive to movement direction and drives subsequent movement. These findings suggest that not only do movement planning and execution exist in orthogonal multi-dimensional space, but that the cue to move does too. One key question arises: what mechanism acts as the starting gun, causing the reorganisation of cortical activity shortly before movement initiation? Inagaki, Svoboda, and colleagues (Inagaki et al., 2022) used optogenetics in tandem with dimensionality reduction of neurophysiological recordings in an attempt to identify the mechanism that causes the reorganisation of cortical dynamics from output-null to output-potent. They found that a signal to initiate originates in subcortical structures; the pedunculo-pontine nucleus (PPN), located in the pons of the midbrain, showed short latency phasic changes in spike rate that were selective to the go cue. These phasic spikes then follow a circuit from midbrain structures, through the thalamus, to the cortex, causing the observed spike in Go mode activity that shifts surrounding activity from the Delay mode into the Response mode. These findings suggest that populations of neurons in the cortex switch their representations from planning to execution, driven by a signal that arises from subcortical structures. Dynamical systems and null states provide a solid framework for how single movements are planned and executed in the motor system (Inagaki et al., 2022; Kaufman et al., 2014; Shenoy et al., 2013). What isn't clear from these models, however, is how sequences of several movements are prepared.

1.2.2 Online planning during movement

Given that sequences of finger presses can be executed very quickly after extended practice (Abrahamse et al., 2013) and evidence suggests the presence of a movement sequence hierarchy (Diedrichsen & Kornysheva, 2015a) including joint representations for movement chunks (Lashley, 1951; Sakai et al., 2003), one might assume that the system would plan several movements at once prior to initiation. However, recent evidence suggests that only a single movement is prepared initially, with planning for the second movement occurring whilst the first is in flight in dorsal premotor and primary motor cortices (Zimnik & Churchland, 2021a).

Churchland and colleagues (Zimnik & Churchland, 2021a) studied online planning during execution by training macaques to make reaching movements from a centre point while they recorded multi-unit neural activity from PMd and M1. The monkeys had to make one of three reaches during each trial: a single reach to a target; a double delayed reach, where two reaches were made with a long pause between; or a compound reach, where two reaches were made with a short pause between. Churchland & colleagues then separated neural activity into preparatory and execution-related signals by projecting activity onto orthogonal dimensions (Elsayed et al., 2016), much akin to the output-null and output-potent dimensions (Kaufman et al., 2014). They hypothesised that if both movements during compound reaches were prepared together, or fused into a new sequence representation, then the neural population should not need to re-enter the preparatory dimension after execution of the first movement. However, they found that neural activity did re-enter the preparatory dimension, and that this happened while the first movement was still ongoing. In fact, the neural traces for the compound reach looked almost identical to those during the double delayed reach, albeit temporally compressed due to the quicker execution. These findings suggest that in the dorsal premotor and primary motor cortex, sequential movements are not pre-planned or fused, but rather these regions are able to plan subsequent movements one-by-one while the prior movement is still being executed. These findings agree with previous findings in M1 which suggest it is responsible for the generation of singular movements rather than sequences (Berlot et al., 2020; Yokoi et al., 2018; Yokoi & Diedrichsen, 2019a), but opposes PMd findings where representations have been found relating to sequential order and chunking (Kornysheva & Diedrichsen, 2014; Yokoi & Diedrichsen, 2019a). One important aspect of the research from Churchland and colleagues is that planning-on-the-fly was found between reaching movements where the transition angles were acute, prompting a significant dwell period on the central target. Fusion, a phenomenon where two reaching movements become seemingly fused according to velocity and jerk (Flash & Hogan, 1985; Todorov & Jordan, 1998), has been observed during reaching tasks where the transition angle between targets is obtuse, prompting shorter dwell time (Sporn et al., 2022). Further research is needed to establish whether behavioural fusion, reduced dwell time, or lower levels of jerk would abolish planning-on-the-fly in neural recordings.

In human behavioural and imaging research, findings suggest that up to three serial movements may be planned in advance by the motor system and any later movements are likely to be planned during the execution of current movements. Ariani et al (2021) had participants execute sequences of finger movements where the size of the viewing window of upcoming presses was controlled, allowing participants to see a varying number of the upcoming sequence elements; either the whole sequence or only one upcoming element in extreme cases. They found that a larger viewing window afforded faster execution up to three presses, with performance not improving when further elements were revealed, suggesting that up to three movement elements were planned prior to execution with the rest having to be planned online during movement. Further, as participants received more practice, their performance improved for viewing windows of up to six elements. Ariani et al labelled this phenomenon the planning horizon, stating that performance improvements over time are likely due to an increase in its capacity (Ariani & Diedrichsen, 2019). In a follow-up preprint released after the publication of Chapter 2, Ariani et al (2023) sought to identify whether pre- and online-planning occurred within distinct anatomical regions. Based on prior research into the representations of motor hierarchical structures, one would expect pre-planning to occur within secondary motor regions and online-planning within M1 (Kornysheva & Diedrichsen, 2014; Russo et al., 2020; Yokoi & Diedrichsen, 2019a). This was indeed the case; fMRI results showed greater activation during planning in PMd and SPL when upcoming sequences consisted of multiple fingers relative to single fingers. In contrast, activity patterns in M1 and primary somatosensory cortex (S1) primarily represented the first element of the upcoming sequence during planning and a temporal summation of patterns belonging to constituent movement elements during execution. Moreover, correlation PCM models showed strong evidence that activity patterns in PMd and SPL were not uncorrelated during planning and execution. These findings contest the null space and dynamical systems hypotheses (Kaufman et al., 2014; Shenoy et al., 2013) by stating that representations are maintained across movement phases albeit on the level detectable by fMRI; using a technique with a greater spatial precision would reveal which mechanism applies in neural populations as opposed to blood oxygenation level dependent (BOLD) responses of humans during a sequence learning task.

1.3 Objectives and summary

The neural mechanisms of movement sequence execution are well-established in terms of motor hierarchical mapping, yet how these same mechanisms operate during the planning period preceding movement is unclear. In the current thesis, I aimed to help close this knowledge gap. Specifically, I investigated how different elements of the hierarchy are implemented neurally across the peri-movement phase. Additionally, based on previous research showing a change in neural population dynamics from planning to execution (Inagaki et al., 2018; Kaufman et al., 2014) that is driven by a signal from subcortical regions (Inagaki et al., 2022), I investigated whether the neural patterns found during movement sequence planning in subcortical regions were identical to those during execution. Moreover, given the importance of suppression in movement planning (Duque et al., 2017) and finger-specific representations found in M1 ipsilateral to movement (Diedrichsen et al., 2013), I identified whether the relative inhibition observed during planning in the active effector (Kornysheva et al., 2019a; Mantziara et al., 2021) caused a similar gradient of suppression in the effector contralateral to movement, or whether there was global inhibition of unused effectors.

Chapter 2 used multivariate pattern decoding analysis of fMRI data in the neocortex to investigate the neural representations of order, timing, and their integration during planning and execution across cortical motor areas contralateral to the performed motor sequence. Additionally, behavioural transfer of known sequence order and timing were assessed relative to new sequences.

Chapter 3 further explored the fMRI dataset collected for chapter 2 to investigate order, timing, and integration across subcortical regions using multivariate pattern analysis within constrained regions of interest. Further, it used dimensionality reduction by principal component analysis to investigate the multivariate distance between representations in planning and execution relative to carefully controlled simulations.

Chapter 4 used behavioural responses to investigate the CQ gradient in a range of participants. Here, I assessed the presence of a mirrored CQ gradient in the hand contralateral to that which was initially cued, identifying a gradient inhibition of fingers controlled by the hemisphere ipsilateral to movement on the active and passive hand during

sequence planning. As a follow-up, I examined the influence of performance and expertise such as musical experience on the strength of the CQ effect.

Chapter 5 discusses and synthesises the findings of the previous chapters with respect to the current literature, notes clinical significance, and identifies future avenues for research.

Chapter 2 - Cortical Integration of Independent Motor Sequence Order and Timing Across Planning and Execution

This chapter is published as:

Yewbrey, R., Mantziara, M., & Kornysheva, K. (2023). Cortical patterns shift from sequence feature separation during planning to integration during motor execution. *Journal of Neuroscience*, *43*(10), 1742-1756.

Author contributions: R.Y., M.M., and K.K. designed research; R.Y., M.M., and K.K. performed research; R.Y. and K.K. analysed data; R.Y. and K.K. wrote the first draft of the paper; R.Y., M.M., and K.K. edited the paper.

2.1 Abstract

Performing sequences of movements from memory and adapting them to changing task demands is a hallmark of skilled human behaviour, from handwriting to playing a musical instrument. Prior studies showed a fine-grained tuning of cortical primary motor, premotor, and parietal regions to motor sequences – from the low-level specification of individual movements to high-level sequence features like sequence order and timing. However, it is not known how tuning in these regions unfolds dynamically across planning and execution. To address this, we trained 24 healthy right-handed human participants (14 females, 10 males) to produce four five-element finger press sequences with a particular finger order and timing structure in a delayed sequence production paradigm entirely from memory. Local cortical fMRI patterns during preparation and production phases were extracted from separate 'No-Go' and 'Go' trials, respectively, to tease out activity related to these peri-movement phases. During sequence planning, premotor and parietal areas increased tuning to movement order or timing, irrespective of their combinations. In contrast, patterns reflecting the unique integration of sequence features emerged in these regions during execution only, alongside timing-specific tuning in the ventral premotor, supplementary motor, and superior parietal areas. This was in line with the participants' behavioural transfer of trained timing, but not of order to new sequence feature combinations. Our findings suggest a general informational state shift from high-level feature separation to low-level feature integration within cortical regions for movement execution. Recompiling sequence features trial-by-trial during planning may enable flexible last-minute adjustment before movement initiation.

2.2 Significance Statement

Musicians and athletes can modify the timing and order of movements in a sequence trial-by-trial, allowing for a vast repertoire of flexible behaviours. How does the brain put together these high-level sequence features into an integrated whole? We found that, trial-by-trial, the control of sequence features undergoes a state shift from separation during planning to integration during execution across a network of motor-related cortical areas. These findings have implications for understanding the hierarchical control of skilled movement sequences, as well as how information in brain areas unfolds across planning and execution.

2.3 Introduction

Skilled sequences of movements performed from memory are regarded as a hallmark of human dexterity (Diedrichsen & Kornysheva, 2015a; Hikosaka et al., 2002a; Rosenbaum et al., 2007). They are essential building blocks of everyday skilled behaviours, from typing, to tying shoelaces, or playing a musical instrument (Figure 2.1a). In addition to the order of movements in a sequence, the temporal accuracy of the movements can be crucial to the success of the task, e.g., when tapping a Morse code. Previous behavioural (Gobel et al., 2011; Kornysheva et al., 2013; Ullén & Bengtsson, 2003), computational (Calderon et al., 2022; Zeid & Bullock, 2019), neurophysiological (Lafuente et al., 2022; Merchant, Pérez, et al., 2013; Zimnik & Churchland, 2021a) and neuroimaging findings (Bengtsson et al., 2004; Kornysheva et al., 2019a; Kornysheva & Diedrichsen, 2014) established that movement order is controlled independently of timing, and vice versa, whenever motor sequences incorporated temporally discrete sub-goals. This includes sequences that are extensively trained and performed from memory without external guidance, characteristic of motor sequence execution in the real world. The integration of movement timing and order has been studied in the context of execution (Kennerley et al., 2004; Kornysheva et al., 2013; Kornysheva & Diedrichsen, 2014; O'Reilly et al., 2008; Shin & Ivry, 2002), but we currently do not know whether the binding of order and timing takes place prior to the initiation of the first movement, and which motor-related cortical areas underly this process.

Neural and haemodynamic activity patterns in contralateral primary motor (M1) and sensorimotor (S1), premotor, and parietal cortices show informational tuning to trained motor sequences (Berlot et al., 2020; Kornysheva & Diedrichsen, 2014; Matsuzaka et al., 2007; Picard et al., 2013; Tanji & Shima, 1994; Wiestler et al., 2014; Wiestler & Diedrichsen, 2013; Wymbs et al., 2012; Wymbs & Grafton, 2015; Yokoi et al., 2018; Yokoi & Diedrichsen, 2019a). Specifically, activity patterns outside the primary motor cortex – premotor, supplementary motor and parietal areas – contain high-level information, e.g., about sequence chunks, positional rank in the sequence (Russo et al., 2020; Tanji & Shima, 1994; Yokoi & Diedrichsen, 2019a) and spatial, rather than body-centred coordinates (Wiestler et al., 2014). Further, activity patterns in these regions can generalise across different pairings of movement order and timing (Kornysheva & Diedrichsen, 2014) (Figure 2.1b). In contrast, activity patterns in contralateral M1/S1 are associated with the planning and execution of

single movements in a sequence (Ariani et al., 2022; Berlot et al., 2020; Yokoi et al., 2018; Zimnik & Churchland, 2021a), body-centred coordinates (Wiestler et al., 2014) and information about unique sequence order and timing integration, suggesting lower-level representations driven by motor implementation (Kornysheva & Diedrichsen, 2014) (Figure 2.1b).

Despite the progress made, it remains uncertain when and where motor-related cortical areas integrate the order and the timing of movements trial-by-trial. One possibility is that premotor and parietal regions show a fixed mapping to high-level independent, and M1/S1 to lower-level integrated sequence features, respectively (Kornysheva & Diedrichsen, 2014). These may be activated simultaneously or sequentially depending on the peri-movement phase, but their informational content could remain stable (Figure 2.1c, “Fixed mapping”). Alternatively, the tuning to high and low-level features may change dynamically with phase with the same regions parsing sequence order and timing during planning but integrating these sequence features during execution (“Dynamic mapping”).

We trained participants to produce five-element finger press sequences comprised of two finger orders and two temporal interval orders (timings) from memory in a delayed production paradigm. To disentangle planning from execution using fMRI, activity was extracted from ‘No-Go’ and ‘Go’ trials, respectively. We utilised multivariate pattern analysis to decode fMRI patterns related to the planned and executed sequence order and timing. Our results provide strong evidence for the integration of sequence order and timing during sequence execution only, but not during planning. Further, they support the idea that contralateral cortical regions are not fixed in their informational content but update their tuning dynamically.

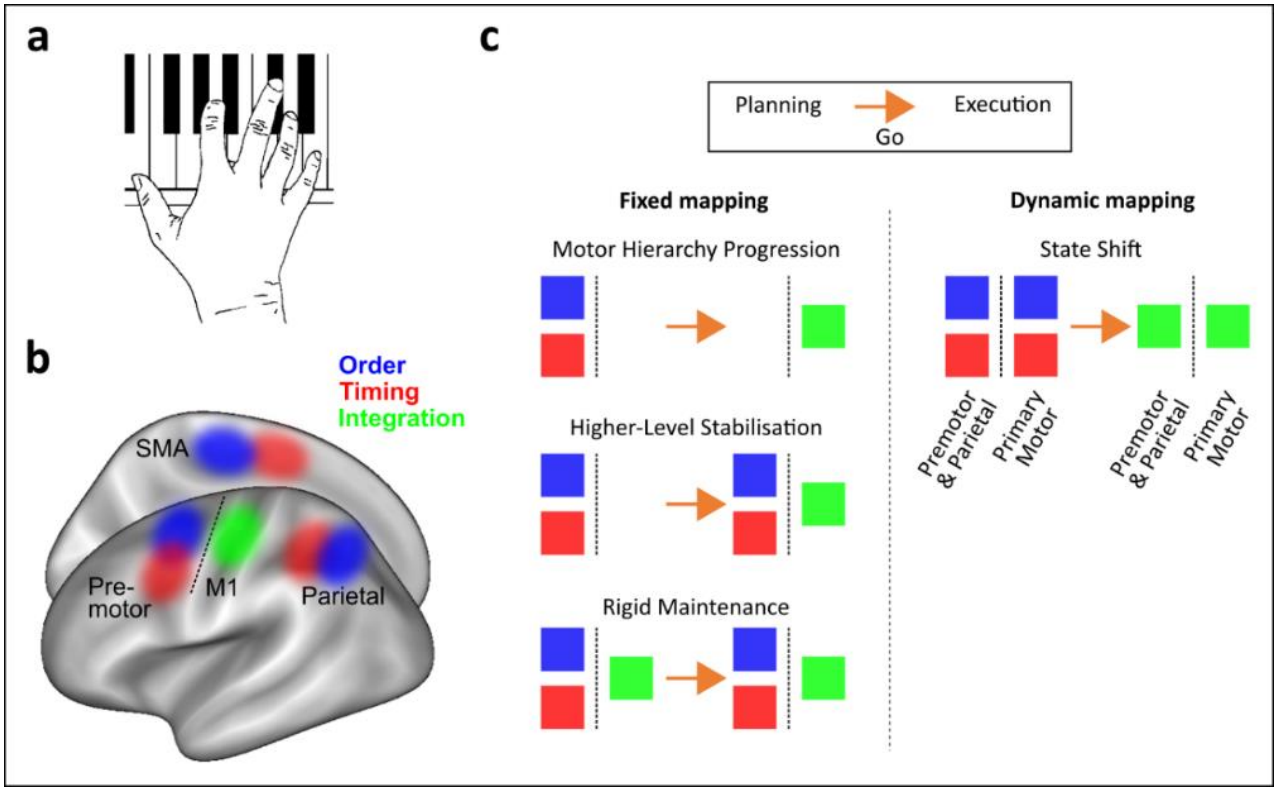

Figure 2.1. Theoretical framework and hypotheses. (a) Skilled sequence production, e.g., when playing a melody on a piano, is characterised by producing movements with a specific order and timing and combining them flexibly trial-by-trial. (b) Previous findings localised independent patterns of order and timing to premotor, supplementary motor, and parietal regions, while their integration was found in the primary motor cortex (M1) (Kornysheva & Diedrichsen, 2014). (c) How does this mapping evolve across planning and execution? "Fixed mapping" hypotheses state that premotor and parietal regions outside of M1 control order and timing as independent motor sequence features, and M1 itself controls the non-linear integration of the two during planning and/or production. In contrast, the "Dynamic mapping" hypothesis proposes that there is a state shift within regions from independent feature control during planning to integration during execution (OSF preregistration: https://doi.org/10.17605/OSF.IO/G64HV).

2.4 Materials and Methods

2.4.1 Participants

24 neurologically healthy participants - 14 females and 10 males (*M* = 21.00 years, *SD* = 1.64) - met all behavioural and imaging requirements after completing the three-day experiment. 23 Participants were right-handed with a mean Edinburgh Handedness Inventory (EHI; https://www.brainmapping.org/shared/Edinburgh.php; adapted from (Oldfield, 1971)) score of 75.22 (*SD* = 20.97, Range: 25-100), one was left-handed with an EHI score of -70. Although our preregistration (osf.io/g64hv) stated we would exclude left-handed individuals, we included this participant as their data was not qualitatively different to the rest of the sample. Data were collected from an additional 17 participants but were

excluded. One participant was excluded due to unforeseen technical difficulties with the apparatus and one participant was excluded due to a corrupted functional scan. 15 further participants did not reach target performance after two days of training. Target performance consisted of an error rate below 20% (*M* = 6.54%, *SD* = 6.03, for the group) and distinct sequence timing structures that transferred across sequence finger orders (see Results section). Participants were recruited either through social media and given monetary reward at a standard rate, or through a participation panel at Bangor University and awarded module credits for their participation. Participants with professional musical qualifications were excluded from recruitment. All participants provided informed consent, including consent to data analysis and publication, through an online questionnaire hosted by Qualtrics (Qualtrics, Provo, UT). This experiment and its procedures were approved by the Bangor University School of Psychology Ethics Committee (Ethics approval number 2019-16478).

2.4.2 Apparatus

Force data from fingers of both the right and left hands were recorded at a sample rate of 1000hz using two custom-built force transducer keyboards (10 channels). Each key had a groove within which the respective fingertip was positioned. A force transducer (Honeywell FS Series, with a range of up to 15 N) was located under each groove and recorded the respective finger force without crosstalk between channels. Force data acquisition occurred in each trial from 500ms before sequence cue onset to the end of the production period in production trials, and the end of the false production period in No-Go trials. The keys could be adjusted in position by sliding them up and down individually along the keyboard plane to achieve the most comfortable position for the hand and wrist when seated during training or in supine position in the MRI scanner, respectively. Once adjusted the position of the keys was fixed. Traces from the right hand were baseline-corrected by the first 500ms of acquisition (500ms before the sequence cue) and smoothed to a Gaussian window of 100ms, trial-by-trial. Button presses were defined as the point at which forces above baseline exceeded a fixed threshold (2.5 N for the first 8 participants and 1 N for the subsequent 16 out of 24 participants). Press timings were identified by the timestamp provided by National Instruments Data Acquisition Software (National Instruments, Austin, TX) associated with the data point at which the respective threshold was exceeded.

During behavioural training sessions, participants were seated at a wooden table approximately 75cm away from a 19-inch LCD LG Flatron L1953HR, at a resolution of 1280 x 1024, at a refresh rate of 60Hz. Their hands were occluded by a horizontally positioned panel on posts around the force boxes. During fMRI sessions, stimuli were presented on an MR Safe BOLDScreen 24", at a resolution of 1920x1200 and a refresh rate of 60Hz. Participants laid supine on the scanner bed and the two force transducers were positioned on a plastic support board resting on their bent upper legs to enable comfortable and stable positioning of the hands.

2.4.3 Behavioural task

Participants were trained to produce four five-finger sequences with defined inter-press-intervals (IPI) from memory in a delayed sequence production paradigm. 'Go' trials began with a fractal image (Sequence cue) presented for 400 milliseconds (ms) which was associated with a sequence. The mapping between fractal image and each sequence was defined randomly for each participant. Following the Sequence cue, a fixation cross was shown to allow participants to prepare the upcoming sequence; display length of this fixation cross was jittered at durations of 600ms, 1100ms, 1600ms, and 2100ms, pseudorandomised across trials within blocks. A black hand with a green background (Go cue) then appeared for 4000ms to cue sequence production. Succeeding the Go cue, another fixation cross was presented in a jittered fashion at durations of 500ms, 1000ms, 1500ms, and 2000ms. Feedback (see feedback section for more details) was then presented to participants for 1000ms, followed by a jittered inter-trial-interval (ITI) duration of 1000ms, 1500ms, 2000ms, and 2500ms. Visually guided (Instructed) 'Go' trials during training were presented in the same fashion albeit featuring a Go cue with a grey background, and a red dot on the tip of each finger on the hand image would move from finger to finger in the target production order and in-pace with the target timing structure. 'No-Go' had the same structure to 'Go' trials, but no Go cue was shown succeeding the preparatory fixation cross. Instead of the Go cue the fixation cross continued to show for an additional 1000ms. As in 'Go' trials, this phase of the trial was followed by a fixation cross, feedback and ITI.

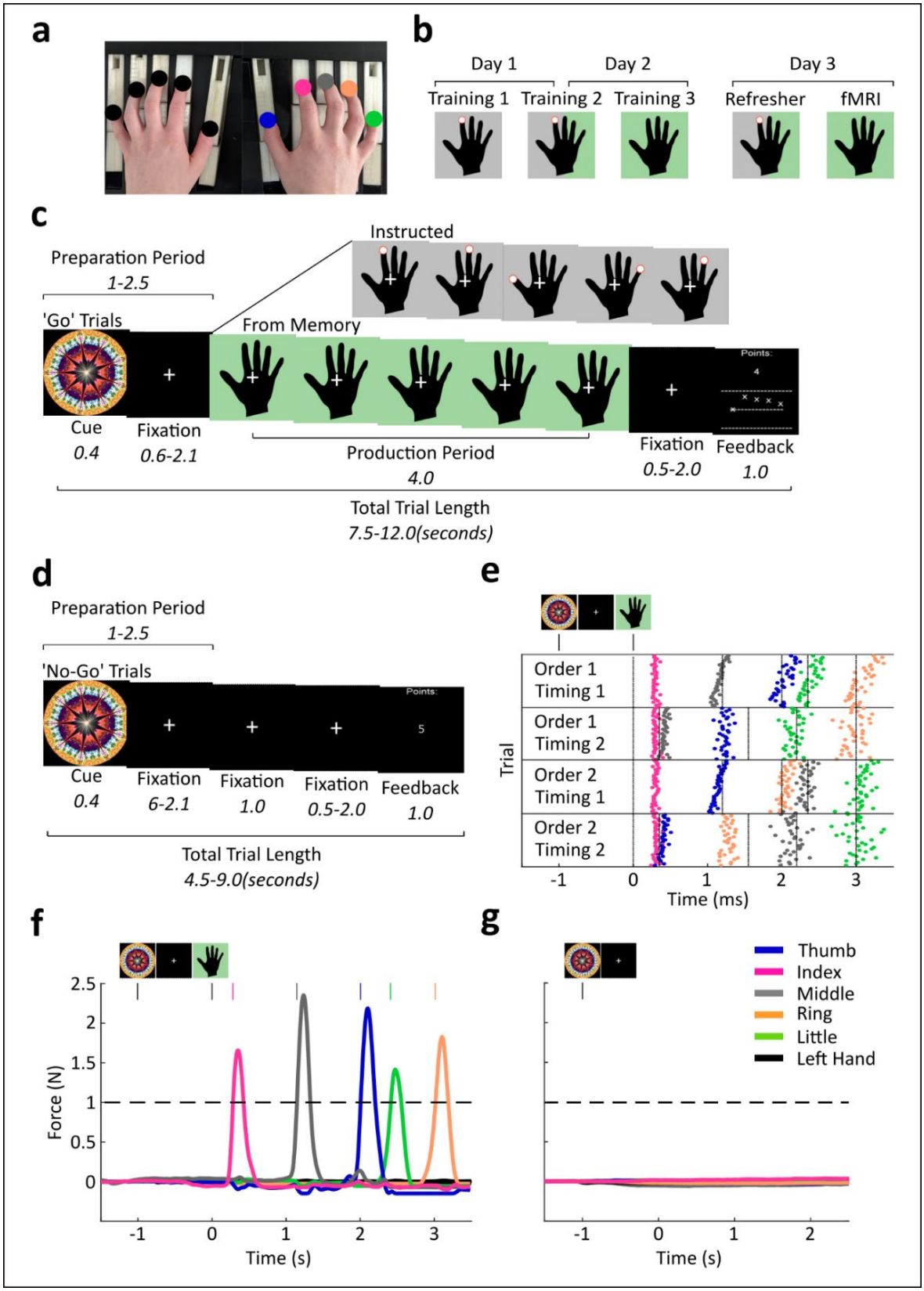

Figure 2.2. Experimental and trial designs. **a**, Participants produced finger presses on a ten-finger force transducer keyboard. The hands were visually occluded from the participants' view by a panel during training and when lying in a supine position during the fMRI session. Target fingers on the right hand are indicated by different colours that also correspond to the legend in later panels. Fingers on the left (inactive) hand are marked as black. **b**, Trial type proportions on each experimental day progressed from 100% instructed (Training 1) to 50/50% mixed (Training 2) to 100% from memory (Training 3) trials during the last stage of

training and during fMRI. See Table 1 for a detailed overview of trial numbers during each session. Black hands with a grey background and a red finger cue indicate visually instructed trials. Black hands with a green background represent trials with sequence production from memory. **c,** 'Go' trials from memory consisted of a Sequence cue, followed by a fixation cross and a Go cue instructing a production period. The occurrence of the Go cue was the onset of the respective hand stimulus. The trial ended with a feedback screen which indicated finger and temporal accuracy relative to a target sequence. Instructed trials, shown as an insert at the top of the image, followed the same trial structure as from memory trials, but displayed visual finger cues to aid production. **d,** 'No-Go' trials consisted of a Sequence cue, followed by a fixation cross without a Go cue, and feedback screen. **e**, A raster plot shows all button press timings in correct trials produced from memory across the entire fMRI session in one representative participant. Horizontal lines separate the different sequences that followed a two finger order by two timing design (see Methods for details). Vertical dotted lines indicate target press timings. Each coloured dot represents a different effector, see corresponding legend. **f**, Example force traces from 10 channels corresponding to the fingers on the right (coloured) and left hands (black) in one representative 'Go' trial during fMRI. The horizontal dashed line represents the finger press threshold, and coloured vertical lines represent the time point at which a press was detected from the respective finger. **g**, Example force traces, as in f, from one representative 'No-Go' trial.

Four target sequences consisted of permutations of two finger orders (Order 1 and 2) and two IPI orders (Timing 1 and 2) matched in finger occurrence and sequence duration. Sequence orders were generated randomly for each participant. All trained sequences began with the same finger press to avoid differences in the first press driving the decoding of sequence identity during preparation (Yokoi et al., 2018). Ascending and descending press triplets and any identical sequences were excluded. Timing structures were the same across participants, to allow for comparison of timing performance across participants. The two trained timing structures consisted of four target IPI sequences as follows: 1200ms-810ms-350ms-650ms (Timing 1), and 350ms-1200ms-650ms-810ms (Timing 2). To assess if participants maintained the target timing structure despite individual tendencies to lengthen or compress overall sequence length, we calculated timing error for each participant relative to their average total production length. This was calculated offline by normalising target and produced IPIs as a percentage of the participant's average total sequence length during the session across sequences, then calculating the cumulative percent deviation from target for each IPI, averaged across trials.

Feedback was given to participants trial-by-trial on a points-based scale ranging from 0 to 10. Points were based on initiation reaction time (RT) and temporal deviation from target timing calculated as a percentage of the target interval length. For initiation reaction time, up to five points were awarded for a fast initiation RT as follows: five points for presses within 200ms of the Go cue, four points for presses within 200-360ms, three points for presses within 360-480ms, two points for presses within 480-560ms, one point for presses

within 560-600ms, and zero points for presses beyond 600ms. For IPI performance, up to five points were awarded based on deviation from target IPI structure in percent of respective interval to account for the scaling of temporal error with IPI length (Rakitin et al., 1998). Five points were awarded for average deviations of IPIs from target for each trial which was lower than 10 percent, four points for 10-20 percent, three points for 20-30 percent, two points for 30-40 percent, one point for 40-50 percent, and zero points for above 50 percent. If the executed press order was incorrect, participants were awarded 0 points for the trial. If the executed press order was correct, they were awarded their earned timing points. To discourage premature key presses in the preparation period of 'Go' trials and 'No Go' trials, 0 points were awarded if participants exceeded a force threshold during preparation above the baseline period. In No-Go trials, five points were awarded if no press was made as instructed. A monetary reward of £10 was offered to the two participants who accumulated the most points across the course of the experiment, to incentivise good performance.

Participants were presented with a feedback screen after each trial showing the number of points achieved in the current trial, as well as feedback on whether they pressed the correct finger at the correct time. Total points accumulated across the whole experiment were shown at the end of each block. A horizontal line was placed in the centre of the screen, with four symbols displayed equidistantly along the line which represented each of the five finger presses. An 'X' indicated a correct finger press, and a '-' indicated an incorrect finger press for each sequence position. The vertical position of these symbols above ("too late") or below ("too early") the line was proportional to the participant's timing of the respective press relative to target IPI (in %). Using these cues, participants could adjust their performance online to ensure maximum accuracy of sequence production and prevent a drift in performance from memory following training. During the first two days of training, auditory feedback in the form of successive rising tones corresponding to the number of points (0-10) were played alongside the visual feedback. Auditory feedback was absent during the fMRI session, to prevent any auditory processing driving decoding accuracy.

2.4.4 Procedure

Training duration was fixed across participants and occurred across the first two days of the experiment over three distinct training stages (see Figure 2.2b for a visual

representation of the training stages, Table 1 for trial numbers during each session). In the first training stage, 80% of all trials were instructed ‘Go’ trials (black hand on grey background, Figure 2.2c), and the remaining 20% were ‘No-Go’ trials. During the second training stage, 40% of trials were instructed ‘Go’ trials, 40% were from-memory ‘Go’ trials (black hand on green background, Figure 2.2c), and 20% were ‘No-Go’ trials (Figure 2.2d). In the third and final stage of training, 80% of trials were from-memory ‘Go’ trials, and 20% were ‘No-Go’ trials. Each stage of training consisted of 240 trials for a total of 720 trials across all three training sections. The third and final day consisted of a short refresher stage of 40 trials, made up of the same proportion of trials as the second stage of training, during which T1 images were collected. Following this refresher stage there was a fMRI stage consisting of 288 trials (48 trials in each block) featuring 50% from-memory ‘Go’ trials and 50% ‘No-Go’ trials.

In addition, before and after the last training stage, participants completed a synchronisation task during which they were asked to synchronize their respective presses to a visual finger cue, as in the first stages of training consisting of four blocks of 32 trials which included trained sequences, sequences with new timings but the same orders (order transfer), sequences with the same timings but new orders (timing transfer), and new sequences. Trial structure was identical to instructed ‘Go’ trials. There were four sequences belonging to each condition and each sequence was shown for eight consecutive exposures (Figure 2.3c) to assess short-term learning gains. We expected that participants would show more accurate synchronization to visual sequences when they encountered trained sequences as well as sequences with a trained finger order or trained timing compared to untrained control sequences following the completion of training.

Table 2.1

Distribution of trial types across experimental phases

	Day 1				Day 2			Day 3	
	Example	Pre-training test	Training 1	Training 2	Training 2	Training 3	Post-training test	Refresher	Test (fMRI)
Instructed trials	4 (33%)	32 (100%)	16 (80%)	8 (40%)	8 (40%)	0	32 (100%)	8 (40%)	0
Memory trials	4 (33%)	0	0	8 (40%)	8 (40%)	16 (80%)	0	8 (40%)	24 (50%)
No-Go trials	4 (33%)	0	4 (20%)	4 (20%)	4 (20%)	4 (20%)	0	4 (20%)	24 (50%)
Total trials per block	12	32	20	20	20	20	32	20	48
Number of blocks	1	4	12	6	6	12	4	2	6

Note. The first half of Training 2 occurred on Day 1, the second half on Day 2.

2.4.5 MRI acquisition

Images were obtained on a Philips Ingenia Elition X 3T MRI scanner using a 32-channel head coil. T1 anatomical scans were acquired using a magnetisation-prepared rapid gradient echo sequence (MPRAGE) scan at a 0.937 x 0.937 x 1 resolution, with a field of view of 240 x 240 x 175 (A-P, R-L, F-H), encoded in the anterior-posterior dimension.

T2*-weighted Functional images were collected across six runs of 230 volumes each with a TR of 2 seconds, a TE of 35ms and a flip angle of 90°. The voxel size was 2mm isotropic, at a slice thickness of 2mm, with 60 slices. These were obtained in an interleaved odd-even echo-planar imaging (EPI) acquisition at a multi-band factor of two. Four images were discarded at the beginning of each run to allow the stabilisation of the magnetic field. The central prefrontal cortex, the anterior temporal lobe and ventral parts of the cerebellum were not covered in each participant. Jitters were employed within each trial during preparation periods, post-production fixation crosses, and inter-trial intervals, to vary which part of the trial is sampled by each TR and therefore give us a more accurate estimate of the hemodynamic response function (HRF) (Serences, 2004).

2.4.6 Pre-processing and first-level analysis

All fMRI pre-processing was completed using SPM12 (Revision 7219) on MATLAB (The MathWorks, Inc., Natick, MA). Slice timing correction was applied using the first slice as a reference to interpolate all other slices to, ensuring analysis occurred on slices which represent the same time point. Realignment and unwarping were carried out using a weighted least-squares method correcting for head movements using a 6-parameter motion algorithm. A mean EPI was produced using SPM's 'Imcalc' function, wherein data acquired across all six runs was combined into a mean EPI image to be co-registered to the anatomical image. Mean EPIs were co-registered to anatomical images using SPM's 'coreg' function and their alignment was checked and adjusted by hand to improve the alignment, if necessary. All EPI runs were then co-registered to the mean EPI image.

For the general linear model (GLM), regressors were defined for each sequence separately for both preparation and production. Preparation- and production-related BOLD responses were independently modelled from 'No-Go' and 'Go' trials, respectively, to tease out activity from these brief trial phases despite the haemodynamic response lag (Logothetis, 2003). The preparation regressor consisted of boxcar function starting at the moment of the Sequence cue in 'No-Go' trials and lasting for the duration of the maximum possible preparation phase (2500 ms). The production regressor consisted of a boxcar function starting at the onset of the first press with a fixed duration of 0 (constant impulse), to capture activity related to sequence initiation and extract sequence production related activity from the first finger press that was matched across sequences within each participant. We aimed at capturing BOLD responses related to neuronal populations that become differentially active for different sequences (Tanji & Shima, 1994), for which a single estimate of sequence production has been used to successfully identify sequence representations in a number of previous fMRI studies (Berlot et al., 2020; Kornysheva & Diedrichsen, 2014; Nambu et al., 2015; Wiestler & Diedrichsen, 2013; Yokoi et al., 2018). We used a separate pilot dataset (N=9) recorded prior to the pre-registration of the study to determine the optimal GLM regressor model for the execution period. To be certain that the constant impulse model provided the best model for sequence production, we assessed contrast values extracted from a spherical region of interest (ROI) centred on M1a (MNI coordinates: [-38 -31 48]) with a radius of 6mm obtained from a separate pilot dataset (N=9) for a model containing variable epoch versus constant impulse regressor for sequence

execution. A repeated measures t-test found that the constant impulse GLM produced significantly higher contrast values (M = 10.89, SD = 3.07) than the variable epoch GLM (M = 3.64, SD = 1.27; $t(8) = 10.24$, $p < .001$, d = 3.41). This may be due to the way that the BOLD response scales non-linearly with movement initiation rather than movement duration or speed (Khushu et al., 2001).

Additionally, we included regressors of no interest: 1) Error trials (incorrect or premature presses during 'Go' trials and presses during No-Go trials) which were modelled from sequence cue onset to the end of the ITI, 2) the preparation period in 'Go' trials (1000-2500 ms from Sequence cue) and 3) the temporal derivate of each regressor. The boxcar model was then convolved with the standard HRF. To remove the influence of movement-related artifacts, we used a weighted least-squares approach (Diedrichsen & Shadmehr, 2005).

2.4.7 Surface reconstruction

Cortical surface reconstruction was conducted on each participant's T1 anatomical image using Freesurfer's recon-all function (Dale et al., 1999). Surface structures were then co-registered to the symmetrical Freesurfer average atlas (Fischl et al., 1999) using surface Caret (Van Essen et al., 2001). Searchlights for multivariate pattern analysis were then defined on each individual surface using the node maps provided by the surface reconstruction and displayed in atlas space.

2.4.8 Cross-sectional and region of interest analysis

Two cross-sections were defined upon the cortical surface: 1) anterior to posterior, running from PMd to OPJ and 2) ventral to dorsal, running from PMv to SMA. These cross-sections were taken from a previous study (Kornysheva & Diedrichsen, 2014). Data points along these axes were extracted to provide a continuous measure along the cortical surface, which was then subjected to a non-parametric permutation analysis to identify clusters which were significantly above baseline (Maris & Oostenveld, 2007). This was conducted as a one-tailed test, with 10,000 permutations, for which Cohen's d effect size was calculated by averaging across the values in each significant cluster (M. Meyer et al., 2021).

ROI analysis was conducted using the Caret toolbox (Van Essen et al., 2001) on ROIs which were defined based on Caret masks used by several previous studies (Kornysheva & Diedrichsen, 2014; Wiestler et al., 2014; Wiestler & Diedrichsen, 2013; Yokoi et al., 2018),

consisting of PMv, PMd, M1, S1, SMA/pre-SMA, SPCa, and SPCp. Note that the preregistration (osf.io/g64hv) referred to the SPCa ROI as "SPC" and S1 and SPCp were added after the pre-registration. This was to enable comparison to more recent results, including those published after the pre-registration, showing S1 (Ariani et al., 2022; Gale et al., 2021) and SPCp involvement in movement planning (Culham & Valyear, 2006; Fitzpatrick et al., 2019; Lindner et al., 2010), as well as to probe the functional differentiation between SPCa and SPCp with respect to sequence representations demonstrated by Yokoi et al. (2018). Z-values for each classifier were averaged within regions to give an overall value for each decoder. These values were calculated from unsmoothed individual data. One-sample t-tests against chance level (zero) then identified significantly above-chance decoding values within these ROIs Bonferroni-corrected for six comparisons. To test the hypotheses in Figure 2.1 (Dynamic vs fixed mapping across planning and execution) we performed a repeated measures ANOVA on decoding values with factors trial phase, region, and classifier.

2.4.9 Multi-variate pattern analysis of fMRI

Multivariate pattern analysis (MVPA) was conducted using a custom-written MATLAB code to detect sequence-specific representations (Kornysheva et al., 2019a; Kornysheva & Diedrichsen, 2014). We used a searchlight of 160 voxels and a maximum searchlight radius of six millimetres. Each searchlight was run on each individual's cortical surface-reconstructed anatomy, projected onto the Freesurfer average atlas (Fischl et al., 1999). The classification accuracy for each searchlight (cf. classification procedures below) was assigned to the centre of each searchlight. A classification accuracy map was generated by moving the searchlight across the cortical surface (Oosterhof et al., 2011). Mean patterns and common voxel-by-voxel co-variance matrices were extracted for each class from training data set (five of the six imaging runs), and then a gaussian linear discriminant classifier was used to distinguish between the same classes in a test data set (the remaining imaging run).

The factorised classification of finger order, timing, and integrated order and timing followed the previous approach (Kornysheva & Diedrichsen, 2014) and performed on betas estimated from the sequence preparation and production periods independently. For the decoding of sequence timing, the classifier was trained to distinguish between two sequences with differing timing but matching order across five runs and was then tested on two sequences with the same two timings paired with a different order in the remaining

run. This classification was then cross-validated across runs and across training/test sequences, for a total of 12 cross-validation folds. For the decoding of sequence order, the classifier was trained to distinguish between two sequences of differing orders paired with the same timing and tested on two sequences with the same two orders when paired with a different timing and underwent the same cross-validation procedure. This method of training and testing the linear discriminant classifier allowed for identification of sequence feature representations that were transferrable across conditions they are paired with and therefore independent. The integrated classifier was trained to distinguish between all four sequences on five runs and then tested on the remaining run. Here, the mean activity for each timing (collapsed across two orders) and finger order (collapsed across two timings) condition within each run was subtracted from the overall activity for each run, separately (Kornysheva & Diedrichsen, 2014). This allowed for the measurement of residual activity patterns that were not explained by a linear combination of timing and order. For better comparability across classifiers, the classification accuracies were transformed to z-scores, assuming a binomial distribution of the number of correct guesses. We then tested these z-scores against zero (chance level) on cortical cross-sections of interest and in pre-defined ROIs across participants for statistical analysis. In addition to the main analysis, we provided an40asely40toryy analysis across the whole cortex by carrying out a random-effects analysis with an uncorrected threshold of $t(23) > 3.48$, $p<0.001$ and a cluster-wise p-value for the cluster of that size on the z-transformed decoding values for order, timing, and integration. This was Bonferroni corrected for two hemispheres and the results, including a full table of significant clusters, are available in Table 3.

2.4.10 Experimental Design and Statistical Analysis

All data collection and analyses were conducted using a repeated measures design. For the behavioural data, we assessed changes in finger force production from baseline during the preparation period in both ‘Go’ and ‘No-Go’ trials using two-tailed paired samples t-tests. We also assessed the length of inter-press intervals and timing error during sequence production using a repeated measures ANOVA with factors timing, order, and interval position. These ANOVAs were conducted both across the group and within each participant to determine effects within individuals. To evaluate accuracy in the synchronisation task, we compared absolute deviation from target interval in the trained, order transfer, and timing

transfer conditions to the new sequence condition using three one-sided paired sample t-tests, in line with previous work (Kornysheva et al., 2013, 2019a; Kornysheva & Diedrichsen, 2014).

To investigate fMRI activity increases in motor related areas during preparation and production, we tested for increases above a baseline along our two cross-sections using a one-tailed non-parametric permutation test with a p-value threshold of .05 and 10,000 permutations (Maris & Oostenveld, 2007). This method was also used to assess Z-transformed decoding accuracy above chance in each of our three classifiers. Further, we ran one-sample t-tests against chance for each classifier within each ROI and trial phase (preparation and production), Bonferroni-corrected for six comparisons (3 classifiers x 2 trial phases). We also ran a repeated measures ANOVA with factors phase, classifier, and region to assess interaction effects, and ran post-hoc pairwise comparisons to investigate a significant interaction between phase and classifier. In addition, we investigated percent signal change and decoding accuracy across cortical hemispheres using whole-brain cluster-based analyses, Bonferroni corrected for two hemispheres (Table 2, Table 3). The significance value was set to p = 0.05 with exact p-values >= 0.001 and effect sizes for each test reported throughout. All statistical tests were performed with MATLAB (MathWorks) and IBM SPSS Statistics 25.0.

2.5 Results

2.5.1 Discrete sequence production from memory

Participants were trained to produce four finger-press sequences from memory with the right hand on a force transducer keyboard (Figure 2.2a). Training consisted of a three-staged transition across two days from trials which visually guided sequence production, towards trials which required sequence production entirely from memory (Figure 2.2b). During functional MRI scans taking place on the third day, participants were required to produce movement sequences from memory only (see Table 1 for trial distribution). Sequences were cued 1000-2500ms before the Go cue by a Sequence cue (abstract fractal image) to prompt the planning of the respective sequence without movement (Figure 2.2c). To isolate fMRI responses to movement planning without contamination from execution patterns, in

addition to ‘Go’ trials, ‘No-Go’ trials were implemented which consisted only of the Sequence cue but did not contain a Go cue (Figure 2.2d). ‘No-Go’ trials made up 20% of trials during training, and 50% of trials during the fMRI session (see Materials and Methods). Sequence planning during the preparation period in ‘Go’ and ‘No-Go’ trials was facilitated through trial-by-trial reward for fast initiation after the Go cue. Fast initiation and accurate sequence performance in ‘Go’ trials could result in up to double the points of ‘No-Go’ trials, in line with a previous study (Mantziara et al., 2021). Thus, to achieve fast and accurate performance and maximise the points, it was beneficial to plan the movement in advance of the Go cue. The target sequences were unique combinations of two finger orders consis’ing of five presses matched in finger press occurrence and two target relative inter-press-interval (IPI) orders involving four IPIs matched in target duration (Figure 2.2e). The finger orders were generated pseudo-randomly for each participant, but each sequence started with the same finger press within each participant to avoid first-finger identity driving the sequence decoding during the preparatory period (Yokoi et al., 2018). Timing 1 and Timing 2 were the same across participants.

The keyboard recorded isometric force trajectories from fingers of both the active right and the passive left hand concurrently during preparation and production (Figure 2.2f, Figure 2.2g). Points were awarded trial-by-trial only if participants did not exceed a force threshold above the baseline period during preparation and ‘No-Go’ trials. In ‘Go’ trials points were calculated based on initiation time after the Go cue, finger press accuracy, and timing accuracy. ‘No-Go’ trials were rewarded when no responses were made above threshold (see Methods). To ensure that participants were not pre-pressing the keys below the force threshold, we checked offline if exerted force of the right hand increased significantly above the42aselyne level. In ‘No-Go’ trials we checked for force increase from the Sequence cue onset to the last possible moment a Go cue could appear if it were a ‘Go’ trial, to represent the preparatory period. Participants did not increase force during ‘No-Go’ trials, and instead showed a small but force reduction (M = 0.154N, SD = 0.09) relative to baseline (M = 0.162 N, SD = 0.09; $t(23) = 3.39$, $p = .003$, $d = 0.69$). A similar small decrease, rather than an increase, was found in the preparation phase of ‘Go’ trials (M = 0.163 N, SD = 0.09) relative to baseline (M = 0.164 N, SD = 0.09; $t(23) = 2.44$, $p = .023$, $d = 0.50$), suggesting that this force decrease associated with planning was not specific to ‘No Go’ trials.

Importantly the data shows that participants did not engage in any subthreshold pre-pressing or rehearsal of the sequence during sequence preparation.

All participants that were included in the study following training produced two distinct timing structures across finger orders when performing the sequences from memory during the fMRI session as instructed, resulting in the expected interaction between sequence timing and interval position at the group level ($F(1.78,40.77) = 73.76$, $p < .001$, $\eta p^2 = .762$, Greenhouse-Geisser corrected, repeated measures ANOVA; Figure 2.3a). Since trained finger orders were different across participants (see Methods), we also assessed the main effects of order and timing and their interaction at the individual level. Here 18 out of the 24 participants showed a significant order by interval position interaction, and 10 showed a significant three-way interaction between timing, order, and interval position. The presence of these idiosyncratic press timing patterns at the individual level suggests the integration of sequence order and timing features. Crucially, sequence timing error showed no difference between timing structures suggesting that there were no systematic differences in difficulty for Timing 1 and Timing 2 at the group level ($F(1,23) = 0.07$, $p = .792$, $\eta p^2 = .003$; Figure 2.3b). At the individual level, 10 participants showed a significant main effect of order, 15 showed a significant main effect of timing, and four showed a significant interaction between order and timing, again suggesting an integration of the two sequence features.

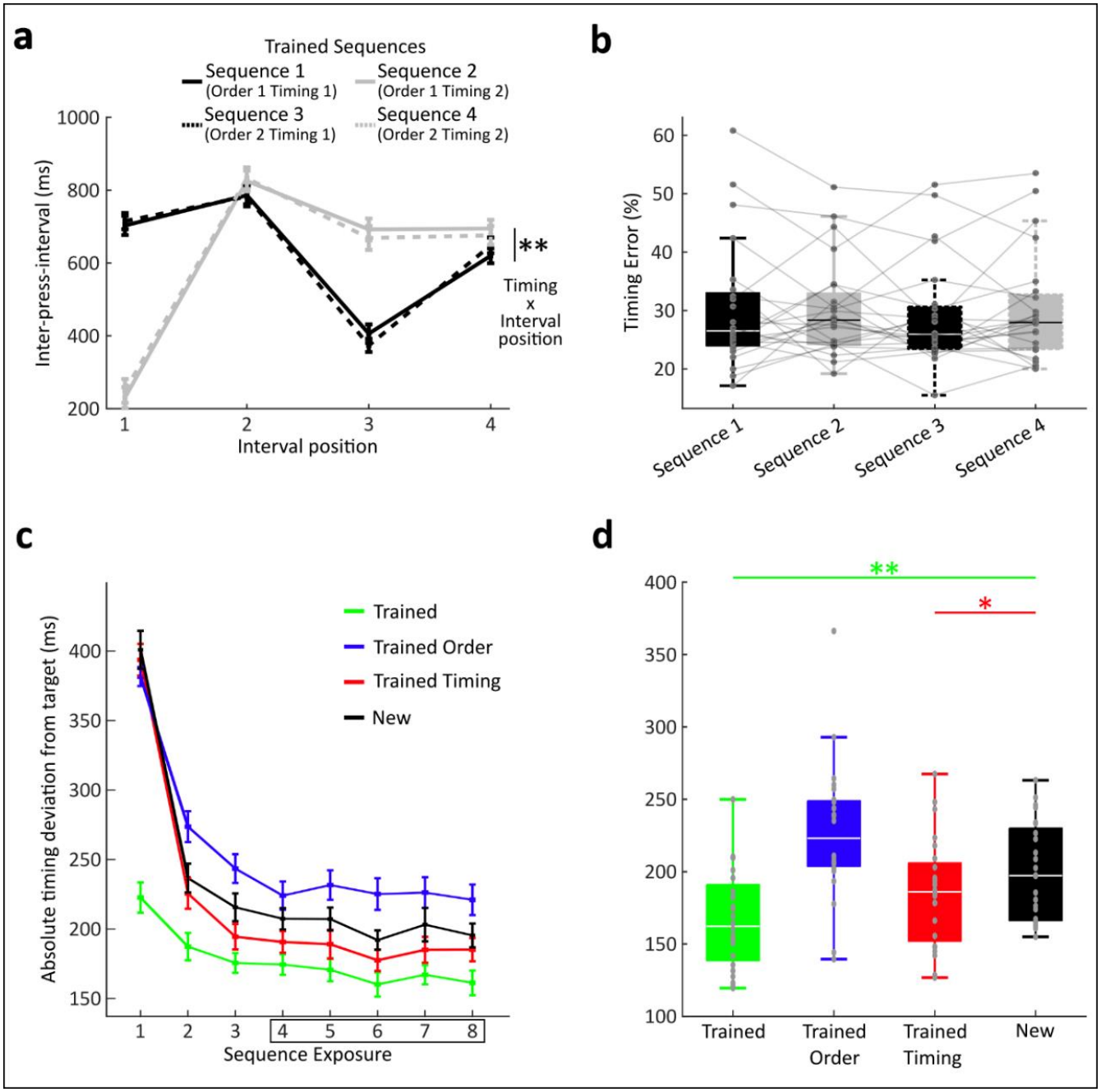

Figure 2.3. Sequence timing and feature transfer. **A**, IPI structure of the four trained sequences during the fMRI session (day 3). An interaction between sequence timing and interval position shows distinct IPI sequences between Timing 1 and Timing 2 across finger order sequences Order 1 and 2. $^{**}p < .01$; repeated measures ANOVA. **B**, Timing error (normalized to the target interval durations, see Materials and Methods) during the fMRI session did not differ between sequences. **c**, Behavioural transfer results from the synchronization task obtained from instructed Go cue trials following the last training stage on day 2. Absolute deviation from target timing is shown across sequence repetitions for trained sequences (green), sequences with trained finger orders, but unfamiliar timing (blue), sequences with trained timing, but unfamiliar order (red), and new sequences with both unfamiliar finger order and timing (black). **D**, Absolute deviation from target timing, as in a, extracted from the fourth to the last sequence repetition as in previous work (e.g., Kornysheva et al., 2019). Significance of t tests to identify performance benefits compared with new sequences is shown by coloured asterisks and horizontal lines. The trained order condition showed an increase in synchronization error (p =0.002, two-tailed t test), suggesting interference rather than benefits related to sequence feature transfer. $^{**}p < 0.01$; $^{*}p < 0.05$; one-sided t test. The boxplots indicate the median as a white

line with the box size delineating the 25th to 75th percentiles, respectively. Lower and upper whiskers correspond the minimum and maximum values, respectively. Outliers are drawn as points.

Learning new sequences is facilitated if the order or the timing of the sequence has been previously trained (Kornysheva et al., 2013, 2019a; Kornysheva & Diedrichsen, 2014; O'Reilly et al., 2008; Shin & Ivry, 2002; Ullén & Bengtsson, 2003). Behavioural transfer to new sequences can be taken as evidence for independent control of sequence order and timing, respectively. Accordingly, we set out to measure behavioural transfer following training. Participants completed a post-training test on Day 2 involving a synchronisation task which assessed how well participants could synchronise to a visually guided sequence. The trials in each condition were presented in a blocked manner with eight repetitions to assess short-term learning gains related to trained finger order and timing (Figure 2.3c) analogous to previous studies (Kornysheva et al., 2013, 2019a; Kornysheva & Diedrichsen, 2014). Since the transfer of trained sequence timing to a new finger order only takes place after three exposures, synchronisation performance was only assessed from the fourth sequence exposure onwards consistent with previously reported analyses (Kornysheva et al., 2013, 2019a; Kornysheva & Diedrichsen, 2014). We compared each condition (trained, order transfer, timing transfer) to new sequences (M = 196.15ms, SD = 34.00) in a one-tailed paired sample t-test. As expected, trained sequences (M = 160.43ms, SD = 33.09) showed a performance advantage ($t(23) = 6.34$, $p > .001$, $d = 1.29$), and so did sequences with trained timing and a new order (M = 182.10, SD = 39.72; $t(23) = 2.09$, $p = .024$, $d = 0.43$), replicating previous findings (Kornysheva et al., 2013, 2019a; Kornysheva & Diedrichsen, 2014) (Figure 2.3d). In contrast to earlier reports, order transfer sequences (M = 223.87, SD = 48.30) showed a worse performance relative to a new sequence ($t(23) = 3.52$, $p = .002$, $d = 0.72$, two-tailed test). Whilst knowledge of both features of a sequence combined, or just its timing, facilitated task performance, knowledge of sequence order hindered future learning of novel sequence acquisition when paired with a new timing structure. This implies that the participants in our study acquired a stronger independent representation of timing than of finger order which was closely integrated with a particular timing structure during production.

2.5.2 Activity increases during preparation and production

Relative increases or decreases in the blood-oxygen level-dependent activity (BOLD) can be dissociated from the presence of informational content in an area, especially as efficiency increases and effort decreases with motor training (Berlot et al., 2020; Wiestler & Diedrichsen, 2013). Movement planning sometimes involves a decrease or no change relative to baseline in motor-related cortical areas whilst information about the upcoming action is still present in these regions (Ariani et al., 2022; Gale et al., 2021). However, planning can also involve increases in BOLD activity in premotor to parietal areas (Ariani et al., 2015; Gallivan et al., 2011; Nambu et al., 2015). To characterise the physiological response in a task that required rapid planning and production of finger sequences from long-term memory, the percent signal change during preparation and production relative to rest were calculated. Preparatory activity was solely sampled from No-Go trials for % signal change and multivariate pattern analyses to separate the BOLD activity related to sequence planning from production in a fast event-related design (see Methods). We then calculated the percent signal change across the cortex (Figure 2.4a) and extracted values along two cross-sections of the cortical surface on the contralateral (left) side to the motor effector (Kornysheva & Diedrichsen, 2014) (Figure 2.4b). These cross-sections extended from anterior to posterior and ventral to dorsal, across premotor to parietal and premotor to supplementary motor regions respectively, because our hypotheses (osf.io/g64hv) on the imaging results during sequence preparation and production were put forward for contralateral premotor, primary motor, and parietal regions, which we expected to be tuned to sequence information based on previous studies (Berlot et al., 2020; Kornysheva & Diedrichsen, 2014; Matsuzaka et al., 2007; Picard et al., 2013; Tanji & Shima, 1994; Wiestler et al., 2014; Wiestler & Diedrichsen, 2013; Wymbs et al., 2012; Yokoi et al., 2018). Whole-brain results are presented in the Supplementary Materials. We carried out one-tailed non-parametric permutation tests along these cross-sections to identify significant clusters where activity increased above baseline (Maris & Oostenveld, 2007). During preparation, a very small, but significant, activity increase was found within ventral premotor cortex (PMv) (p = .002), and a marginally significant increase within dorsal premotor cortex (PMd) (p = .050; Figure 2.4b), suggesting large variability across participants. During production, activity increases were found across the majority of contralateral motor-related regions, with one large cluster across PMd, M1, sensorimotor cortex (S1), anterior superior parietal cortex (SPCa), and posterior superior parietal cortex (SPCp) (p < .001), and another cluster which

spanned the cross-section from PMv to PMd ($p < .001$). The cross-section overlapping with anterior supplementary motor area (SMA) did not show a significant activity increase from rest during production. However, note that the section of the SMA directly posterior to the cross-section did show a significant activity increase (Table 2 for whole-brain contrast cluster analysis).

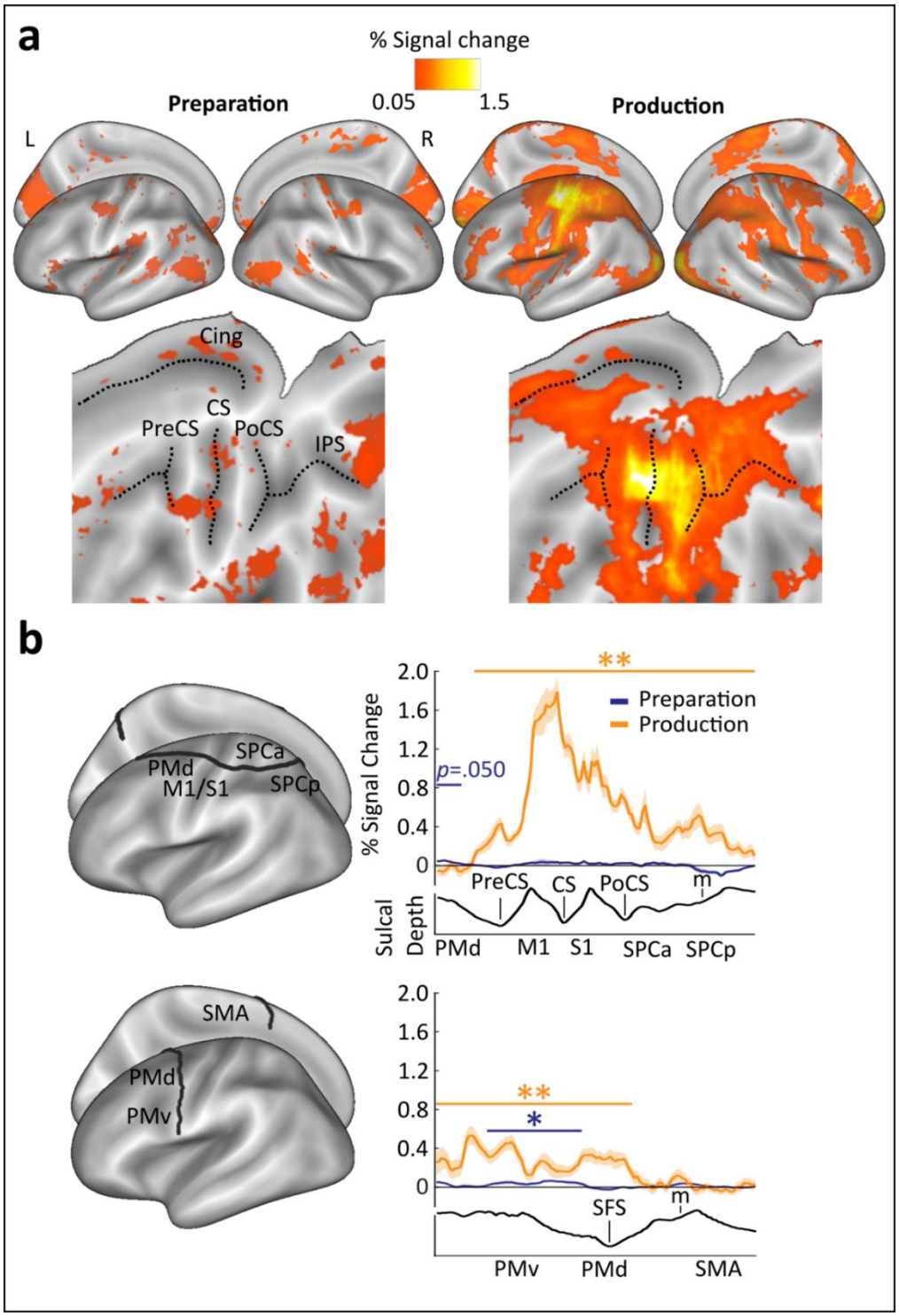

Figure 2.4. Percent signal change during preparation and production. **A**, Inflated surface maps are shown in top panels and flat maps in bottom panels, displaying mean % signal change during preparation (left panels)

and production relative to rest (right panels), respectively. For significant surface-based clusters across the cortex, see Table 2. **B**, Mean % signal change relative to rest for both preparation (blue lines) and production (orange lines), plotted on cross-sections running from rostral premotor cortex, through the hand area, to the occipito-parietal junction (top) and on a profile running from the ventral, through the PMd, to the SMA (BA6; bottom). Clusters with increases above baseline are denoted by the coloured horizontal lines and asterisks, calculated using one-tailed nonparametric permutation tests. Cing, Cingulate; CS, central sulcus; IPS, intraparietal sulcus; m, medial wall; OPJ, occipito-parietal junction; PoCS, postcentral sulcus; PreCS, precentral sulcus; SFS, superior frontal sulcus. **p > 0.01; *p > 0.05; one-sided t test. Shaded areas around the lines in b and c represent standard error of the sample mean.

Overall, no or small BOLD increases were observed across regions on the contralateral premotor-to-parietal axis during the short period of sequence planning. These results are in line with recent findings involving the motor planning of well-trained actions, e.g., common object manipulations like grasping and lifting, or tapping with the same finger (Ariani et al. 2022, Gale et al. 2021).

Table 2.2

Surface-based clusters with significant % signal change above rest

					MNI		
Contrast Versus Rest	Area (Brodmann Area)	Extent	*p* (cluster)	Peak *t*	X	Y	Z
Preparation	**Contralateral**						
	Extrastriate Vis Cortex (BA18)	4886.16	<.001	7.21	-12	-60	-5
	Pre-SMA (BA32)	2249.6	<.001	6.99	-11	14	50
	Primary Auditory Cortex (BA41)	940.58	<.001	7.84	-44	-29	11
	Posterior Cingulate (BA23)	733.45	<.001	6.86	-11	-38	31
	Anterior Insula (BA48)	706.11	<.001	6.55	-37	-12	3
	Occipitotemporal Area (BA37)	698.86	<.001	6.39	-38	-62	2
	Anterior Insula (BA48)	523.72	<.001	6.67	-46	18	11
	M1 (BA4)	483.3	<.001	6.86	-46	-10	44
	Inferior Parietal (BA39)	480.37	<.001	5.48	-50	-59	26
	Extrastriate Vis Cortex (BA18)	477.2	<.001	6.19	-20	-90	6
	S1 (BA2)	429.79	<.001	5.06	-18	-39	59
	Orbitofrontal (BA47)	373.43	<.001	6.82	-23	29	2
	Superior Parietal (BA7)	293.49	<.001	5.52	-21	-49	51
	Posterior Cingulate (BA23)	274.22	<.001	6.71	-13	-55	26
	Pre-SMA (BA32)	231.75	<.001	5.46	-9	46	6
	Middle Temporal (BA21)	179.26	<.001	6.06	-46	-37	-3
	Middle Temporal (BA21)	125.41	<.001	6.18	-54	-26	-7
	Inferior Parietal (BA39)	122.42	<.001	5.42	-50	-71	16
	Anterior Insula (BA48)	115.35	<.001	4.46	-28	31	29
	Extrastriate Vis Cortex (BA19)	98.81	<.001	5.38	-19	-53	3
	Wernicke's Area (BA22)	92.06	<.001	4.82	-53	-19	3
	Occipitotemporal Area (BA37)	86.6	<.001	4.75	-43	-41	-19
	Anterior Prefrontal (BA10)	54.95	0.007	4.49	-6	56	13
	Wernicke's Area (BA22)	53.73	0.008	4.5	-57	-37	3
	Anterior Insula (BA48)	53.07	0.009	4.35	-54	-1	11
	Posterior Cingulate (BA23)	51.92	0.01	6.21	-4	-26	38
	Anterior Insula (BA48)	51.89	0.01	5.99	-55	3	14
	Primary Auditory Cortex (BA42)	48.98	0.014	4.71	-57	-37	16

	Superior Parietal (BA5)	39.88	0.043	5	-12	-44	45
	Ipsilateral						
	Extrastriate Vis Cortex (BA18)	2605.25	<.001	7.71	14	-73	-8
	Extrastriate Vis Cortex (BA19)	1523.99	<.001	7.2	21	-83	16
	S1 (BA3)	1498.75	<.001	7.89	37	-26	37
	Superior Parietal (BA5)	1142.07	<.001	7.88	17	-53	47
	Occipitotemporal Area (BA37)	883.28	<.001	7.65	46	-63	-1
	Ventral Temporal (BA20)	671.28	<.001	6.27	49	-37	14
	Superior Parietal (BA40)	336.82	<.001	5.56	34	-52	49
	Anterior Cingulate (BA24)	282.58	<.001	5.86	6	31	12
	Extrastriate Vis Cortex (BA18)	274.65	<.001	4.87	23	-87	3
	Anterior Insula (BA48)	268.99	<.001	6.19	41	-24	20
	Superior Parietal (BA40)	245.49	<.001	5.49	31	36	35
	Anterior Insula (BA48)	159.52	<.001	6.36	55	-8	13
	Pre-SMA (BA32)	145.62	<.001	5.05	10	54	22
	Middle Temporal (BA21)	122.81	<.001	4.83	53	-50	3
	Pre-SMA (BA32)	106.49	<.001	5.86	5	44	7
	Anterior Cingulate (BA24)	93.31	<.001	4.94	9	11	30
	Subgenual Area (BA25)	56.97	0.003	5.21	4	22	6
	Posterior Cingulate (BA23)	56.86	0.003	5.13	4	-12	34
	S1 (BA3)	48.96	0.008	5.22	54	-17	37
	Middle Temporal (BA21)	48.93	0.008	4.64	49	-34	-4
	Posterior Cingulate (BA23)	44.43	0.015	5.35	4	-30	32
	Pre-SMA (BA32)	43.95	0.016	4.43	6	48	27
	Dorsolateral Prefrontal (BA9)	40.09	0.026	4.57	12	34	46
	Ectosplenial Area (BA26)	36.16	0.045	4.43	6	-45	25
Production	**Contralateral**						
	Superior Parietal (BA40)	9012.24	<.001	13.05	-34	-34	38
	Extrastriate Vis Cortex (BA18)	1166.68	<.001	7.05	-30	-86	-12
	SMA (BA6)	741.62	<.001	9.5	-3	-16	59
	M1 (BA4)	717.53	<.001	8.91	-53	-1	30
	Extrastriate Vis Cortex (BA18)	701.31	<.001	6.37	-18	-71	-2
	Extrastriate Vis Cortex (BA18)	561.59	<.001	7.03	-20	-86	-21
	Anterior Insula (BA48)	400.9	<.001	6.84	-33	2	7
	Extrastriate Vis Cortex (BA18)	174.37	<.001	5.88	-15	-92	-12
	Posterior Cingulate (BA23)	103.37	<.001	5.43	-5	-5	38
	Anterior Insula (BA48)	86.36	<.001	7.69	-26	13	16
	Primary Auditory Cortex (BA41)	79.07	<.001	5.6	-48	-44	25
	Broca's Area (BA45)	77.51	<.001	5.8	-45	30	32
	Extrastriate Vis Cortex (BA18)	45.13	0.001	4.98	-37	-69	-16
	Ipsilateral						
	Anterior Insula (BA48)	2828.07	<.001	9.24	51	-42	34
	Extrastriate Vis Cortex (BA19)	2365.33	<.001	7.46	46	-73	-21
	Extrastriate Vis Cortex (BA18)	1295.15	<.001	6.91	9	-81	32
	M1 (BA4)	974.65	<.001	7.87	55	-4	35
	V1 (BA17)	542.45	<.001	5.52	9	-71	5
	SMA (Medial BA6)	513.52	<.001	8.01	4	-14	61
	PMd (Dorsal BA6)	285.07	<.001	7.48	29	-7	48
	Extrastriate Vis Cortex (BA18)	266.94	<.001	6.91	21	-89	-13
	M1 (BA4)	239.01	<.001	8.4	33	-21	56
	Posterior Cingulate (BA23)	159.35	<.001	6.4	8	-24	24
	Anterior Cingulate (BA24)	70.39	<.001	5.71	9	11	31
	Pars Opercularis (BA44)	62.97	<.001	5.49	48	19	33
	Pars Triangularis (BA45)	42.9	0.008	5.16	43	34	32
	Pars Triangularis (BA45)	39.1	0.014	4.87	38	40	18

Note. Results of surface-based random effects analysis (N = 24) with an uncorrected threshold of $t(23) > 3.48$, $p > 0.001$. *p* (cluster) is the cluster-wise *p* value for the cluster of that size. The *p* value is corrected over the cortical surface using the area of the cluster (Worsley et al., 1996) and Bonferroni-corrected for two hemispheres. The cluster coordinates reflect the location of the cluster peak in MNI space.

Table 2.3

Surface-based clusters with significant above-chance classification accuracy for the decoding of sequences and their constituent features (order and timing)

					MNI		
Classifier	Area (Brodmann Atlas)	Extent	*p* (cluster)	Peak *t*	X	Y	Z
Integrated Preparation							
Integrated Production	**Contralateral**						
	Superior Parietal (BA7)	606.08	<.001	7.27	-17	-63	56
	Superior Parietal (BA5)	183.08	<.001	6.6	-14	-47	46
	Extrastriate Vis Cortex (BA19)	62.85	0.008	4.67	-47	-66	-19
	S1 (BA2)	46.26	0.05	4.34	-28	-44	58
	Ipsilateral						
	Inferior Parietal (BA39)	69.53	0.004	5.81	51	-54	29
	Superior Parietal (BA7)	63.4	0.008	5.01	16	-65	49
Order Preparation	**Contralateral**						
	Extrastriate Vis Cortex (BA18)	61.68	0.012	4.33	-23	-73	-18
	Extrastriate Vis Cortex (BA18)	56.03	0.022	5.04	-23	-82	-13
	Ipsilateral						
	Extrastriate Vis Cortex (BA18)	199.36	<.001	5.56	9	-80	30
	Extrastriate Vis Cortex (BA19)	80.09	0.004	4.9	21	-62	-5
Order Production	**Contralateral**						
	Extrastriate Vis Cortex (BA18)	118.04	<.001	6.51	-24	-94	-10
Timing Preparation	**Ipsilateral**						
	Extrastriate Vis Cortex (BA18)	58.41	0.026	4.69	19	-81	-22
Timing Production	**Contralateral**						
	SMA (BA6)	130.73	<.001	5.13	-3	3	53
	Broca's Area (BA44)	128.93	<.001	4.94	-49	9	13
	S1 (BA3)	114.82	<.001	5.78	-50	-14	39
	Superior Parietal (BA40)	76.95	0.01	5.57	-40	-45	36
	Extrastriate Vis Cortex (BA19)	59.21	0.044	4.36	-35	-81	16
	Inferior Parietal (BA39)	57.46	0.05	4.25	-35	-57	28
	Ipsilateral						
	M1 (BA4)	199.04	<.001	6.08	52	-11	40
	PMv (Ventral BA6)	164.2	<.001	6.26	55	7	23
	Inferior Parietal (BA39)	155.11	<.001	5.76	39	-48	27
	Pars Opercularis (BA44)	151.26	<.001	5.42	41	22	35
	Inferior Parietal (BA39)	93.54	0.002	5.14	35	-60	28
	Pars Triangularis (BA45)	59.82	0.034	4.21	43	27	17

Note. Table of significant surface-based clusters across the cortex (as in Table 2) for the order, timing, and integrated classifiers.

2.5.3 Multi-variate pattern analysis (MVPA)

We used MVPA to identify cortical areas that showed systematic changes in BOLD activity patterns between sequences with different finger orders, temporal structures, and unique

combinations of the latter. Using a whole brain searchlight of 160 voxels (Oosterhof et al., 2011), we trained a linear discriminant analysis (LDA) classifier to distinguish between sequences in a one-run-out cross-validation method – an approach that has been validated with pattern simulations in a previous study (Kornysheva & Diedrichsen, 2014). Specifically, we looked for regional activity patterns that either transferred across or were unique for specific combinations of order and timing. The order classifier was used to decode between sequences with different finger orders, regardless of their pairing with a timing feature, whereas the timing classifier was trained to decode between sequences with different finger timings regardless of their pairing with a specific finger order. These two classifiers allowed the identification of regions which contained above chance decoding of sequence order and timing independently of the other sequence feature, respectively (Figure 2.5a). The integrated classifier decoded residual patterns after subtracting averaged sequence order and timing related patterns for each run separately, in order to detect regions which hold information on sequence identity that is not driven by a simple summation of order and timing information (see Methods).

To reveal the continuous profile of feature decoding along contralateral motor regions on the cortical surface, we employed the same permutation test approach (Maris & Oostenveld, 2007) as in the % signal change analysis for each of the three classifiers, for preparation and production, separately (Figure 2.5b). During preparation, a significant cluster was found for finger order within SPCp (p = .040, d = 0.60), and a marginally significant cluster for timing decoding was identified within PMv (p = .054, d = 0.62). During production, above chance decoding was shown for the integrated classifier within PMd in two clusters (p = .002, d = 0.81; p = .044, d = 0.63; on anterior to posterior and ventral to dorsal cross-sections, respectively) and S1, which extended into M1 and SPCa (p = .007, d = 0.79). Above chance decoding of timing was found within SPCa (p = 0.016, d = 0.70), PMv (p < .001, d = 0.79), and SMA (p = .045, d = 0.53).

Next, we examined how well sequence features could be decoded from ROIs during preparation and production. These regions covered premotor to superior parietal areas: PMd, PMv, M1, S1, SMA/pre-SMA, SPCa, and SPCp. First, to identify above chance decoding of sequence information in these areas, one-sample t-tests were performed on the z-values extracted from each of the pre-defined ROIs during both preparation and production for

timing, order, and integrated classifiers (Figure 2.5c). These t-tests were Bonferroni corrected six times, to account for phase (2) by classifier (3) within each pre-defined ROI. During preparation, the above chance was found in SPCp for sequence order decoding ($t(23) = 2.74$, $p = .036$, $d = 0.56$), with marginally significant, but equal sized above chance accuracy in SPCp for sequence timing ($t(23) = 2.51$, $p = .060$, $d = 0.51$, Bonferroni-corrected). During production, classification increased above chance for sequence timing in SMA/pre-SMA ($t(23) = 2.71$, $p = .036$, $d = 0.56$, Bonferroni-corrected), PMv ($t(23) = 3.00$, $p = .018$, $d = 0.61$, Bonferroni-corrected), and SPCa ($t(23) = 2.67$, $p = .042$, $d = 0.55$, Bonferroni-corrected). Further, classification increased above chance for order-timing integration in S1 ($t(23) = 3.69$, $p = .003$, $d = 0.75$, Bonferroni-corrected), PMd ($t(23) = 3.06$, $p = .018$, $d = 0.63$, Bonferroni-corrected), SPCa ($t(23) = 4.36$, $p < .001$, $d = 0.89$, Bonferroni-corrected), and SPCp ($t(23) = 3.20$, $p = .012$, $d = 0.65$, Bonferroni-corrected).

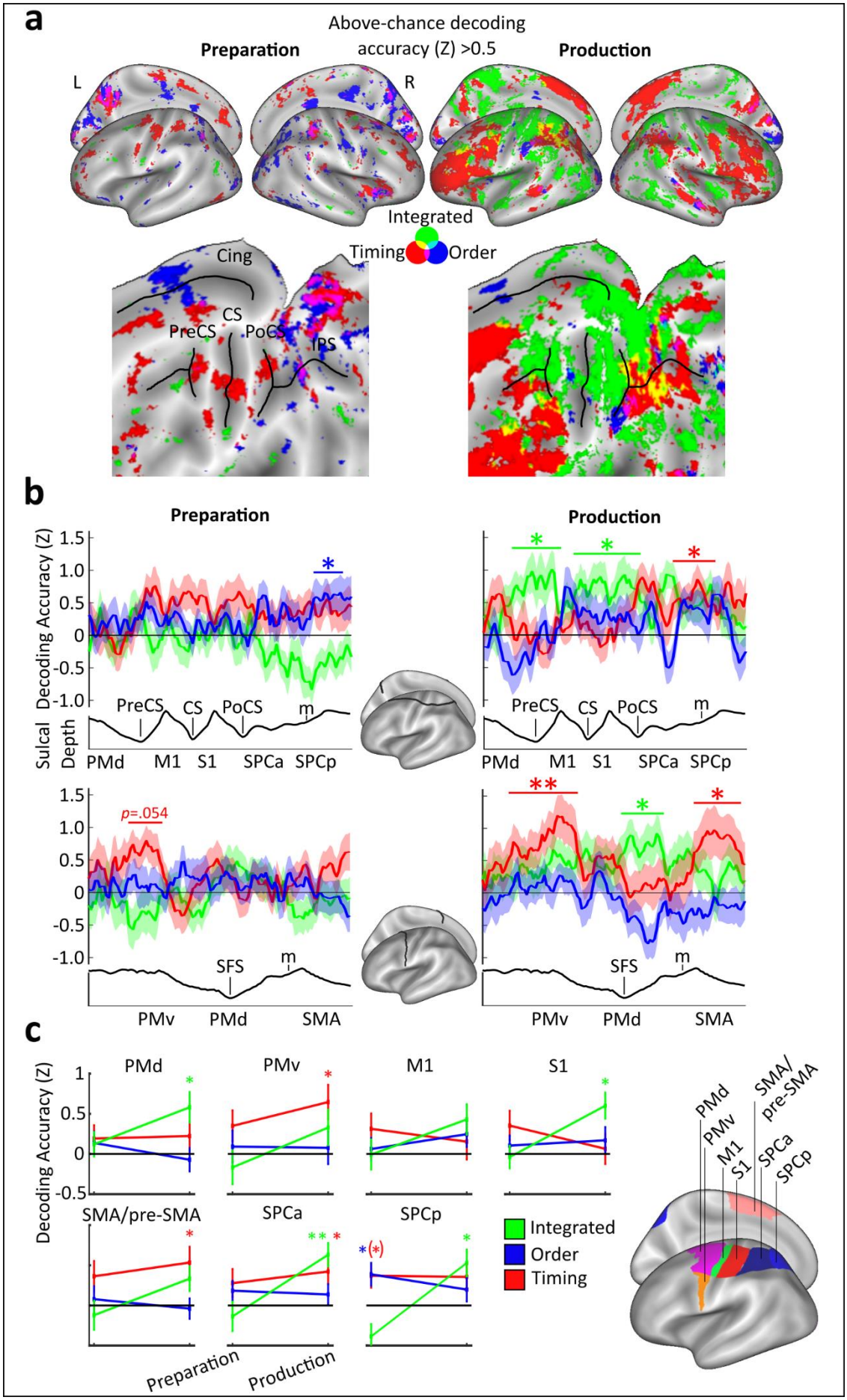

Figure 2.5. Multivariate pattern classification results. **A**, Inflated surface (top panels) and flat maps (bottom

panels), showing mean decoding z-accuracy values above chance for finger order (blue), timing (red), and integrated sequence patterns (green) (Kornysheva & Diedrichsen, 2014). For the corresponding significant surface-based clusters across the cortex, see Table 3. **B**, Mean decoding z-accuracy values for each classifier along the cross-sections explained in Figure 2.4b. Coloured asterisks indicate the respective above-chance clusters for each classifier during preparation and production. **C**, Searchlight z-accuracy values were extracted using predetermined ROIs (Wiestler and Diedrichsen, 2013; Kornysheva and Diedrichsen, 2014; Yokoi et al., 2018) shown in the left panel. Coloured asterisks indicate decoding above chance. (*) p=0.060; **p > 0.01; *p > 0.05; one-sided t test above chance (Bonferroni-corrected for six comparisons within each ROI).

ROI analyses were only performed in the hemisphere contralateral to the movement in line with our hypotheses. For explorative purposes, we also carried out searchlight analyses across the whole cortex including the ipsilateral surface, which were cluster- and Bonferroni-corrected for two hemispheres (Table 3). On the ipsilateral side, significant clusters during preparation were only found for order in the extrastriate visual cortex (p < .001, p = .004). During production, significant clusters were found for timing in M1 (p < .001), PMv (p < .001), inferior parietal (p > .001), and three clusters in lateral prefrontal (p > .001, p = .002, & p = .034) regions, with significant clusters for integration in inferior (p = .004) and superior parietal regions (p = .008). These findings suggest a general shift towards integration across phase across the cortex, with several regions also representing timing during production.

Finally, we set out to test our main hypotheses (Figure 2.1, osf.io/g64hv) regarding an interaction between peri-movement phase (preparation, production), classifier (timing, order, integrated) and region (PMd, PMv, M1, S1, SMA/pre-SMA, SPCa, SPCp). A repeated-measures ANOVA revealed a main effect of phase ($F($1,23) = 9.49, p = .005, ηp^2 = .292), substantiating a general increase of decoding accuracy across regions and classifiers during production. The main effect of region was not significant (F(3.84,88.42) = 0.45, p = .763, ηp^2 = .019, Greenhouse-Geisser corrected), suggesting that all the contralateral cortical ROIs had a comparable contribution to sequence decoding across trial phases. Importantly, we found a phase by classifier interaction (F(2,46) = 10.34, p = .044, ηp^2 = .127), which was driven by an overall increase in the integrated classifier accuracy from preparation (M = -0.10, SE = 0.13) to production (M = 0.49, SE = 0.11) (p = .003, *95% CI* [.217, .971], Bonferroni corrected). Finally, we found no interaction of phase by region (F(3.20,73.50) = 0.79, p = .512, ηp^2 = .033, Greenhouse-Geisser corrected), or phase by classifier by region (F(5.40,124.18) = 1.63, p = .151, ηp^2 = .066, Greenhouse-Geisser corrected). In sum, this supports the hypothesis that tuning of these regions to high and low-level features of

sequences changes dynamically depending on trial phase, rather than region, with a state shift towards sequence feature integration after movement initiation across multiple regions.

2.6 Discussion

Activity along the cortical premotor to parietal axis has been associated with motor sequence control, from its hierarchical organisation (Gerloff et al., 1997; Kennerley et al., 2004; Russo et al., 2020; Sakai et al., 2003; Wiestler et al., 2014; Yokoi & Diedrichsen, 2019a; Zimnik & Churchland, 2021a) to sequence order and timing (Crowe et al., 2014; Kornysheva & Diedrichsen, 2014; Merchant, Pérez, et al., 2013; Ramnani & Passingham, 2001; Shima & Tanji, 1998a; Wiestler et al., 2014). Yet how sequence-related computations in these regions unfold across planning and execution remains uncertain. Do these cortical areas retain a fixed tuning to sequence features and their integration throughout planning and execution? Or do they switch their content dynamically from before to after movement initiation? Here, we examined how motor cortical areas integrate informational content on the order of finger movement sequences and their timing across the planning and execution phases. Sequence decoding from activity patterns revealed that high-level features of sequence organisation remain separate during movement planning and are integrated into unique patterns upon movement initiation in premotor and parietal areas.

2.6.1 Cortical patterns switch their tuning from planning to execution

Our results demonstrate a generalised dependency of cortical representations on peri-movement phase, with a global shift across regions towards order and timing integration at the transition from sequence planning to execution. This indicates that most cortical motor-related areas do not rigidly map onto higher- versus lower-level representations of sequential organisation, as assumed by earlier studies that focussed on sequence execution alone (Diedrichsen et al., 2013; Kornysheva & Diedrichsen, 2014; Yokoi & Diedrichsen, 2019a). Instead, pattern activity tuning in these regions changes dynamically upon motor initiation (Figure 6). Such a state switch in motor-related patterns echoes previous findings for the primary motor and dorsal premotor cortices in the context of single movements. These show that preparatory neural population activity occupies a different state space

("output-null") from production to prevent readout from downstream areas during planning (Kaufman et al., 2014; O'Shea & Shenoy, 2016; Zimnik & Churchland, 2021a). Here, cortical motor planning patterns are not simply subthreshold versions of execution activity patterns controlled by inhibitory gating within the cortex or downstream (Cisek & Kalaska, 2005; Duque & Ivry, 2009b), but a qualitatively different neural activity pattern. Our results support the notion of a largely distinct functional tuning during motor planning across regions on the premotor to parietal axis in the context of sequential movements.

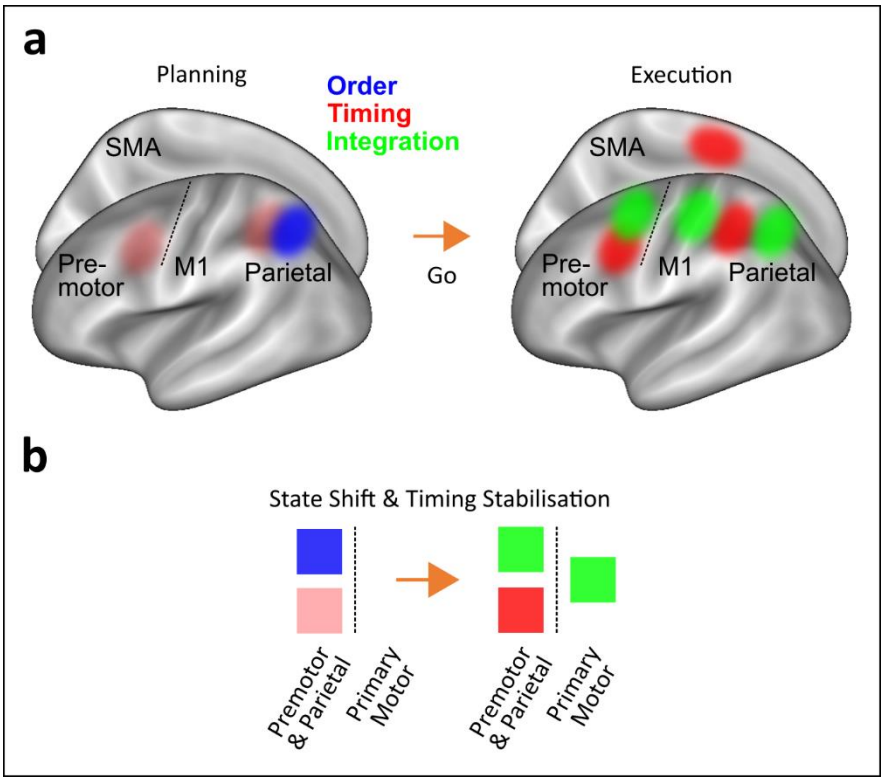

Figure 2.6. Schematic representation of sequence feature control during planning and integration across regions on the premotor-to-parietal axis contralateral to the movement. **a,** Inflated cortical surface showing a schematic summary of the fMRI pattern decoding results. **b**, These findings suggest that there is a shift within regions from planning to execution driven by the emergence of patterns related to the integration of sequence order and timing (Dynamic mapping: State shift). This is accompanied by pattern stabilisation and increase within medial and lateral premotor and parietal areas related to timing (Fixed mapping: Higher-level stabilisation). Notably evidence for the control of movement order independently of its lower-level integration with timing is restricted to the planning phase only. Semi-transparent clusters of timing-related pattern decoding above chance reflect Bonferroni corrected p-values between 0.05 and 0.06 during planning.

2.6.2 Lack of sequence feature integration prior to motor initiation

As participants trained to perform the four finger sequences over two days and entirely from memory, one may expect that this level of practice would result in their retrieval as one integrated spatio-temporal synergy (Gentner et al., 2010). However, we found that information about motor sequence order and timing of the upcoming sequence was parsed

trial-by-trial and integrated after motor initiation only. One possibility is that the two-by-two task design may encourage participants to hold onto higher level representations of movement order and timing. However, in previous tasks where only one combination of order and timing was trained, transfer of known order and timing to new combinations was still found, showing that the separation is not dependent on the task structure, but arises automatically (Kornysheva et al., 2013; Ullén & Bengtsson, 2003).

Although previous work has shown that planning-related activity in motor areas is predictive of movement features such as speed, force, and trajectory of the upcoming movement (Pearce & Moran, 2012; Wong et al., 2016; Yang et al., 2015), these may be regarded as part of planning a holistic motor synergy (D'Avella et al., 2003; Overduin et al., 2015; Shenoy et al., 2013). In contrast, for discrete sequence learning there is now ample evidence that higher-level sequence features such as movement order and timing are encoded independently (Bengtsson et al., 2004; Kornysheva & Diedrichsen, 2014; Ullén & Bengtsson, 2003; Zeid & Bullock, 2019) and remain so separate during planning (Kornysheva et al., 2019a; Mantziara et al., 2021), despite training across multiple days and entirely memory-guided production. Specifically, sequence planning is dominated by higher-level control of motor sequences without precise implementation parameters, e.g. movement order without speed or timing information (Mantziara et al., 2021), and ordinal position without effector information (Kornysheva et al., 2019a). Further, the neural generation of sequence elements with a discrete timing goal (instructed delay or rapid succession) shows no fusion in M1, despite long-term training and fusion at the muscular level (Zimnik & Churchland, 2021a). Yet, when and how integrated control is engaged during planning of more continuous overlapping movement sequences is uncertain. Rather than engaging a dedicated timing system as is observed with discrete movements here and in previous work (Bengtsson et al., 2004; Kornysheva & Diedrichsen, 2014; Medina et al., 2005; Ullén & Bengtsson, 2003), continuously overlapping movements have been shown to employ a state-dependent control system which integrates sensorimotor states of effectors (Diedrichsen et al., 2007; R. B. Ivry & Schlerf, 2008; R. B. Ivry & Spencer, 2004; Kornysheva, 2016) . Thus, we predict that integrated control for continuous sequences would occur throughout planning and execution, unlike for discrete motor sequences.

What triggers sequence feature integration trial-by-trial? We propose that contralateral motor-related cortical regions activate movement order and timing plans separately until a sensory stimulus like the Go cue triggers the binding of the corresponding neural patterns. This binding may occur through subcortical, e.g. thalamic input triggering an appropriate state for motor execution of specific combination of features (Inagaki et al., 2022; Wang et al., 2018). Delaying the binding of sequence features to the production phase and maintaining higher-level separation may allow the system to retain maximum flexibility trial-by-trial, should task demands change.

2.6.3 Independent patterns for sequence timing but not finger order are reinstated during execution

We found a stark asymmetry between sequence order and timing during the sequence production phase. In contrast to the independent patterns for finger order, the activity patterns tuned to sequence timing increased (PMv) or emerged (SMA/pre-SMA, SPCa) during production. Thus, cortical patterns for sequence timing accompanied the emergence of sequence-specific integrated patterns, unlike patterns related to sequence order which were restricted to the planning phase. This asymmetry was also observed at the behavioural level in the transfer task. Here, trained timing could be quickly recombined with a new order in line with previous work (Kornysheva et al., 2013, 2019a; Kornysheva & Diedrichsen, 2014; Ullén & Bengtsson, 2003). In contrast, producing the same finger order with a new timing was associated with poorer performance, unlike a previous study involving a delayed sequence production from memory (Kornysheva et al., 2019a). This interference effect suggests that participants were unable to separate the trained order from their timing during execution, which directly parallels the prominence of integrated and the lack of independent finger order tuning during motor production.

2.6.4 M1 lacks information about sequences despite a large activity increase during execution

Our results show a lack of sequence feature separation or integration in contralateral M1 during preparation and only limited evidence for integration above chance during production extending out from the greater peak in S1. This occurs despite a large activity increase in M1 during production. While this contrasts with several older neuroimaging

studies (Kornysheva & Diedrichsen, 2014; Nambu et al., 2015; Wiestler & Diedrichsen, 2013; Wymbs & Grafton, 2015), recent findings show that information held within M1 is not related to sequence control. Activity patterns in M1 do not change with sequence learning (Berlot et al., 2020, 2021a) and reflect the processing of individual movements, particularly, the first press of a sequence (Yokoi et al., 2018; Yokoi & Diedrichsen, 2019a). Further, there has been no experimental evidence that sequential movements are neurally fused in M1 into holistic sequence representations: Constituent movements remain individuated in M1 regardless of sequential context (Russo et al., 2020; Zimnik & Churchland, 2021a). Thus, matching the first finger press across trained sequences in each participant may explain why we see no prominent sequence feature decoding from M1 in contrast to a previous study on sequence timing and order (Kornysheva & Diedrichsen, 2014).

2.6.5 Extending the motor planning framework to sequential actions

The framework for single movement motor planning proposes that the motor system enters a preparatory state that is distinct from movement execution (Churchland et al., 2010; Kaufman et al., 2014; Shenoy et al., 2013). Recent findings also suggest a distinction between the selection of motor goals and motor implementation planning, which formulate 'what' movements to execute and 'how' to execute them, respectively (Haith & Bestmann, 2020; Wong et al., 2015), converging with the idea of hierarchical motor sequence control (Diedrichsen & Kornysheva, 2015a; Yokoi & Diedrichsen, 2019a). Here, we propose that sequence order and timing features are specified during planning as 'what' elements representing higher-level control, and integrated during execution as 'how' elements, representing lower-level implementation. Crucially, our results suggest that individual regions can undergo a state shift from 'what' to 'how' control depending on the peri-movement phase. Future electrophysiological research should address whether the same neuronal populations are involved in both types of control within areas, and determine the neural origin and exact time point that triggers the informational state shift.

Chapter 3 - Hippocampus Retrieves the Order of Skilled Typing Sequences During Movement Planning

This chapter is in preparation as:

Yewbrey, R., & Kornysheva, K. (2024). Hippocampus retrieves the order of skilled typing sequences during movement planning. [In Prep]

Author contributions: R.Y. and K.K. designed research; R.Y. and K.K. performed research; R.Y. and K.K. analysed data; R.Y. and K.K. wrote the first draft of the paper; R.Y. and K.K. edited the paper; R.Y. and K.K. wrote the paper.

3.1 Abstract

It is widely accepted that plasticity in the subcortical motor basal ganglia-thalamo-cerebellar network plays a significant role in the learning and control of long-term memory for new procedural skills, such as the formation of the learnt population trajectories in the striatum and the adaptive sensorimotor mapping in the cerebellum. However, recent findings reported the involvement of a wider cortical and subcortical brain network in the consolidation and control of skilled actions, including an area traditionally associated with declarative memory – the hippocampus. Here, we probe how different levels of the motor hierarchy – high-level features during planning and their integration during sequence execution are activated in subcortical areas with and without direct mapping to motor output centres. An fMRI dataset (N=24) collected after participants learnt to produce four typing sequences entirely from memory over several days was examined for the overall BOLD signal change and informational content in subcortical regions-of-interest during planning and execution. Although there was a widespread activity increase in striatal, thalamic, and cerebellar motor regions in the perimovement phase, the associated activity did not contain information on the motor sequence identity or its constituent features. In contrast, hippocampal activity increased during planning and was predictive of the order of the upcoming sequence of movements. Our findings show that the hippocampus is involved in movement sequence planning, specifically the retrieval of serial order from memory in a task that involves retrieving different sequences of movements trial-to-trial, similar to skilled human actions such as typing or handwriting. These findings question traditional classifications of motor memory and carry potential implications for the rehabilitation of individuals with relevant neurodegenerative disorders.

3.2 Introduction

Motor skill acquisition involves cortico-striato-cerebellar circuits linked via interlocking loops in the thalamus (Bostan & Strick, 2018). As motor skills are learnt, the dominant assumption is that there is a transition from associative to motor reference frames (Dayan & Cohen, 2011; Hikosaka et al., 2002b; Verwey, 2023b), accompanied by a shift in skill encoding to cortical and subcortical areas with direct or indirect projections to brainstem and spinal control centres, particularly the putamen and Lobules V and VI of the cerebellum (Thompson & Kim, 1996). This is thought to underlie the formation of a motor "repertoire" and the procedural control of fine-grained kinematics and sensorimotor maps (Diedrichsen & Kornysheva, 2015b).

However, neurophysiology and neuroimaging of skilled sequence learning and control in humans and animal models demonstrated that activity in motor cortical regions is not tuned to whole sequences of movements, but to individual movement elements of a skilled sequence (Shima & Tanji, 2000; Yokoi & Diedrichsen, 2019b; Zimnik & Churchland, 2021b). Moreover, the network of areas involved in the later stages of learning continues to extend beyond core motor cortical and subcortical hubs. This applied to skills after prolonged training over weeks or months (Averbeck et al., 2003; Berlot et al., 2020, 2021b; Mushiake et al., 2006; Shima & Tanji, 1998b) or sequence production from memory without external guidance (Yewbrey et al., 2023). The associated patterns of activity have been linked to higher-order control of skilled motor sequences such as their serial order and timing (Kornysheva & Diedrichsen, 2014), as well as the transfer of movement components of a sequence to new sequences to enable flexibility, characteristic of skilled motor control in humans. Furthermore, there is growing evidence that the hippocampus, traditionally associated with declarative memory formation, and for a long-time neglected in motor control of skilled actions, contributes to the consolidation of procedural sequential skills (Albouy et al., 2008, 2008, 2013; Buch et al., 2021; Lungu et al., 2014).

Whilst the cortical control of sequential skills has been characterised in detail functionally over the last three decades, the complementary contribution of striatal, cerebellar, and hippocampal areas to skilled motor sequence control remains debated. In particular, it is unclear whether these are functionally in higher-level organisation versus lower-level implementation of skilled movement sequences during the peri-movement phase, i.e.

during planning or execution. Outcomes are directly relevant to the development of interventions to rehabilitate skilled motor control in individuals suffering from neurological and neurodegenerative disorders (Parkinson's Disease, Cerebellar Ataxia and Alzheimer's Disease) affecting the respective brain regions disproportionately.

The functional role of the basal ganglia (BG) during motor learning has historically been attributed to action selection, by activating target movement plans and inhibiting competing movements (Frank, 2011; Gurney et al., 2001; Mink, 1996; Redgrave et al., 1999). During sequential movement learning in particular, the dorsolateral striatum (equivalent to the putamen in humans) of the BG has been shown to concatenate movement chunks (Friend & Kravitz, 2014; Graybiel, 1998; Wymbs et al., 2012) and is sensitive to the temporal and ordinal structure of sequences (Bednark et al., 2015). Moreover, multi-unit recordings in the dorsomedial striatum (analogous to the caudate nucleus in humans) show ramping activity which scales across the temporal length of inter-movement intervals (Emmons et al., 2017; Wang et al., 2018), showing a sensitivity to the temporal structure of sequential movements. These findings suggest that BG are responsible for the specification of high-level movement sequences features.

In contrast, more recent findings suggest that the ventrolateral striatum in BG is a low level controller of learnt sequences of movements, reflecting movement kinematics of an overtrained skill (Dhawale et al., 2021; Harpaz et al., 2022). Recent supporting evidence in rodents has shown that low-level kinematics, but not high-level sequential structure (i.e. movement order), are disrupted when the dorsolateral striatum is perturbed using optogenetics (Mizes et al., 2023a), with intact movement kinematics can be generated by the BG being preserved in the case of cortical lesions (Kawai et al., 2015). While a considerable amount of evidence in this debate comes from non-human animals, there is human neuroimaging evidence for distinguishable movement sequence activity patterns in the BG using multivariate distance measures (Berlot et al., 2020). However, whether these patterns are related to high-level action selection, or low-level kinematics, requires further investigation.

The thalamus is often thought to solely relay sensory input, particularly vision (Adams et al., 2002; Sherman, 2007). Recently, however, the function of the motor thalamus (ventral lateral nucleus) has been broadened from a sensory relay (Bosch-Bouju et al., 2013) to a

region that actively modulates cortical activity, encourages interregional coupling, and focuses cortical activity (Shine et al., 2023), with modulatory action also extending to the BG, and CB (Shine, 2021). This action is present during movement planning and works alongside the cortex to maintain preparatory activity (Guo et al., 2017). Moreover, during the execution period, the motor thalamus relays a signal from the pons to the cortex to initiate movement, causing the neural dynamics of the motor cortex to reorganise (Inagaki et al., 2022). However, whether these preparatory and execution-related roles of the thalamus consist of high- or low-level movement sequence information is unclear.

The cerebellum (CB) has long been associated with sensorimotor prediction and adaptation for online motor control, evidenced best by cerebellar ataxia (Diener & Dichgans, 1992; Miall et al., 2007) and eye blink conditioning (Christian & Thompson, 2003). However, more recent findings have suggested that the CB is also involved in movement planning, driving the cortex through different states of preparatory activity (Chabrol et al., 2019; Li & Mrsic-Flogel, 2020). Indeed, when the CB of mice is perturbed during planning, they made fewer correct directional licks (Gao et al., 2018). However, this seemed to impact subsequent movement direction whilst kinematics remained stable. Despite the CB's established history of kinematic definition during execution, it is not clear whether planning in the CB represents higher-level movement features or movement kinematics.

Whilst the basal ganglia and cerebellum have been the main subcortical focus of research in skill acquisition and sensorimotor learning, the hippocampus has long been overlooked, in line with the landmark studies of procedural memory in amnesic patients with medial temporal lobe damage (Brooks & Baddeley, 1976; Cohen & Squire, 1980). However, there is increasing evidence that the original taxonomy is not straightforward for skill acquisition and control in the real-world with both procedural and declarative memory playing a part in sensorimotor adaptation and skill learning. In particular there is increasing evidence that the hippocampus is involved in sequence learning and consolidation during movement sequence learning (Albouy et al., 2008, 2013; Buch et al., 2021; Doyon et al., 2009; Lungu et al., 2014). Recent findings suggest that the hippocampus defines movement order, by developing effector-independent representations of movement sequences during learning (Albouy et al., 2015). Evidence from magnetoencephalography (MEG) also suggests the medial temporal lobe plans an abstract template for the parallel preordering of actions

during sequence planning (Buch et al., 2021; Kornysheva et al., 2019b) and replaying sequences during short rest periods interspersed with practise. However, the exact localisation of this neural activity to the medial temporal lobe using MEG is debatable, and higher spatial resolution of fMRI is required to substantiate these findings.

Here, we set out to tease apart the roles of subcortical areas associated with motor skill learning and control – basal ganglia, thalamus, cerebellum, and hippocampus – in movement sequence planning and execution from memory. Using multivariate pattern analysis of fMRI data we investigated the activity patterns related to higher-level sequence feature selection and lower level sequence-specific implementation in the peri-movement phase during which participants produced movement sequences with a particular order and timing structures from memory (Yewbrey et al., 2023). We found that that the hippocampus plays a role in 65orting movement sequences, particularly in recalling the high-level sequential order from memory. In contrast, increases in activity in during the production phase were not associated with sequence-specific information, suggesting that these were instead involved in low-level control of constituent movement elements used across sequences.

3.3 Results

3.3.1 Activity increases from preparation to production in the contralateral putamen, caudate, thalamus, and ipsilateral cerebellum, but not the hippocampus

We trained 24 participants to produce four five-finger sequences from memory using their right hand. Behavioural training progressed from production under visual instruction to production from memory across two days. On the final third day, participants produced the sequences entirely from memory in an MRI scanner whilst activity across the whole brain was recorded. To isolate neural patterns relating to movement production from those relating to movement preparation, we used two independent trial types: Go trials (Figure 3.1a), to sample production activity, and No-Go trials (Figure 3.1b), to sample preparatory activity. Go trials began by cueing the upcoming sequence with an abstract fractal image, followed by a fixation cross, then a black hand with a green background (Go cue) indicated that the sequence should be executed (Figure 3.1c). A further fixation cross, then

performance feedback, followed. No-Go trials were almost identical, however did not display a Go cue. Rather, a fixation cross remained on the screen for an extended period. Feedback followed, and participants were rewarded for not producing any presses (see Methods and materials). More details regarding the experimental design and behavioural findings are available in a previous paper which examined the role of cortical motor areas (Yewbrey et al., 2023).

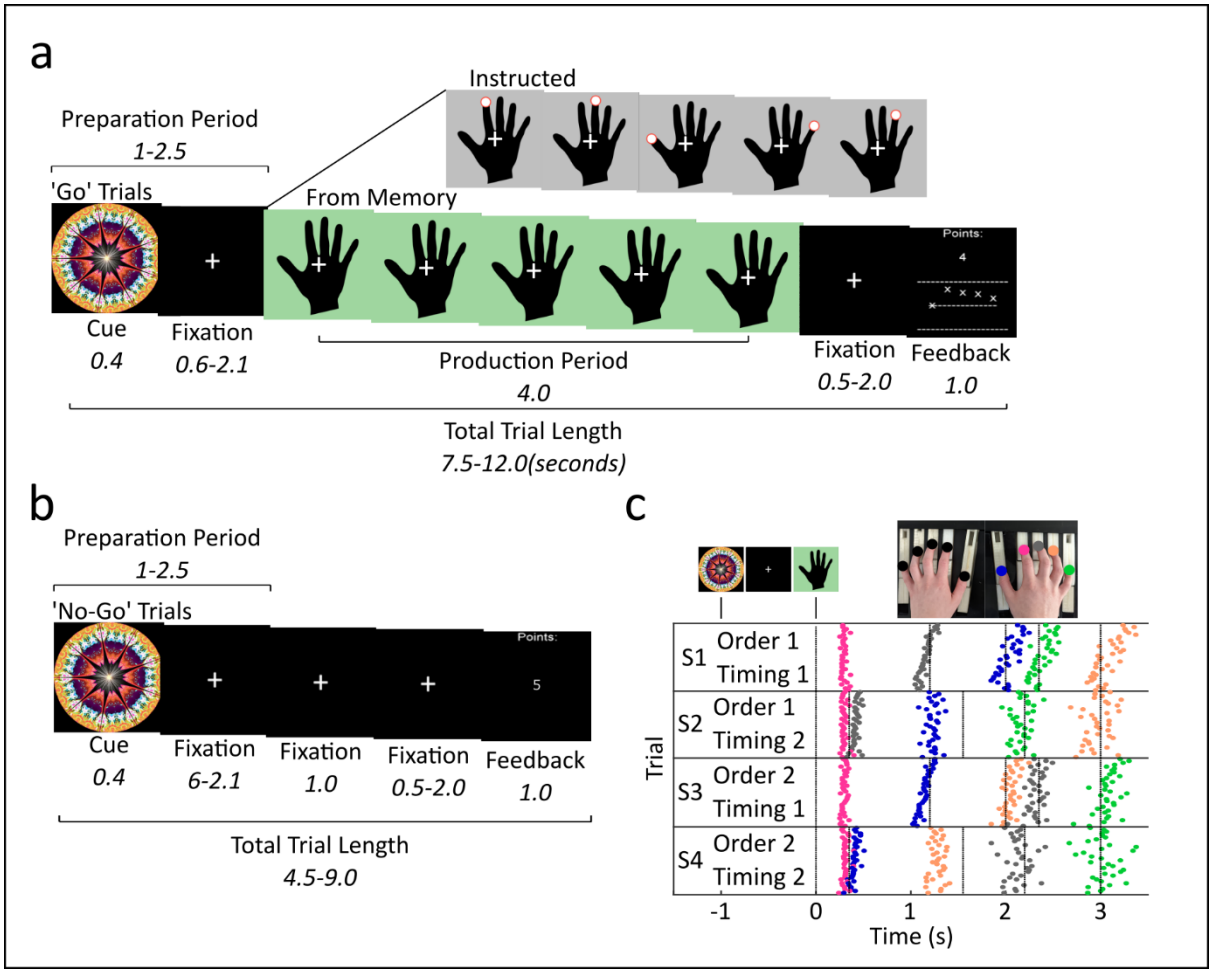

Figure 3.1. Trial types and target sequences. **a**, participants were trained to produce sequences from memory via visual instruction in 'Go' trials. The target sequence for each trial was indicated by an abstract fractal cue which succeeded a short preparation period. A black hand with a grey (instructed; a red cue indicated which finger to press with a set temporal structure) or green (from memory; participants had to produce the sequence without the visual cue) appeared to indicate the go cue. A short fixation period followed, after which feedback was provided based on the accuracy and timing of the sequence. **B**, on 50% of trials, the go cue would be replaced by an extended fixation cross. Participants were subsequently rewarded for not making a press during these 'No-Go' trials. **C**, all trials for one participant are plotted with the colour indicating which button was pressed according to the image above the plot. Target sequences consisted of permutations of two timings and two orders, constituting S1 through S4. Participants performed the sequences using the right hand on a 10-finger force transducer.

Firstly, we examined whether the subcortical regions of interest with connections to the active effector (right hand) were active during the preparation and production of movement sequences. We extracted percent signal change relative to rest from the left thalamus, left caudate, left putamen, and right CB lobules 4 and 5. In addition we extracted activity from the bilateral hippocampus in line with its role in skill learning and memory (Albouy et al., 2015; Doyon et al., 2009; Kornysheva et al., 2019b). We defined all regions using each participant's individual anatomy (see Methods and materials). The extracted percent signal change values from across all voxels belonging to each region were then averaged for each participant during preparation and production and we identified significant increases or decreases in activity compared to a baseline of zero (Figure 3.2a, b). All tests were Bonferroni corrected twice to account for phase (2) in each pre-defined ROI. During preparation, we observed significantly above baseline activity in the caudate ($t(23) = 3.28$, $p = .006$, $d = 0.67$), putamen ($t(23) = 2.67$, $p = .028$, $d = 0.55$), and hippocampus on both the left ($t(23) = 6.28$, $p < .001$, $d = 1.28$) and right ($t(23) = 4.63$, $p < .001$, $d = 0.94$) sides. No significant difference relative to baseline was found in the thalamus nor in lobules 4 and 5 of the CB during preparation ($p > .114$, $d < 0.41$). During production, significantly above baseline activity was observed in all subcortical area with connections to the active effector – contralateral thalamus ($t(23) = 7.54$, $p < .001$, $d = 1.54$), caudate ($t(23) = 2.66$, $p = .028$, $d = 0.54$), putamen ($t(23) = 4.21$, $p < .001$, $d = 0.86$), CB lobule 4 ($t(23) = 5.61$, $p < .001$, $d = 1.15$), and CB lobule 5 ($t(23) = 12.22$, $p < .001$, $d = 2.49$). The hippocampus, however, showed significantly below baseline activity during production in the left ($t(23) = 2.45$, $p = .044$, $d = 0.50$) and right ($t(23) = 3.19$, $p = .008$, $d = 0.65$) hemispheres. In sum, only basal ganglia and hippocampus were active during sequence preparation from memory. During production only subcortical and cerebellar areas with direct relevance to the active effector increased their activity, whereas hippocampal activity decreased.

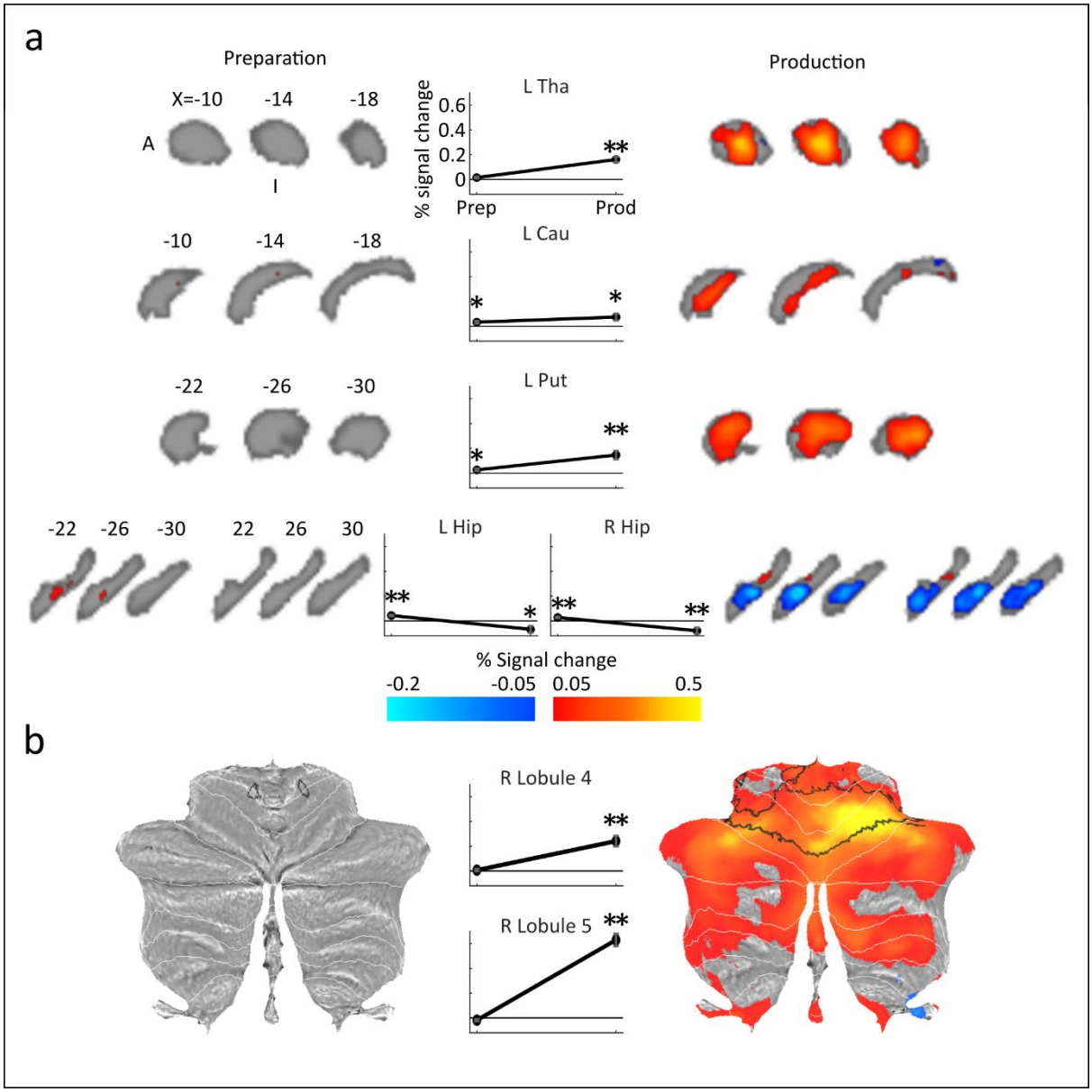

Figure 3.2. Percent signal change in subcortical regions during preparation and production. **A**, volumetric slices of each subcortical region displaying percent signal change for preparation and production, far left and right respectively. Centre shows the level of percent signal change when averaged across each subcortical region. ** $p < 0.01$; * $p < 0.05$; two-sided t test against 0. Error bars represent standard error of the sample mean. **B**, as above, for cerebellum. Black outline indicates significant clusters. Tha, thalamus; Cau, caudate nucleus; Put, putamen; Hip, hippocampus.

We then localised the peak activations within each subcortical area by identifying significant clusters of activation using a random effects analysis (Figure 3.2a, b). All results were corrected using SPM's small-volume correction and Bonferroni corrected twice to account for phase (2). During preparation, we found significant clusters of activation in the caudate's ventral anterior head ($t(23) = 6.02$, *pFWE* = .008, extent = 101, MNI coordinates: x=-16, y=22, z=-5), anterior body ($t(23) = 5.56$, *pFWE* = .020, extent = 83, x -16 y 22 z 7), and dorsal anterior tail ($t(23) = 5.55$, *pFWE* = .008, extent =106, MNI coordinates: x=-12, y=-6,

z=17), posterior putamen (t(23) = 5.71, *pFWE* < .001, extent = 228, MNI coordinates: x=-32, y=-14, z=9), anterior left hippocampus (t(23) = 7.97, *pFWE* < .001, extent = 766, MNI coordinates: x=-26, y=-22, z=-15), anterior right hippocampus(t(23) = 6.33, *pFWE* < .001, extent = 471, MNI coordinates: x=38, y=-20, z=-17), and CB right lobule five extending into right lobule four (t(23) = 5.09, *pFWE* = .002, extent = 205, MNI coordinates: x=17, y=-45, z=17). During production, we found significant clusters of activation widespread in the thalamus which centred middle posterior (t(23) = 14.29, *pFWE* < .001, extent = 851, MNI coordinates: x=-16, y=-24, z=5), the anterior tail of the caudate (t(23) = 5.24, *pFWE* < .001, extent = 208, MNI coordinates: x=-10, y=0, z=9), posterior putamen (t(23) = 7.06, *pFWE* < .001, extent = 783, MNI coordinates: x=-28, y=-18, z=3), and CB lobules 4 and 5 (the peak of which is in lobule 6, outside of our pre-defined ROIs; t(23) = 8.46, *pFWE* < .001, extent = 20079, MNI coordinates: x=7, y=-69, z=-16). In sum, while thalamus, BG, and cerebellum show general increases in activity throughout both movement phases relative to rest, hippocampus instead shows an increase during preparation and a decrease during production.

3.3.2 Sequence order, but not timing and integration, is present in subcortical regions – linear discriminant analysis

Whilst activity increases and decreases can show where there are changes in the use of neural resources, it does not inform us what informational content is represented in the underlying activity patterns. To identify the presence of sequence order and timing control, which may be considered higher-level sequence features and aspects of action selection, the four sequences that participants were trained to produce were permutations of two different order (finger press order) structures and two different timing (inter-press-interval arrangement, or rhythm) structures. We trained and tested an LDA classifier to distinguish between the neural patterns elicited by each order, regardless of the timing condition it was paired with, to identify independent representations of movement order (Kornysheva & Diedrichsen, 2014; Yewbrey et al., 2023). This constituted the accuracy values for the order decoder. A complimentary decoder was vice versa trained and tested to distinguish between the neural patterns of different timings when paired with different orders, providing the accuracy values for the timing decoder. A final decoder was trained and tested to distinguish between the residual patterns unique to each order-timing combination,

indicative of each sequence's idiosyncratic movement kinematics and provided values for the integrated decoder. All decoders were cross validated across six imaging runs and, for order and timing, across conditions, then converted into z scores (see Methods and materials).

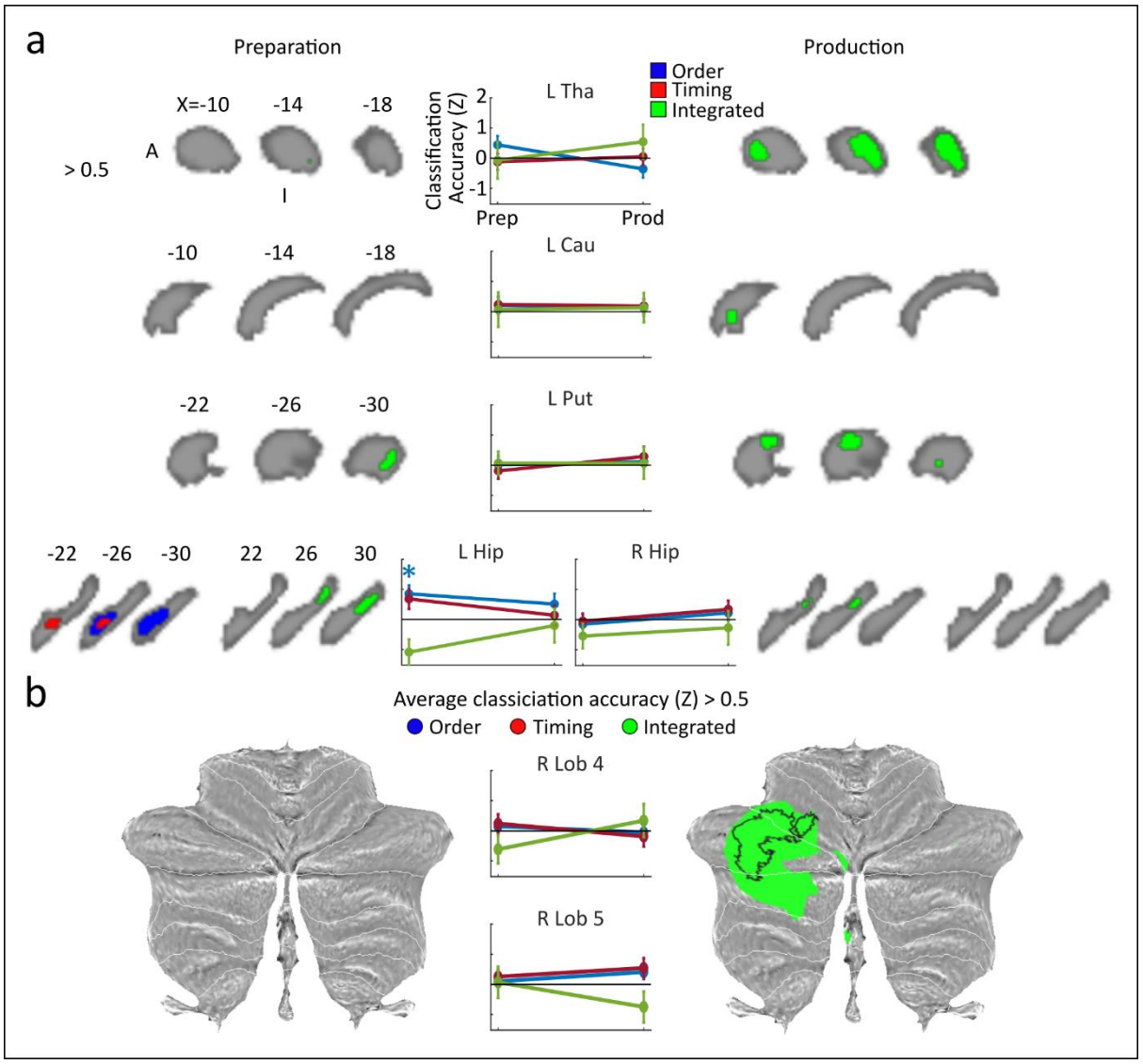

Figure 3.3. Linear discriminant analysis results. **A**, volumetric slices of each subcortical region displaying classification accuracy for each classifier during preparation and production, far left and right respectively. Centre shows classification accuracy when averaged across each subcortical region. * $p < 0.05$; one-sided t test against chance (Bonferroni-corrected for six comparisons within each ROI). Error bars represent standard error of the sample mean. **B**, as above, for cerebellum. Black outline indicates significant cluster. Tha, thalamus; Cau, caudate nucleus; Put, putamen; Lob 4, lobule four; Lob 5, lobule five.

We first tested whether ROI showed above chance decoding accuracy (Figure 3.3a, b). To do so, we obtained accuracy values for each of our three classifiers during preparation and production when considering all voxels within each ROI. We then assessed accuracy values in each region using one-tailed one-sample t-tests against a chance level of zero. All tests

were Bonferroni corrected six times to account for classifier (3) and phase (2) in each pre-defined ROI. During preparation, we found significantly above chance decoding of order in the left hippocampus ($t(23) = 3.00$, $p = .018$, $d = 0.61$). During production, we found no evidence of significantly above-chance decoding accuracy in the ROIs ($p > .264$, $d < 0.36$). These results suggest that the left hippocampus is involved in the planning of the ordinal structure of movement sequences.

Whilst considering all present voxels contained within a region is informative as to the general inclination of a region's processing, it does not inform us as to which subregions may be driving decoding accuracy the most. This is especially true when it comes to subcortical regions such as the thalamus, which shows differing functional and anatomical connectivity throughout its various subregions and nuclei (Kumar et al., 2017). Therefore, we performed volumetric searchlight analyses using 160 voxel searchlights for each decoder, constrained to each subcortical ROI (Figure 3.3a, b). The accuracy value for each given searchlight was assigned to the centre voxel. We then identified significant clusters using a random effects analysis on the produced accuracy maps and applied SPM's small-volume correction in a similar manner to the contrast activity cluster analysis. We Bonferroni corrected significance values for each cluster six times, to account for classifier (3) and phase (2). During preparation, we found a significant cluster for the order decoder in the anterior body of the left hippocampus ($t(23) = 5.74$, $pFWE < .001$, extent = 379, MNI coordinates: x=-32, y=-22, z=-11). No significant clusters were found to survive corrections during production, although prior to corrections a significant integrated cluster was found in the superior thalamus during production ($t(23) = 4.68$, $pFWE = .041$, extent = 51, MNI coordinates: x=-18, y=-26, z=15). These findings reinforce that the hippocampus, particularly the anterior body, is involved in the planning of sequential movement order. Sequence timing and its non-linear integration with sequence order, however, do not seem to be represented in motor-related subcortical regions.

3.3.3 Sequence representations differ across preparation and production

Given that our target subcortical regions show different activity levels alongside changes in informational content across preparation and production, we wanted to investigate whether there was a substantial change in the neural patterns themselves prior to and during movement. One possibility if that the patterns present during preparation undergo

linear scaling to exceed a set threshold and initiate movement, where unintended initiation is thought to be prevented by suppression in 72orticespinal circuits (Duque & Ivry, 2009a). Alternatively, these patterns may belong to entirely independent distributions, meaning that they are altogether distinct. The presence of similar neural patterns has been evidenced in single finger movements using fMRI (Ariani et al., 2022), whereas distinct neural patterns have been shown in multi-unit recordings of neural populations (Kaufman et al., 2014). Accordingly, we assessed the within-sequence, across-phase Euclidean distance between conditions in our fMRI data across principal components using multi-dimensional scaling of the representational dissimilarity matrix. Since we saw substantial activity changes across all regions except for the caudate from preparation to production, the first principal component is set to represent the different levels of activity as it captures the dimension with the greatest variance across the conditions. Therefore, we quantified the Euclidean distance between each sequence's position during preparation and production in a 2D space with the axes comprising of principal components two and three.

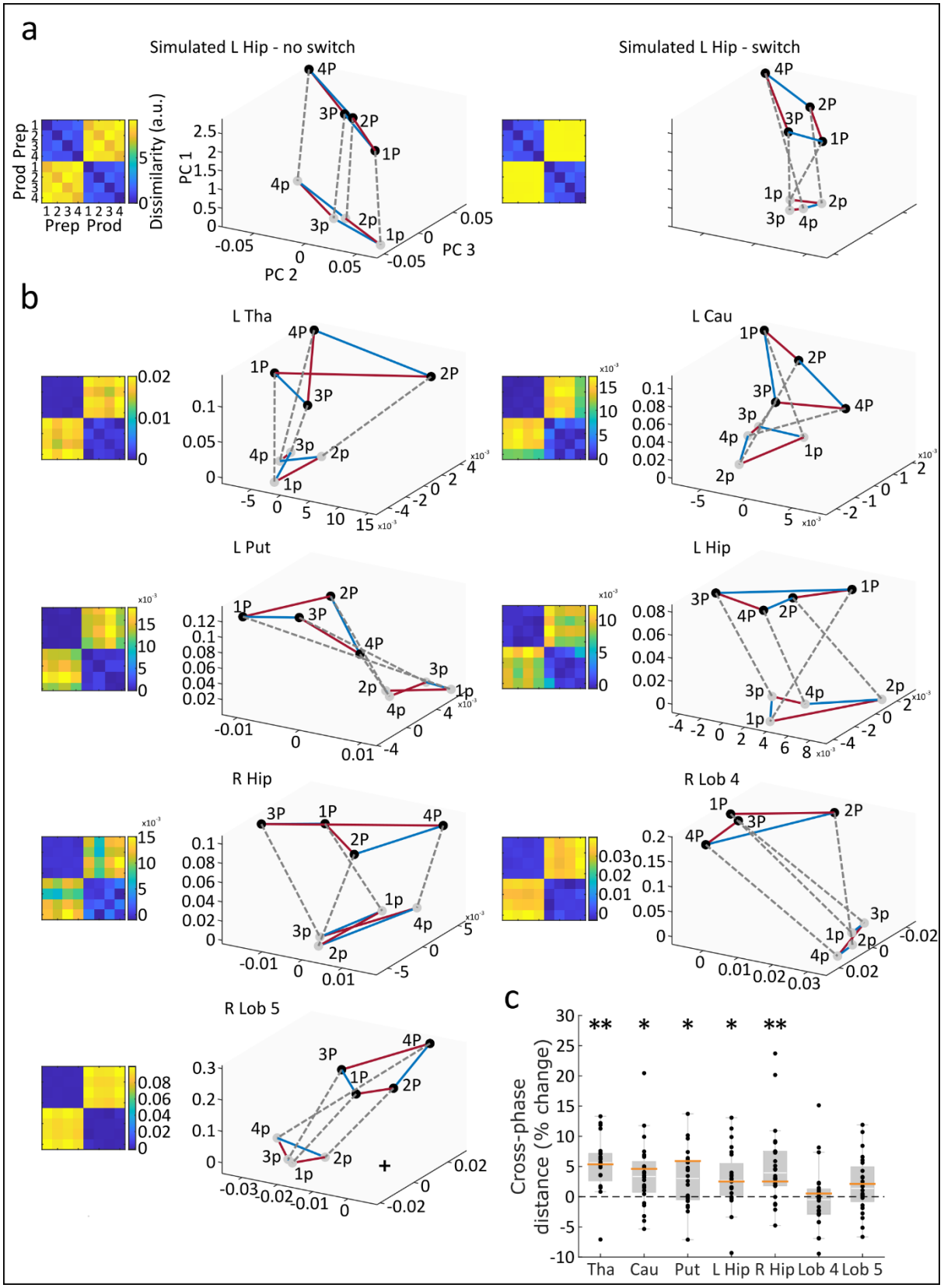

Figure 3.4. Simulated and empirical cross-phase Euclidean distances using multi-dimensional scaling. **a**, multi-dimensional scaling plots of simulated fMRI data along principal components 1, 2, and 3, showing four simulated sequence conditions across two phases. Red lines connect simulated sequences with different timings but the same order, whereas blue lines indicate sequences with different orders but the same timing. Dotted grey lines are drawn between the same sequence during preparation and production. Preparation and

production were either generated using the same distribution (left panel; no switch) or different distributions (right panel; switch). **b**, multi-dimensional scaling plots of empirical data from target ROIs showing all four sequences during preparation and production. **c**, averaged Euclidean distance between preparation and production within sequences once PC1 is excluded, calculated relative to those same distances from the simulated no switch data with matched signal to noise ratios. This represents differences for all sequences between preparation and production which cannot be explained by differences in overall activity. Orange horizontal lines represent the same distances in the simulations when a switch is induced. * $p < 0.05$; ** $p < 0.001$; one-sided t test against simulated no distance with matched noise, 0 (Bonferroni-corrected for seven comparisons). Tha, thalamus; Cau, caudate nucleus; Put, putamen; Lob 4, lobule four; Lob 5, lobule five.

If one were to assume that activity patterns during production are simply upscaled versions of those during preparation, the hypothetical distance between patterns after removal of the first principal component should be zero. However, given a level non-zero level of noise in our data, these distances are unlikely to equal zero which would bias our results away from indicating a maintained distribution. To control for this, we simulated fMRI data sets with the same conditions as our empirical data and generated preparation and production from either the same distribution (no switch) or different distributions (switch), whilst matching their signal to noise ratios to our regions of interest (Figure 3.4a). Additionally, we scaled this cross-phase distance by the average of distances within preparation and production (Figure 3.4b). We then performed one-tailed, one-sample *t*-tests against zero to identify significantly elevated Euclidean distance in each of our subcortical regions, Bonferroni corrected seven times for region (Figure 3.4c). We found significant elevation in the thalamus ($t(23) = 6.06$, $p < .001$, $d = 1.24$), caudate ($t(23) = 3.20$, $p = .014$, $d = 0.65$), putamen ($t(23) = 3.12$, $p = .017$, $d = 0.64$), hippocampus in the left ($t(23) = 3.05$, $p = .020$, $d = 0.62$) and right ($t(23) = 3.93$, $p = .002$, $d = 0.80$) hemispheres. No significant differences were found in CB lobule 4 ($t(23) = 0.37$, $p = 1.00$, $d = 0.08$) and CB lobule 5 ($t(23) = 2.05$, $p = .182$, $d = 0.42$). These results suggest that all subcortical regions apart from CB show significantly higher cross-phase distances than a matched simulation which does not predict a change in distributions across phase, providing evidence for distinct neural patterns for movement sequences prior to and during movement.

3.4 Discussion

Learning and control of skilled motor sequences (“muscle memories”) has been associated with subcortical motor-related brain areas – basal ganglia, the cerebellum, and,

more recently, the hippocampus (Buch et al., 2021; Harpaz et al., 2022; Khilkevich et al., 2018). However, there are unresolved debates on the contribution of these areas to high-level action selection and lower-level movement implementation, respectively (Christian & Thompson, 2003; Frank, 2011; Gao et al., 2018; Mizes et al., 2023a). Here, we examined brain activity patterns within effector-related striatal, thalamic, and cerebellar, as well as bilateral hippocampal regions while participants were preparing and executing well-trained motor sequences from memory in the fMRI scanner. Specifically, we probed whether these regions showed activity in line with sequence-sensitive tuning to high-level sequence features – finger order and timing, as opposed to their lower-level integration for sequence execution (Figure 3.5). Further, we assessed whether the neural patterns during planning in those subcortical areas were simply a subthreshold version of those during execution (Cisek & Kalaska, 2005; Duque & Ivry, 2009a), or qualitatively distinct neural states (Kaufman et al., 2014) implying a state shift in neural activity related to phase. Although both hippocampal and effector-related striatal regions showed increased activity during sequence planning, only the hippocampal patterns showed higher-level sequence order tuning during planning. In contrast striatal, thalamic, and cerebellar regions increased activity during production yet lacked sequence-specific patterns across any of the phases, suggesting their role may be related to low-level kinematic control of individual movement elements, rather than a particular sequence of movements. All regions, apart from the cerebellum, showed fundamental shifts in the activity patterns from planning to execution, suggesting that initiating movements involves a general shift in the neural control of sequential movements.

3.4.1 The hippocampus pre-orders upcoming movements

The hippocampus has traditionally been associated with episodic recall in the non-motor domain and is key to the preservation of event order (Davachi & DuBrow, 2015). However, new evidence suggests its involvement in the consolidation of motor skills, e.g. via hippocampo-neocortical replay patterns supporting rapid wakeful consolidation during short rest periods interspersed with sequence learning (Buch et al., 2021). Our fMRI pattern analysis revealed that the hippocampus retrieves high-level information on the upcoming sequence during movement planning – the finger order of the sequence regardless of its timing.

One possibility is that the hippocampus engages in serial order replay during preparation, which is temporally compressed approximately 20-fold relative to the acquired skill and is associated with skill consolidation (Buch et al., 2021). Alternatively, it may be setting up the order through parallel competitive preparation of the upcoming sequence elements – competitive queueing (Kornysheva et al., 2019b). This framework suggests that upcoming movements are planned in parallel prior to serial execution during production using a parallel playing layer (Averbeck et al., 2002; Houghton & Hartley, 1995). Whilst only invasive recording in patients and concurrent EEG-fMRI studies would be able to arbitrate between these two scenarios, they demonstrate that the hippocampus is involved in the control of highly trained sequences of movements, specifically in retrieving sequence order from long-term memory.

Previous findings suggest that the superior parietal lobule (SPL) also plays a role in the definition of movement order during planning (Yewbrey et al., 2023) and represents effector non-specific movement intentions (Henderson et al., 2022; Shushruth et al., 2022). The SPL and hippocampus share extensive connections through the ‘where’ pathway in the dual stream model of memory (Huang et al., 2021) and interact closely during navigation tasks to convert world-centered coordinates into body-centered coordinates (Rolls, 2020; Whitlock et al., 2008). As such, interaction between hippocampus and SPL may serve to map the abstract order generated by the hippocampus (Kornysheva et al., 2019b) onto intrinsic reference frames (Wiestler & Diedrichsen, 2013) prior to execution (Figure 3.5).

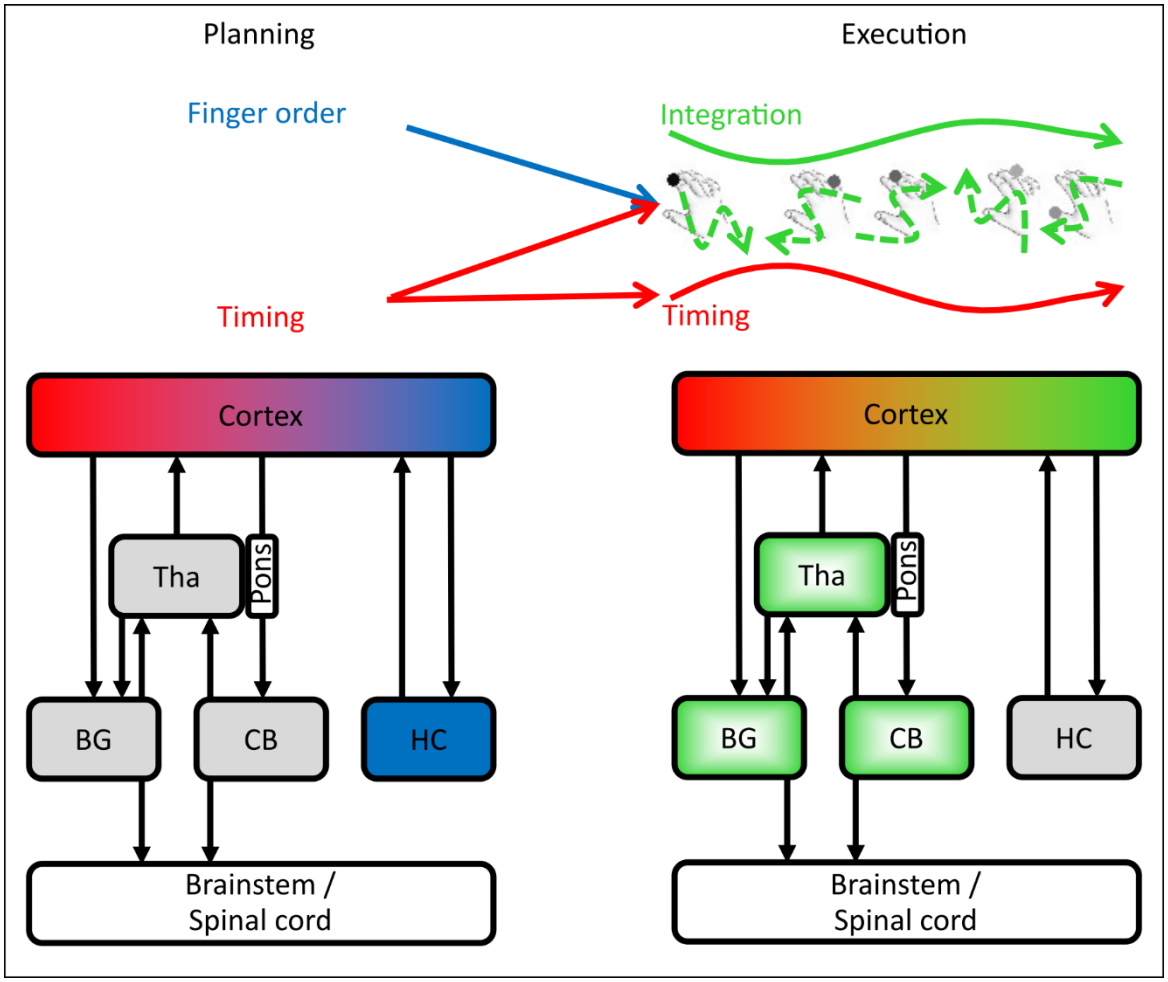

Figure 3.5. Schematic representation of sequence feature control during planning and execution. Higher level sequence features, order (blue) and timing (red), are defined by cortex and hippocampus during planning. During execution, the activity patterns in hippocampus, basal ganglia, and thalamus shift while the cortex integrates order and timing into low-level sequence specific trajectories (green), while maintaining higher-level independent movement timing. The green gradient fill in thalamus, basal ganglia, and cerebellum indicates regions that implement individual sequential elements. Tha, thalamus; BG, basal ganglia; CB, cerebellum; HC, hippocampus.

3.4.2 Effector-relevant striatal, thalamic, and cerebellar activity lacks sequence-specific tuning

While the hippocampus showed clear evidence for a high-level selection of upcoming serial order, we found no evidence for effector-relevant contralateral striatal, thalamic, and ipsilateral cerebellar activity containing sequence-specific information of any sort. These findings speak against both the hypothesized role of the striatum in action selection and its integration of sequence features for kinematic control of the whole sequence as one motor program. This appears to contrast results from rodent models (Mizes et al., 2023a) where optogenetic lesions lead to kinematic deficits in sequence production. However, this mapping breaks down in rodents when highly trained sequences share elements with other

sequences the animal has been exposed to, e.g. lever presses appearing in a different order (Mizes et al., 2023b). This is analogous to many motor skills in humans, such as typing, handwriting and music production where elements are reused in different permutations, including highly trained ones. Importantly this also applied to the factorial design of our study. Thus, kinematic control in the striatum is likely associated with singular movements, rather than whole sequences, which our experiment would be unable to detect due to all sequences containing the same constituent movements.

Surprisingly, we did not observe any engagement in ipsilateral effector-relevant cerebellar regions during motor sequence planning. This includes both the absence of overall activity increase and the lack of above-chance accuracy in decoding sequences, despite recent animal studies suggesting their role in motor planning. This suggests that cerebellar motor regions contribute to the online control of individual movement elements during movement production, rather than the planning and execution of a whole sequence. The latter preserves the possibility of cerebellar involvement in planning, including the planning of individual actions “on the fly” once the production of a sequence has started (Ariani et al., 2021; Ariani & Diedrichsen, 2019). Sequence tuning could be found in cerebellar regions known to be interconnected with prefrontal areas (Crus I). Notably, this tuning occurred again exclusively during motor execution, emphasizing its role in online control rather than pre-execution planning.

Despite participants’ ability to fluently produce the target movement sequences from memory after two days of training, the movement kinematics for the upcoming sequence are not pre-planned. Rather, the order and timing of sequences is recombined trial-by-trial likely through communication with the cortex, which has shown a mechanism whereby the order and timing are planned and subsequently integrated during execution (Yewbrey et al., 2023). This maintenance of separation up until the go cue likely affords the individual the ability to adjust movement plans should task demands suddenly change.

3.4.3 Multidimensional scaling reveals a widespread shift in sequence pattern activity across planning and execution

Motor planning in the cortex has been proposed to be a scaled down version of execution, held at bay by suppression in corticospinal circuits (Cisek & Kalaska, 2005; Duque

& Ivry, 2009a). More recently, however, planning activity has been proposed to exist in an output-null dimension to execution, where increases and decreases in output from neurons projecting to the same source cause no net change in activity, but prepare the system to shift into the output-potent dimension (Kaufman et al., 2014, 2016), including for sequences of movements (Yewbrey et al., 2023). Our current results suggest that this shift also takes place in multiple subcortical areas: striatum, thalamus, and hippocampus. Here, sequence-related activity patterns across planning and execution were significantly distinct across the perimovement phases. This could not be explained by a simple upscaling through changes in activity and matched by our no-change simulations of the same dimensions that considered empirical noise levels in those areas. This could be driven by either separate populations becoming active at different times around movement execution or changes of the patterns of the same neuronal pool, which can only be resolved with invasive recordings in these areas.

3.4.4 Implications for clinical disorders

Here we show that the hippocampus, but not the basal ganglia-cerebellar-thalamic loop is contributing to the planning of skilled movement sequences produced from memory. Thus, breakdowns in movement sequence execution in Parkinson's Disease (Wilkinson et al., 2009) and Cerebellar Ataxia (Doyon et al., 1997) cannot be explained by deficits in the planning or execution of entire sequences. Instead we hypothesize that they might be a result of the reduced capacity to implement the online control of individual movement elements (Dhawale et al., 2021; Mizes et al., 2023a). In contrast, our results predict that Alzheimer's Disease which is associated with a degeneration of the hippocampal formation and the medial temporal lobe (Dubois et al., 2016), affects everyday movement sequence production such as handwriting and ideomotor action organization (Förstl & Kurz, 1999) because of the inability to retrieve the correct order of the upcoming movement elements. We hypothesize that this applies particularly to contexts where movement sequences need to be retrieved flexibly from long-term memory, such as often the case in everyday skilled action use which utilises the same elements from the motor repertoire across different ordinal sequences, e.g., typing, handwriting and tool use. In summary, our results question traditional classifications of motor skill memory and control, along with their associated

subcortical substrates. Research on skilled movement planning in these clinical populations is needed to inform appropriate rehabilitation interventions and support.

3.5 Methods and materials

3.5.1 Participants

24 neurologically healthy participants (14 females and 10 males; mean age = 21.00 years, SD = 1.64 years) met all behavioural and imaging requirements after completing the three-day experiment. 23 participants were right-handed with a mean Edinburgh Handedness Inventory (https://www.brainmapping.org/shared/Edinburgh.php; adapted from Oldfield, 1971) score of 75.22 (SD = 20.97, range: 25-100), one was left-handed with an Edinburgh Handedness Inventory score of -70. Although we stated that we would exclude left-handed individuals in our preregistration (www.osf.io/g64hv), we included this participant's data in our analyses as they were not qualitatively different from the rest of the sample. Data from an additional 17 participants were excluded for the following reasons: one due to unforeseen technical difficulties with the apparatus, one because of a corrupted functional scan, and 15 further participants did not reach target performance after two days of training. Target performance consisted of an error rate < 20% (mean = 6.54%, SD = 6.03%, for the group) and distinct sequence timing structures that transferred across sequence finger orders; the full details regarding the exclusion criteria have been described elsewhere (Yewbrey et al., 2023). Participants were recruited either through social media and given monetary reward at a standard rate, or through a participation panel at Bangor University and awarded module credits for their participation. Individuals with professional musical qualifications were excluded from recruitment. All participants provided informed consent, including consent to data analysis and publication, through an online questionnaire hosted by Qualtrics. The Bangor University School of Psychology Ethics Committee approved this experiment and its procedures (ethics approval number 2019-16478).

3.5.2 Apparatus

Two custom-built force transducer keyboards captured presses from all 10 fingers on the right and left hands of participants as they produced movement sequences. Each key had a small groove where participants placed their finger and could be adjusted for comfort

according to the size of the participant's hand. Below each key, a force transducer sampled force at 1000 Hz (Honeywell FS Series, with a range of up to 15N). The keys were not depressible. Force acquisition occurred in each trial from 500ms before sequence cue onset to the end of the production period in production trials, and the end of the false production period in No-Go trials. Traces from the right hand were baseline-corrected trial-by-trial using the first 500ms of acquisition (500ms before the sequence cue) and smoothed to a Gaussian window of 100ms. Button presses were defined as the point at which forces exceeded a fixed threshold relative to baseline (2.5N for the first 8 participants and 1N for the subsequent 16 of 24 participants). During behavioural training sessions, participants were seated at a wooden table ~75 cm away from a 19-inch LCD LG Flatron L1953HR, at a resolution of 1280 x 1024 and a refresh rate of 60Hz. Their hands were occluded during behavioural sessions by a horizontal panel on posts positioned above the force boxes. During fMRI sessions, stimuli were presented on an MR Safe BOLDScreen 24-inch monitor, at a resolution of 1920 x 1200 and a refresh rate of 60Hz. Participants laid supine on the scanner bed, and the two force transducers were positioned on a support board resting on their bent upper legs to enable comfortable and stable positioning of the hands.

3.5.3 Behavioural task

Participants were trained to produce four five-finger sequences with defined inter-press intervals (IPIs) from memory in a delayed sequence production paradigm. Go trials began with an abstract fractal image (Sequence cue), which was associated with a sequence. Following the Sequence cue, a fixation cross was shown to allow participants to prepare the upcoming sequence. A black hand with a green background (Go cue) then appeared to cue sequence production from memory. Succeeding the Go cue, another fixation cross was presented. Feedback was then displayed to participants based on their performance during the preceding production period, finally followed by an inter-trial interval where a fixation cross was displayed. During training, participants learned the sequences through repeated exposure to visually guided (Instructed) Go trials. These Instructed Go trials were functionally identical to From Memory Go trials, but featured a Go cue with a grey background and a red dot on the tip of each finger on the hand image, which moved from finger to finger in the target production order and in-pace with the target timing structure. No-Go trials had the same structure as Go trials, but the go cue did not appear following the

preparatory fixation cross. Instead, the fixation cross continued to show for an extended period. This was succeeded by a further fixation cross, feedback, and ITI, as in Go trials.

The four five-finger target sequences consisted of permutations of two finger orders (Order 1 and 2) and two IPI orders (Timing 1 and 2) matched in finger occurrence and sequence duration. Sequence orders were generated randomly for each participant, making sure to avoid ascending and descending press triplets and any identical sequences. Furthermore, each participant's trained sequences began with the same finger press to avoid differences in the first press driving the decoding of sequence identity during preparation (Yokoi et al., 2018). Timing structures were the same across participants, which consisted of four target IPI sequences as follows: 1200ms – 810ms – 350ms – 650ms (Timing 1), and 350ms – 1200ms – 650ms – 810ms (Timing 2).

The trial-by-trial feedback used a points-based scale, ranging from 0 to 10. Points were awarded based on initiation reaction time and temporal deviation from target timing. 0 points were awarded if the executed press order was incorrect. If the executed press order was correct, participants were awarded their earned timing points. In No-Go trials, 5 points were awarded if no press was made as instructed. Participants were presented with a feedback screen after each trial showing the number of points achieved in the current trial, as well as visual feedback on whether they pressed the correct finger at the correct time. A horizontal line was drawn across the centre of the screen, with four symbols displayed equidistantly along the line representing each of the five finger presses. Correct presses were indicated by an "X" symbol and incorrect presses were represented by a "–" symbol, for each respective sequence position. The vertical position of these symbols above ("too late") or below ("too early") the horizontal line was proportional to the participant's timing of the respective press relative to target IPI. Using these cues, participants were able to adjust their performance online to ensure maximum accuracy of sequence production. During the first two days of training, auditory feedback in the form of successive rising tones corresponding to the number of points (0 – 10) was played alongside the visual feedback. Auditory feedback was absent during the fMRI session, to prevent any auditory processing driving decoding accuracy. All aspects of the behavioural task for this experiment are described in greater detail in a previous study (Yewbrey et al., 2023).

3.5.4 Procedure

Training duration was consistent across participants and occurred across the first two days of the experiment over three distinct training stages. In the first training stage, 80% of all trials were instructed Go trials, and the remaining 20% were No-Go trials. During the second training stage, 40% of trials were instructed Go trials, 40% were from-memory Go trials, and 20% were No-Go trials. In the third and final stage of training, 80% of trials were from-memory Go trials, and 20% were No-Go trials. The third day took place inside of the MRI scanner and consisted of a short refresher stage, made up of the same proportion of trials as the second stage of training, during which T1 images were collected. Next, there was an fMRI stage consisting of six imaging runs, featuring 50% from-memory Go trials and 50% No-Go trials. In addition, before and after the last training stage, participants completed a synchronization task which has been described elsewhere (Yewbrey et al., 2023).

3.5.5 MRI acquisition

Data were acquired using a 32-channel head coil in a Philips Ingenia Elition X 3T MRI scanner. T1 anatomical scans at a 0.937 x 0.937 x 1 resolution were acquired using MPRAGE, encoded in the anterior-posterior dimension with an FOV of 240 x 240 x 175 (A-P, R-L, F-H). For the functional data, T2*-weighted scans were collected across six runs of 230 volumes at a 2 mm isotropic resolution, with 60 slices at a thickness of 2 mm. The functional images were acquired at a TR of 2s, a TE of 35 ms, and a flip angle of 90°. These were obtained at a multiband factor of 2, in an interleaved odd-even EPI acquisition. To allow the stabilization of the magnetic field, four images were discarded at the beginning of each run. The whole brain of most participants was covered, except for the central prefrontal cortex, the anterior temporal lobe, and ventral parts of the cerebellum. Jitters were used within each trial during preparation periods, post-production fixation crosses, and I, to give us a more accurate estimate of the Hemodynamic Response Function (HRF) by varying which part of the trial is sampled by each TR (Serences, 2004).

3.5.6 Pre-processing and first-level analysis

All fMRI pre-processing steps were completed using SPM12 (revision 7219) in MATLAB (The MathWorks). We applied slice timing correction using the first slice as a reference to interpolate all other slices to, ensuring analysis occurred on slices which represent the same

time point. Realignment and unwarping were conducted using a weighted least-squares method correcting for head movements using a 6-parameter motion algorithm. A mean EPI was produced using SPM's Imcalc function, wherein data acquired across all six runs were combined into a mean EPI image to be co-registered to the anatomical image. Mean EPIs were co-registered to anatomical images using SPM's coreg function, and their alignment was checked and adjusted by hand to improve the alignment, if necessary. All EPI runs were then co-registered to the mean EPI image. For the GLM, regressors were defined for each sequence separately for both preparation and production, resulting in eight regressors of interest per run. Preparation- and production-related BOLD responses were independently modelled from No-Go and Go trials, respectively, to tease out activity from these brief trial phases despite the haemodynamic response lag (Logothetis, 2003). The preparation regressor consisted of boxcar function starting at the onset of the Sequence cue in No-Go trials and lasting for the duration of the maximum possible preparation phase (2500ms). The production regressor consisted of a boxcar function starting at the onset of the first press with a fixed duration of 0 (constant impulse), to capture activity related to sequence initiation and extract sequence production-related activity from the first finger press that was matched across sequences within each participant. We aimed at capturing BOLD responses related to neuronal populations that become differentially active for different sequences (Tanji & Shima, 1994), for which a single estimate of sequence production has been used to successfully identify sequence representations in several previous fMRI studies (Berlot et al., 2020; Kornysheva & Diedrichsen, 2014; Nambu et al., 2015; Wiestler & Diedrichsen, 2013; Yokoi et al., 2018). Additionally, we included several regressors of no interest: (1) error trials (incorrect or premature presses during Go trials and presses during No-Go trials), which were modelled from sequence cue onset to the end of the ITI; (2) the preparation period in Go trials (1000-2500 ms from Sequence cue); and (3) the temporal derivate of each regressor. The boxcar model was then convolved with the standard HRF. To remove the influence of movement-related artifacts, we used a weighted least-squares approach (Diedrichsen & Shadmehr, 2005). This resulted in us obtaining beta weight images for each of the eight conditions per scanning run, for all six runs. We further calculated the percent signal change during preparation and production relative to rest and compared each to a baseline of zero using two-tailed one-sample *t*-tests (Figure 3.2a). These tests were Bonferroni-corrected two times, to account for phase (2) within each pre-defined ROI.

Additionally, we identified significant clusters of activity constrained to each ROI using a random effects analysis with an uncorrected threshold of $t(23) > 3.48$, $p < 0.001$ and a cluster-wise p value for the cluster of that size (Worsley et al., 1996).

3.5.7 Subcortical and cerebellar regions of interest

We used Freesurfer's automatic segmentation (Dale et al., 1999) to segment subcortical regions of interest consisting of the thalamus, caudate nucleus, putamen, and hippocampus, from each participant's T1 anatomical image. We then resliced each region's mask into the same resolution as the functional images (2x2mm isotropic) and further masked them using functional activity. Only beta weights from voxels within these subcortical functional masks were extracted, constraining analyses to voxels belonging to subcortical regions of interest. Further, to assess the spatial organisation of multivariate patterns, we defined 160-voxel volumetric searchlights with a maximum radius of 6 mm in native space within each subcortical region of interest. LDA accuracy and RSA dissimilarity values (see Linear discriminant analysis and Representational similarity analysis sections) obtained were assigned to the centre voxel of the active searchlight.

For the CB, we used the SUIT cerebellar toolbox (Diedrichsen, 2006) to segment the whole structure based on individual anatomical T1 images. We then resliced the lobular probabilistic cerebellar atlas (Diedrichsen et al., 2009) into each participant's native space to acquire masks for CB lobules 4 and 5. We then resliced these masks into functional resolution and further masked them using functional activity. Beta weights were extracted from these regions using these masks to constrain analyses to voxels of interest. Additionally, we defined a 160-voxel volumetric searchlight across the whole cerebellum using each participant's individual anatomy. LDA accuracy and RSA dissimilarity values were assigned to the centre voxel of the active searchlight in a similar manner to the subcortical analysis. Classification accuracy and distance maps were subsequently resliced into SUIT space to display group results on a cerebellar surface flatmap (Diedrichsen & Zotow, 2015).

3.5.8 Linear discriminant analysis

LDA was used to detect sequence-specific representations (Kornysheva et al., 2019b; Kornysheva & Diedrichsen, 2014; Yewbrey et al., 2023), programmed in a custom-written MATLAB (The MathWorks) code. We extracted mean patterns and common voxel-by-voxel

covariance matrices for each class from the training dataset (five of the six imaging runs), and then a gaussian linear discriminant classifier was used to distinguish between the same classes in the test dataset (the remaining imaging run). The factorized classification of finger order, timing, and integrated order and timing followed the previous approach (Kornysheva & Diedrichsen, 2014; Yewbrey et al., 2023) and was performed on betas estimated from the sequence preparation and production periods independently. For the decoding of sequence order, the classifier was trained to distinguish between two sequences with different orders but matching timing across five runs and was then tested on two sequences with the same orders paired with a different timing in the remaining run. This classification was then cross-validated across runs and across training/test sequences, for a total of 12 cross-validation folds. For the decoding of sequence timing, the classifier was trained to distinguish between two sequences with differing timings paired with the same order and tested on two sequences with the same two timings paired with a different order and underwent the same cross-validation procedure. This method of training and testing the linear discriminant classifier allowed for identification of sequence feature representations that were transferrable across conditions they are paired with and therefore independent. The integrated classifier was trained to distinguish between sequences on five runs and then tested on the remaining run. Here, the mean activity for each timing (collapsed across two orders) and finger order (collapsed across two timings) condition within each run was subtracted from the overall activity for each run, separately (Kornysheva & Diedrichsen, 2014; Yewbrey et al., 2023). This allowed for the measurement of residual activity patterns that were not explained by a linear combination of timing and order, rather spatiotemporal idiosyncrasies that would result in the generation of unique kinematics for the respective sequence that were not transferrable to others. However, due to a unique feature possessed by the 2x2 design, the subtraction of each condition's mean activity patterns from the data resulted in the patterns of opposing sequence pairs (e.g., order 1, timing 1 and order 2, timing 2) becoming identical. For this reason, we trained our classifier to distinguish between the sequence pairs that remained distinct, resulting in a 50% chance accuracy.

We normalised classification accuracy by transforming to z scores, assuming a binomial distribution of the number of correct guesses (Kornysheva & Diedrichsen, 2014). We then

tested these z scores against zero (chance level) in subcortical and cerebellar ROIs across participants for statistical analysis. Z-score transformed classification accuracy maps were subjected to a random effects analysis, similar to the RSA distance maps, with an uncorrected threshold of $t(23) > 3.48$, $p < .001$ and a cluster-wise p value for a cluster of that size (Worsley et al., 1996). Analyses that considered all voxels within respective regions of interest were also subjected to one-tailed one-sample *t* tests relative to zero, Bonferroni-corrected 6 times to account for phase (2) X classifier (3), to identify decoding accuracy above chance level. We also ran repeated measures ANOVAs on regional distance measures with factors of phase, classifier, and region to assess interaction effects and ran post-hoc pairwise comparisons to investigate significant interaction effects.

3.5.9 Multi-dimensional scaling

We firstly multivariately pre-whitened beta weights prior to multi-dimensional scaling to increase the reliability of our distance measurements, using a regularised estimate of the overall noise-covariance matrix (Walther et al., 2016). We then identified the first three principal components in our pre-whitened beta weights using classical multi-dimensional scaling of the variance-covariance matrix. This method plots all eight conditions in 3D space according to the first three eigenvectors (principal components) associated with the largest eigenvalues. Given that activity levels varied significantly within regions across preparation and production (see Results), we measured the Euclidean distance between preparation and production within each sequence upon exclusion of the first principal component, since the largest eigenvalues are likely associated with differences in activity levels across phase. Hence, we calculated the Euclidean distance between points plotted in the 2D space represented by principal components one and two. However, given a non-zero level of noise in the data, the Euclidean distance between two points will be biased away from zero. We therefore simulated fMRI activity patterns with a matched number of voxels and signal to noise ration relative to the mean across participants of each ROI collected in the empirical data. We then calculated the cross-phase within-sequence Euclidean distances to provide baselines for the one-sample t-tests carried out in each region (Bonferroni corrected seven times for region). Additionally, these distances were scaled and normalised according to the average of the average distances between conditions during preparation and production respectively.

Chapter 4 - The Fingers on the Contralateral Hand Show a Mirrored Suppression Gradient During Unimanual Movement Sequence Planning

This chapter is in preparation as:

Yewbrey, R., Wright, H., Sadnicka, A., & Kornysheva, K. (2024). The Fingers on the Contralateral Hand Show a Mirrored Suppression Gradient During Unimanual Movement Sequence Planning [In Preparation].

R.Y., H.W., A.S., and K.K. conceived the experiment; R.Y., A.S., and K.K. formulated the hypotheses; R.Y. collected the data; R.Y., H.W., and K.K. designed the analysis; R.Y. and K.K. performed the analyses; R.Y. and K.K. wrote the original version of the manuscript; All authors contributed to editing of the manuscript.

4.1 Abstract

Movement elements in a sequence are planned in parallel via competitive queueing (CQ). The pre-activation of each element is weighted by its ordinal position in the upcoming sequence, with the degree of separation associated with the quality of sequence execution. Effectors that are not included in the upcoming sequence show reduced availability relative to target effectors. This effect is also shown in motor-evoked potentials during single movement delayed response tasks and is thought to reduce the likelihood of executing unintended competing movements. However, it is unclear how competition from Unused effectors is resolved when planning multiple movements in parallel. For example, during unimanual finger sequence production, the pre-activation of fingers in the used hand from the traditional CQ gradient may cause finger-specific inhibition in the contralateral unused hand, resulting in a mirrored gradient of availability. Alternatively, the CQ gradient may cause matching pre-activation in the unused hand but be held back from execution by global suppression, or show no differentiation at all. Here, we trained participants to produce two finger sequences: one with the right hand, and one with the left, and used probe trials to evaluate the availability of fingers on the Used and Unused hand when participants prepared an upcoming sequence. Alongside a traditional CQ gradient, we identified a mirrored gradient in the unused hand where the finger homologous to the one in the first serial position showed the lowest availability, followed by fingers homologous to later positions. A stronger CQ gradient in the unused hand was associated with faster movement times, suggesting that it might be beneficial to behaviour. Additionally, the impact of expertise playing video games, but not music or sports, predicted a stronger CQ gradient in the used hand during sequence planning. These results point to interhemispheric inhibition of individual fingers which helps to resolve competitive processes during rapid movement planning.

4.2 Introduction

The fluent production of several movements in succession underpins many abilities that are uniquely human. From playing a musical instrument to executing a dance routine, all require skilled production of movement sequences. The planning of upcoming movement sequences is thought to be crucial to execution (Haith & Bestmann, 2020; Lashley, 1951; Wong et al., 2015) with competitive queueing (CQ) models suggesting that each movement element is planned in parallel, weighted by its ordinal position in the sequence (Houghton, 1990). Multivariate analysis has identified such weighting in the probability of neural patterns, revealing the presence of a CQ gradient during sequence planning in both primates and humans (Averbeck et al., 2002; Kornysheva et al., 2019b). The size of this CQ gradient was shown to be a reliable indicator of subsequent behavioural performance, with a steeper gradient predicting greater execution accuracy. Moreover, the CQ gradient has been identified behaviourally by probing the availability of the upcoming sequence's constituent movements at the point of initiation (Mantziara et al., 2021). This study also found that the responses in an unused effector, such as the thumb when target sequences consist of the four fingers, shows reduced availability compared to effectors that are used in the sequence. However, it is unclear whether all non-target effectors show an indiscriminate reduction in availability, or whether some are impacted more than others (Duque et al., 2017).

Evidence from transcranial magnetic stimulation (TMS) shows that when the target effector of an upcoming movement becomes known, unused effectors become suppressed along the corticospinal circuit (Duque et al., 2005; Leocani et al., 2000; Sohn et al., 2003). Interhemispheric inhibition of ipsilateral M1 during unimanual hand movements has been well documented (Chettouf et al., 2020), where activation of contralateral M1 results in interhemispheric inhibition through transcallosal connections (Ferbert et al., 1992; Jones et al., 1979; B.-U. Meyer et al., 1995). Further, research investigating fMRI activity patterns in the ipsilateral primary motor cortex (M1) during unimanual finger movements show global suppression, underneath which finger-specific activity patterns are almost identical to those in the contralateral M1 (Diedrichsen et al., 2013). However, competing evidence suggests that suppression during movement planning is modulated by the unselected effe'tor's relevance to the task, with more closely associated effectors being suppressed to a greater

extent, specifically in the context of upper and lower limb movements (Labruna et al., 2014). Such inhibition is thought to reduce competition between movements during action selection implying local, modulated suppression of unused effectors (Bestmann & Duque, 2016). If focal inhibition is used to resolve competitive processes in the planning of single movements, it may play a similar role in the resolution of the CQ gradient when planning movement sequences. Given that the CQ gradient shows parallel planning of individual fingers, modulated by their ordinal position in the upcoming sequence (Kornysheva et al., 2019b; Mantziara et al., 2021), it is possible that the pre-activation gradient also causes suppression in the ipsilateral hemisphere and, by extension, the unused hand contralateral to the upcoming movement. Furthermore, the strength of the CQ gradient predicts the quality of subsequent performance; it may also be possible that the gradient in the unused effector predicts performance in a similar manner.

However, there are several other predictors of movement sequence performance in addition to the quality of motor plans, such as experience playing musical instruments (Sobierajewicz et al., 2018). Musicians can produce successive complex notes with great temporal precision, professional dancers and sporting athletes can execute strings of whole-body movements with little effort, and experienced video gamers often perform great feats of fine motor control. Whilst experience in these forms of expertise has been closely linked to general cognitive (Benz et al., 2016; Choi et al., 2020; Teixeira-Machado et al., 2019) and motor (Landry & Champoux, 2017) benefits, the exact mechanisms that facilitate performance in sequential motor learning tasks, including an overall decrease in production time (Sobierajewicz et al., 2018) and greater timing accuracy when sequences have a fixed temporal structure (Kincaid et al., 2002), are less well-studied. Performance benefits during movement sequence learning tasks have been associated with improvements in motor planning (Ariani & Diedrichsen, 2019), so could expertise lead to greater performance by increasing the efficiency of the CQ process? While this has not been measured directly, research has identified a reduced movement-related cortical potential (MRCP), an increase in amplitude of neural recordings shortly prior to movement initiation (Hallett, 1994), in trained musicians relative to untrained controls (Wright et al., 2012a). This effect was also found when participants underwent extended practice with a musical instrument and suggests that expertise results in more efficient planning processes during motor learning

tasks (Wright et al., 2012b). Moreover, musicians show greater interhemispheric inhibition (Ridding et al., 2000) and a larger corpus callosum (Schlaug et al., 1995) compared to non-musicians, suggesting competition-related interhemispheric inhibition may be greater in those with musical expertise.

Given the unclear role of interhemispheric inhibition of unused effectors in the planning of movement sequences, we trained participants to produce movement sequences on the right and left hands from memory and probed the availability of fingers both used and unused hands during planning. Moreover, with established neural and behavioural differences between individuals with expertise and untrained controls, we investigated the relationship between the amount of music, sports, dance, and video games expertise each participant had with their behavioural signatures of planning in both used and unused effectors. We identified a CQ gradient in the used hand and a mirrored gradient of suppression in the unused hand, with the strength of latter unpredictive of performance. Moreover, we found that expertise was unpredictive of planning signatures, but the number of years participants spent playing musical instruments predicted the speed of sequence execution.

4.3 Results

We trained 58 participants to produce two four-finger sequences from memory as fast and accurately as possible in a delayed sequence production paradigm. The task required both hands; one sequence was produced using the right hand, the other using the left. Two days of training transitioned participants from producing sequences under visual guidance to entirely from memory across three distinct stages (Figure 4.1a). During a final third day, after a short refresher block, a test phase required the sequences to be produced entirely from memory. Sequence production trials began with an abstract visual Sequence Cue displayed 1s prior to the onset of the Go Cue where the participants had to produce the target sequence as fast and accurately as possible (Figure 4.1b). After production, participants received feedback based on the speed and accuracy of their performance. Participants learned to associate both Sequence Cues with their respective sequence through repeated exposure to visually guided trials during training. To ensure performance

reached a similar level of skill to previous research (Yewbrey et al., 2023), we defined a skilled group of participants with an error rate less than 20% during the test phase. These 47 skilled participants produced the target sequences with initial reaction time (RT) *M* = 410.40 ms (*SD* = 66.00), movement time (MT) *M* = 642.50 ms (*SD* = 227.37), and error rate *M* = 10.5 % (*SD* = 5.08). Additionally, to include a greater level of variance to investigate the correlates of skilled performance, we defined a second group of participants who actively engaged in the task despite showing higher error rates than those in the skilled group (see Materials and methods). The 58 participants in this broader group, which also included those in the skilled group, produced the target sequences with RT *M* = 416.67 ms (*SD* = 79.28), MT *M* = 651.04 ms (*SD* = 220.11), and error rate *M* = 14.00 % (*SD* = 9.28). Moreover, since our two target sequences were performed on opposite hands, we wanted to ensure that performance was equal across both with regards to RT, MT, and error rate. In the skilled group, two-tailed, paired samples *t*-tests revealed no significant difference between sequence one (right hand) and two (left hand) for RT (sequence one, *M* = 416.00, *SD* = 72.76; sequence two, *M* = 406.16, *SD* = 64.86; $t(46) = 1.50$, $p = .140$, $d = 0.22$), MT (sequence one, *M* = 638.12, *SD* = 233.40; sequence two, *M* = 638.23, *SD* = 229.12; $t(46) = 0.01$, $p = .994$, $d = 0.00$), and error rate (sequence one, *M* = 11.10, *SD* = 6.80; sequence two, *M* = 9.89, *SD* = 6.48; $t(46) = 0.96$, $p = .340$, $d = 0.14$). We observed similar results in the broader group, with no significant difference between sequence one and two for RT (sequence one, *M* = 429.17, *SD* = 118.49; sequence two, *M* = 416.00, *SD* = 85.20; $t(46) = 1.10$, $p = .272$, $d = 0.15$), MT (sequence one, *M* = 645.87, *SD* = 221.32; sequence two, *M* = 654.10, *SD* = 234.28; $t(46) = 0.56$, $p = .575$, $d = 0.07$), and error rate (sequence one, *M* = 14.20, *SD* = 11.00; sequence two, *M* = 13.71, *SD* = 11.52; $t(46) = 0.29$, $p = .771$, $d = 0.04$), suggesting that both sequences were produced similarly, even when considering a broader range of performance during the task.

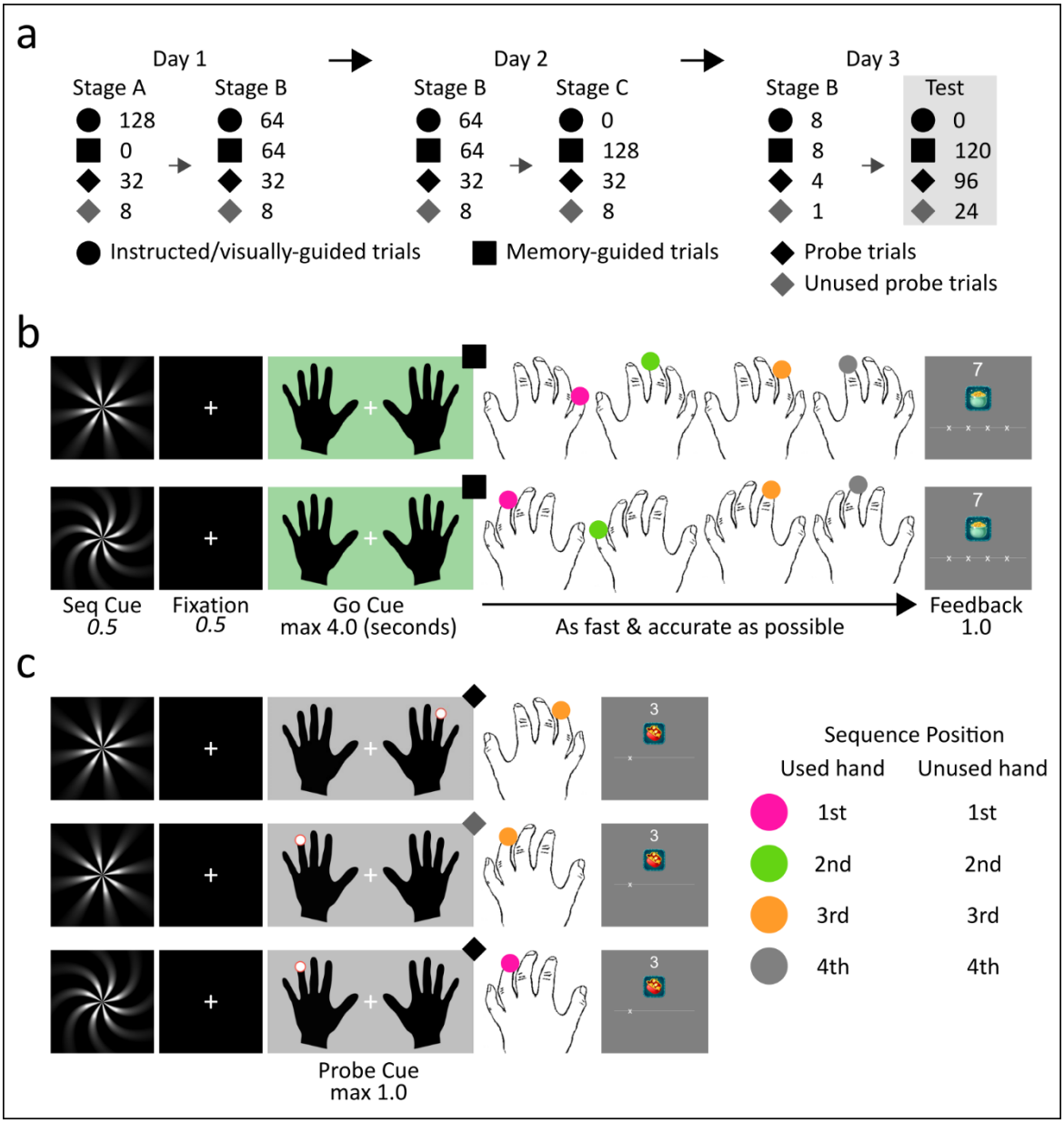

Figure 4.1. Design and experimental conditions. **a**, Trial numbers across the three days of the task, showing the progression of production trials from entirely visually-guided trials (Stage A) to half visually-guided half memory-guided (Stage B) to entirely from memory (Stage C, test). Probe trials were present throughout all Stages of the experiment. The test phase, highlighted by the grey outline, is the focus for analysis. **b**, Production trials consisted of an abstract sequence cue, followed by a fixation cross and a Go Cue which signalled the onset of the production period. The target sequence was produced entirely using the right hand or entirely using the left. Succeeding production, feedback was shown with points awarded depending on speed and accuracy of execution. **c**, Probe trials were almost identical to production trials, but a single press was visually instructed instead of a Go Cue. When the instructed press was a part of the target sequence (Used hand), its position was assigned depending on its position in the sequence. When the instructed press was on the hand contralateral to the target hand (Unused hand), its position was assigned depending on the position of the homologous contralateral finger in the sequence. Seq Cue, Sequence Cue.

4.3.1 Competitive queuing of upcoming finger presses on the prepared hand is reversed on the unprepared hand

To test for the availability of each movement in the sequence shortly prior to execution (Mantziara et al., 2021), half of the trials during the test phase were Probe trials (Figure 4.1c). These Probe trials were identical to regular production trials during the preparation phase but instead of a Go Cue prompting the entire sequence, a Probe Cue prompted the visually-guided production of a single press and its reaction time and error rate indicated its availability at the time of initiation (Mantziara et al., 2021). Additionally, we introduced probe trials that would cue a sequence on one hand but prompt a press on the contralateral hand that is not used to produce the target sequence. The position of these Unused probe trials was labelled according to the position of the homologous contralateral finger in the target sequence (Figure 4.1c). For example, when a sequence on the right hand is cued and the index finger is in the first position, an Unused probe which prompts the index finger of the left hand would be assigned to position number 5. Measuring the strength of the CQ gradient in Unused probes allowed us to investigate whether greater availability in the target effector results in an increased inhibition in the homologous effector on the contralateral side. In addition, to remove RT-related variance across participants, all probes were calculated as a percentage relative to the median RT of the first position for each participant, resulting in position one being set to a baseline of zero percent (Mantziara et al., 2021).

We first sought to assess the presence of a CQ gradient in both used and unused effectors in the skilled group of participants, to analyse a comparative skill level to previous research (Yewbrey et al., 2023). To test for a modulation of finger press availability for fast and accurate production by position on the prepared and unprepared hand, we ran a 2 X 4 repeated measures ANOVA with factors Used/Unused and probe position (1, 2, 3, 4) on RT relative to the first Used probe position (Figure 4.2a). We found a significant main effect of Used/Unused ($F(1,46) = 106.50$, $p < .001$, $\eta p^2 = 0.70$), where Unused probes showed significantly slower relative RT ($M = 11.41\%$, $SE = 1.44$) compared to Used probes ($M = 25.27\%$, $SE = 2.39$), and a main effect of probe position ($F(2.34,107.72) = 6.34$, $p = .001$, $\eta p^2 = 0.12$, Greenhouse-Geisser corrected), with pairwise comparisons (Bonferroni corrected 4 times for position) identifying significant increases from position 1 to positions 2 ($p = .010$, 95% CI [0.94, 9.62]) and 3 ($p = .008$, 95% CI [1.09, 9.95]) respectively. We also found a significant interaction effect ($F(2.49,114.74) = 39.33$, $p < .001$, $\eta p^2 = 0.46$, Greenhouse-

Geisser corrected), which pairwise comparisons (Bonferroni corrected 8 times for Used/Unused X position) found to be driven by significant increases within all positions from Used to Unused (position 1, $p < .001$, 95% CI [24.27, 33.93]; position 2, $p < .001$, 95% CI [6.50, 15.41]; position 3, $p < .001$, 95% CI [5.10, 11.93]; position 4 $p < .001$, 95% CI [4.17, 9.52]), significant increases within Used probes from position 1 to positions 2 ($p < .001$, 95% CI [8.70, 20.00]), 3 ($p < .001$, 95% CI [10.76, 20.87]), and 4 ($p < .001$, 95% CI [9.37, 21.61]), and a significant decrease within Unused probes from position 1 to position 4 ($p = .002$, 95% CI [2.00, 11.56]). These results indicate a gradient is present within Used probes, albeit only between position one and others. Also, Unused probes show overall slower reaction times compared to Used probes, in addition to a mirrored gradient where availability decreases between positions 1 and 4.

To ensure that these RT effects were not driven by changes in the speed accuracy trade-off, we performed a similar analysis with error rate (Figure 4.2b). After converting the number of errors into a percentage relative to the first position in each participant, with the first position set to 0%, we performed another 2 X 4 repeated measures ANOVA with factors Used/Unused and probe position to assess relative errors. We found a significant main effect of Used/Unused ($F(1,46) = 8.91$, $p = .005$, $\eta p^2 = 0.16$), where Unused probes showed greater relative error ($M = 8.52$, $SE = 1.46$) compared to Used probes ($M = 13.68$, $SE = 2.12$). While there was no main effect of probe position ($F(3,138) = 1.45$, $p = .230$, $\eta p^2 = 0.03$), there was a significant Used/Unused X probe position interaction ($F(3,138) = 12.47$, $p < .001$, $\eta p^2 = 0.21$). Pairwise comparisons (Bonferroni corrected 8 times for Used/Unused X position) revealed significant elevations from Used to Unused probes in positions 1 ($p < .001$, 95% CI [11.31, 24.92]) and 2 ($p = .049$, 95% CI [0.02, 12.30]), significant increases within Used probes from position 1 to positions 2 ($p < .001$, 95% CI [3.96, 15.51]), 3 ($p < .001$, 95% CI [6.44, 17.80]), and 4 ($p < .001$, 95% CI [5.54, 18.92]), and no significant differences within Unused probes. However, in Unused probes, a decrease from position 1 to position 3 was close to significance after Bonferroni corrections ($p = .089$, 95% CI [-0.86, 20.02]). These results suggest the presence of an error gradient like that of RT in Used probes, and a similar albeit weaker and near-significant gradient in Unused probes. Therefore, the effects that we observed with relative RT are similarly represented in error rates, and do not appear to be the result of a change in the speed-accuracy trade off. The

presence of an interaction effect with similar directionality in both RT and error rate results suggests that the inhibition of the unused hand is focal, rather than a global effect.

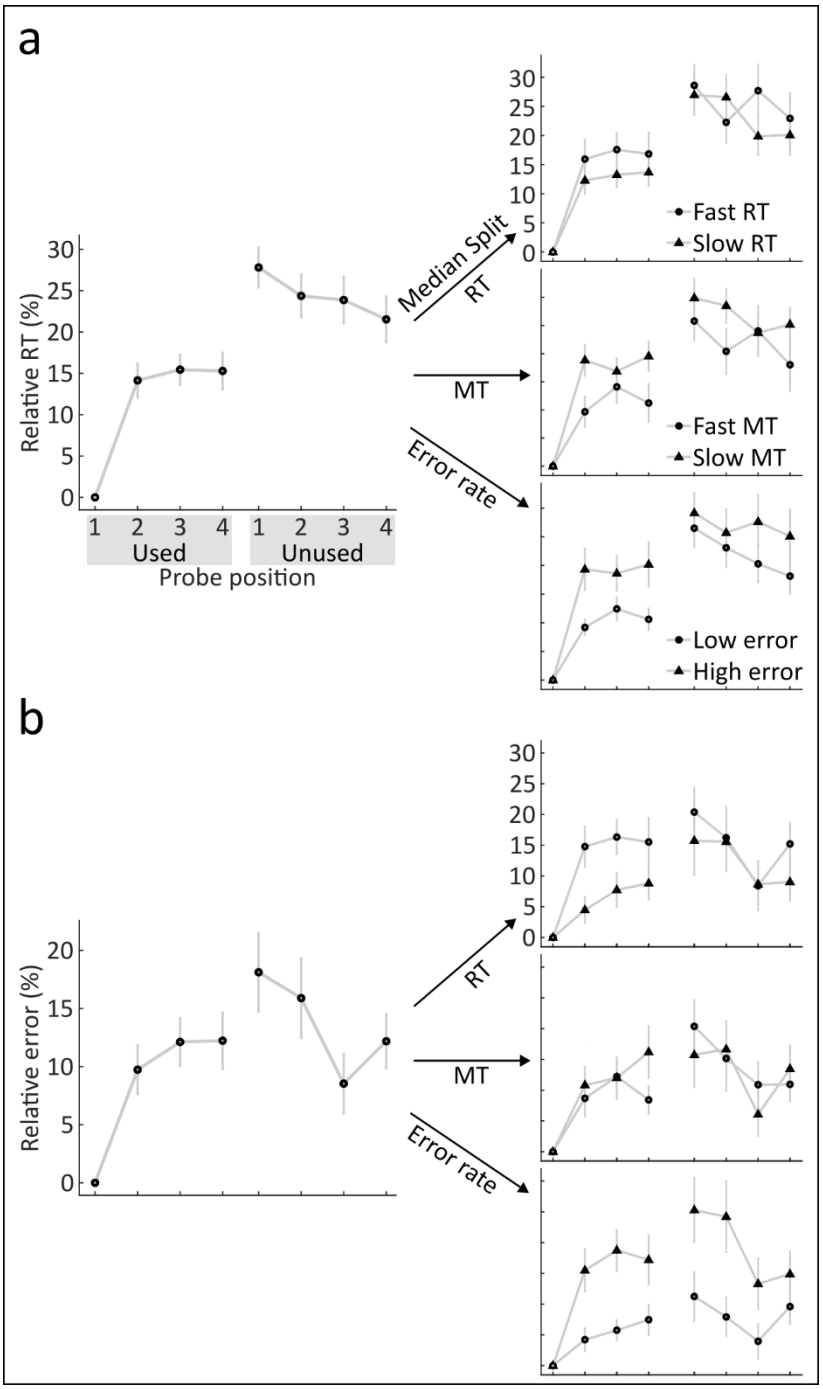

Figure 4.2. CQ gradients for relative RT and relative error. **a,** Left panel, RT of each Probe target position, calculated relative to the RT of the first Probe target position. Right panel, relative RT, as in the left panel, median split according to three performance measures in Go trials: RT, MT, and error rate. **b,** As in a, for press errors of each position relative to the first.

Next, we wanted to see whether an increase in the strength of the CQ gradient in the used hand showed a relationship with the strength of the gradient in the unused hand. To do so, we first calculated the average difference between adjacent Used probe positions

($2^{nd} – 1^{st}$, $3^{rd} – 2^{nd}$, and $4^{th} – 3^{rd}$) for both relative RT and relative error rate for each participant, where higher values suggest greater competitive queueing. We then performed the same calculation for the Unused probe positions, where positive values suggest identical competitive queueing in the unused hand and negative values suggest that later items in a sequence show greater availability compered to earlier items. We ran a Spearman correlation on the resultant values and found a significant positive correlation between the Used and Unused relative RT differences (*rho* = .328, *p* = .025; Figure 4.3a), and a non-significant correlation between Used and Unused relative error differences (*rho* = .110, *p* = .460; Figure 4.3b). These results suggest an increase in CQ gradient on the used hand correlates with an increase in a matching gradient on the unused hand, despite a mirrored gradient in Unused probes observed across the whole group (Figure 4.2a). Together, these findings show a general mirrored CQ gradient in Unused probes across participants that becomes less pronounced the greater the CQ gradient is in Used probes.

We then wanted to test whether the strength of the CQ gradient in the Used hand correlated with the overall inhibition in the Unused hand, so we correlated the relative difference between Used probes with the average relative measures in the Unused hand for both RT (Figure 4.3c) and error rate (Figure 4.3d). Both respective measures correlated significantly (*rho* = .845, *p* < .001; *rho* = .460, *p* = .001), suggesting that greater pre-planning of upcoming movements in the used hand results in greater overall suppression of the unused hand.

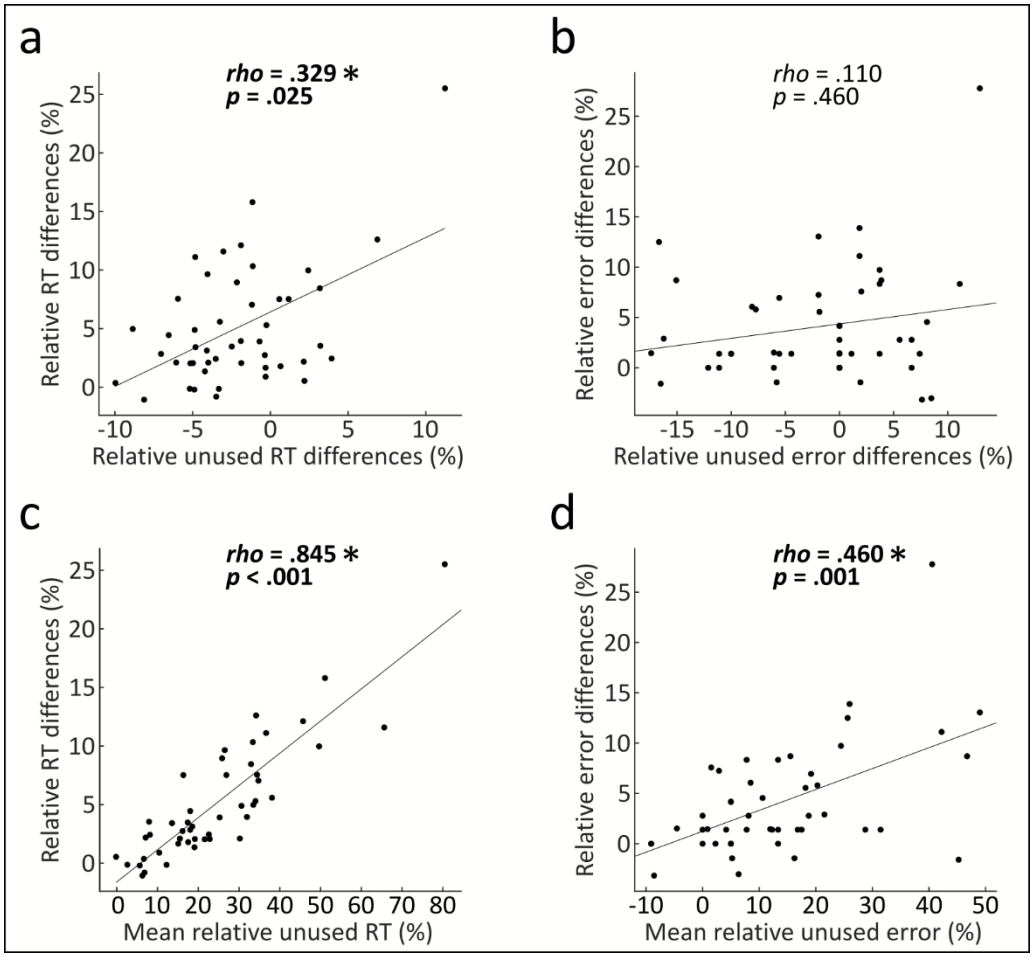

Figure 4.3. Correlations between used and unused CQ gradients. **a,** To measure the strength of the CQ gradient, we took the sum of the mean difference between adjacent positions (–nd - 1st, –rd - 2nd, and –th - 3rd) based on RTs relative to the first position (Probe trials). Greater differences represent a steeper gradient, suggesting greater pre-ordering of upcoming movements during the preparatory period. We then calculated a homologous value for the adjacent positions of Unused probes and ran a Spearman correlation between the two values. Positive values of relative Unused differences equate a CQ gradient that matches the traditional gradient where earlier elements are more available, whereas negative values represent a mirrored gradient where each successive element is more available than the last. **b,** As in a, but for the sum of the mean relative error rate difference between adjacent positions. **c**, Correlation between the sum of the mean relative RT differences between Used probe positions, as in a, with the mean relative RT values of the unused probes. **d,** as in c, but for relative error. *p < .005, Spearman correlation.

4.3.2 Performance correlates with the strength of the used, but not unused, CQ gradient

Given that we observe a CQ gradient in participants, we wanted to assess whether the strength of the gradient was correlated to subsequence performance. To investigate this, we first performed a median split of the skilled group based on three performance factors during Go trials: RT, MT, and error rate, resulting two groups of 23 high- and low-performing participants for each split: low RT and high RT, low MT and high MT, and low error rate and high error rate. Since we had an odd number of participants, the median performing participant from each analysis was excluded. We then calculated the average difference

between adjacent Used probe positions (–nd - 1st, –rd - 2nd, and –th - 3rd) for both relative RT and relative error rate for each participant and compared the values across the high- and low-performing groups for each median split using one-tailed independent samples *t*-tests as we hypothesised significantly greater CQ RT and error gradients for the higher-performing group. For RT gradient, the RT median split showed higher CQ RT gradients in the higher-performing group albeit non-significantly ($t(44) = 0.83$, $p = .409$, $d = 0.25$). For the other splits, however, the lower-performing groups showed greater CQ RT gradients, with MT median split not significant ($t(44) = 1.92$, $p = .061$, $d = 0.57$), but error median split being significant ($t(44) = 2.21$, $p = .032$, $d = 0.65$) in two-tailed *t*-tests. Additionally, we repeated these median split tests for the strength of the unused CQ RT gradients using two-tailed *t*-tests. We found no significant differences across groups for the RT median split ($t(44) = 0.28$, $p = .781$, $d = 0.08$), MT median split ($t(44) = 0.76$, $p = .449$, $d = 0.23$), and error median split ($t(44) = 1.27$, $p = .210$, $d = 0.38$). Next, we assessed the CQ error gradients using median splits. The RT median split showed non-significant higher CQ error gradients in the higher-performing group ($t(44) = 1.40$, $p = .085$, $d = 0.41$, one-tailed). However, both MT ($t(44) = 1.56$, $p = .126$, $d = 0.46$, two-tailed) and error rate ($t(44) = 2.00$, $p = .055$, $d = 0.58$, two-tailed) showed non-significant lower CQ gradients in the higher-performing groups. For the unused CQ error gradients, neither the RT ($t(44) = 0.19$, $p = .853$, $d = 0.06$), MT ($t(44) = 1.00$, $p = .323$, $d = 0.30$), nor error ($t(44) = 1.50$, $p = .143$, $d = 0.44$) median splits showed significant differences across the groups in two-tailed tests. These results suggest that used CQ gradients possess some relationship to performance, whereas unused CQ gradients do not.

To further assess the relationship between CQ and the quality of performance, we ran Spearman correlations between the relative gradients and initiation RT, movement time, and error rate during Go trials, to assess whether the strength of the CQ gradient showed a relationship with performance (Figure 4.4a, b). Based on previous findings, we expected both relative RT and relative error rate to negatively correlate with initiation RT (Mantziara et al., 2021), so we ran one-tailed correlations to attempt to replicate these findings. Relative RT showed a negative but non-significant correlation with initiation RT ($rho = -.069$, $p = .322$), while relative error and initiation RT showed a near-significant negative correlation ($r = -.242$, $p = .050$). Although neither of these correlations are statistically

significant, they replicate the direction of the relationship found previously. For the rest of the correlations, we ran two-tailed Spearman correlations. Next, we correlated relative RT and relative error with movement time, to see if those with more pronounced CQ gradients executed sequences faster or slower. We found a significant positive correlation with relative RT (r = .368, p = .012) and a positive non-significant correlation with relative error (r = .111, p = .458), suggesting those with greater CQ RT gradients performed the sequences slower overall. Finally, we correlated relative RT and relative error with finger error rate, which showed a positive non-significant correlation with relative RT (r = .266, p = .071) and a significant positive correlation with relative error (r = .315, p = .031), suggesting that those with a greater CQ error gradient produced more errors during Go trials than those with a smaller gradient.

In addition to assessing the relationship between Used probes and performance, we also wanted to assess whether Unused probes correlated with performance (Figure 4.4b). Significant correlations would suggest that inhibiting the effector contralateral to movement is important for skilled performance of movement sequences. When performing two-tailed Spearman correlations between relative Unused RT and performance, we found no significant correlations with initiation RT (r = .058, p = .700), movement time (r = .141, p = .342), nor error rate (r = .062, p = .678). We found the same pattern for relative Unused error, where no significant two-tailed Pearson's correlations were found with initiation RT (r = -.003, p = .985), movement time (r = .249, p = .092), nor error rate (r = -.284, p = .053). These results suggest relative inhibition of the fingers on the hand contralateral to movement is not related to the subsequent performance quality of the sequence.

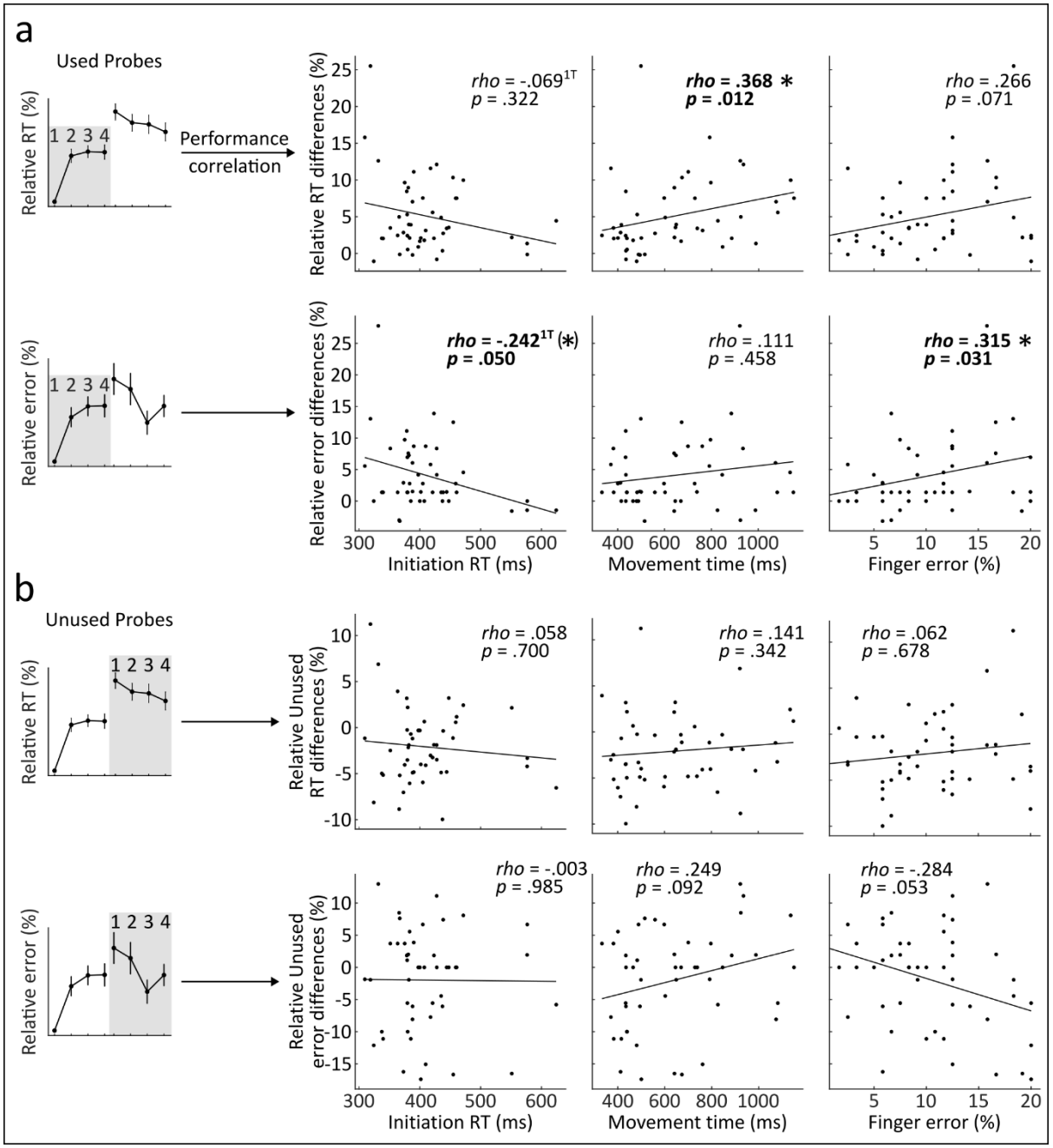

Figure 4.4. CQ gradient correlations with several performance metrics. **a**, To assess how the strength of pre-ordering related to the quality of performance, we correlated the steepness of the relative RT and relative error CQ gradients with initiation RT, movement time, and finger error in Go trials. **b,** As in a, but for Unused probes (Probe trials which prompted a press from the hand that wasn't used to execute the target sequenc[e,] 5[th]-6t[h,] 6[th]-7t[h,] 7[th]-8th). *p < .005, (*)p = .005, Spearman correlation; 1T, one-tailed test.

4.3.3 The CQ gradient is predicted by hours per week playing video games and several performance variables, where the suppression gradient is predicted by movement time

Having identified which elements of performance correlated with the extent of planning, we then looked to assess whether expertise predicted the strength of the CQ gradient in the Used hand and the suppression gradient in the Unused hand. We asked participants

regarding their musical, dance, sports, and video gaming experience: how many years of practice they had, and how many hours per week they practiced. These variables were then used as predictors, alongside performance variables (initiation RT, movement time, and finger error), in four stepwise forward multiple regression models to predict the strength of planning gradients: relative Used RT differences, relative Used error differences, and their respective Unused counterparts. At each step, variables were chosen based on their correlation with the outcome variable and included if their p-value reached a forward criterion of $p <= .050$. For relative Used RT differences, four predictor variables were entered into the model: movement time, hours per week spent gaming, error rate, and initiation RT (Figure 4.5a). Of all predictors, initiation RT was the only negative predictor. For relative Used error differences and relative Unused RT differences, there were no significant predictors entered into the model. For relative Unused error differences, movement time was the only predictor and was positive (Figure 4.5b). This suggests that slower sequence execution, more weekly time spent gaming, higher error rates, and quicker initiation time may result in a greater CQ gradient. Moreover, slower sequence execution also may result in a greater suppression gradient in the Unused hand.

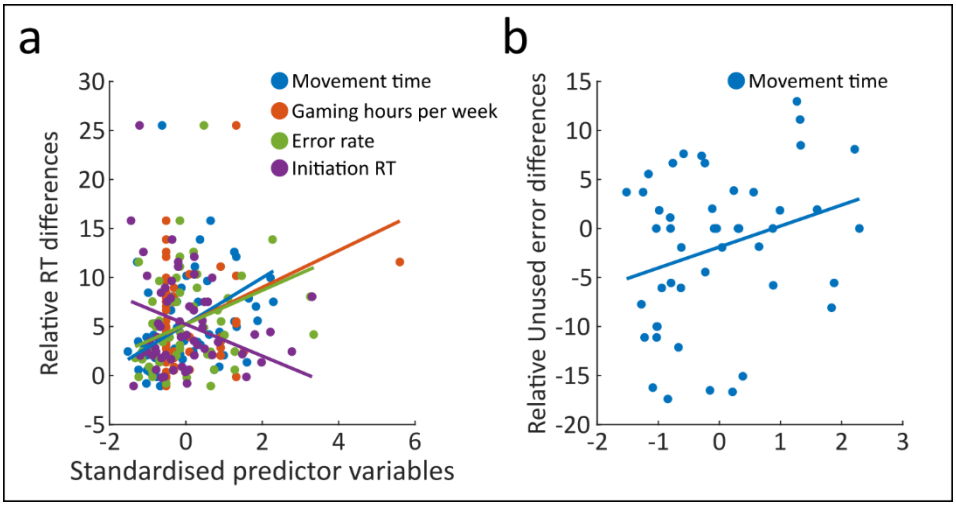

Figure 4.5. Surviving predictors of CQ RT and Unused error gradients following stepwise forward multiple regression. **a,** Performance and expertise variables were entered into a stepwise forward multiple regression model to assess which variables predicted the relative RT differences shown in the CQ gradient. Four predictors survived the forward criterion of $p <= .050$: movement time, hours per week spent gaming, error rate, and initiation RT. **b,** Analysis as in a but for the relative differences for Unused error, representing an error suppression gradient. Movement time was the only predictor that achieved the criteria to be added to the model.

4.4 Discussion

4.4.1 A suppression gradient mirrors the usual CQ gradient in the unused hand

The existence of a CQ gradient for the planning of skilled movement sequences has been established by research using both neural recordings (Kornysheva et al., 2019b) and behavioural measures of reaction time and error rate (Mantziara et al., 2021), however how this system interacts with unused effectors and how it relates to expertise is unclear. Here, we show that alongside the pre-ordering of upcoming movements, the motor system also seems to display a gradient of focal inhibition in matching fingers on the contralateral hand. While the neural mechanism underlying this focal inhibition is not clear based on our current research, the primary motor cortex (M1) has been found to induce cross-callosal inhibition in the opposite M1, ipsilateral to movement (Ni et al., 2009) and unimanual movements elicit almost identical finger-specific activity patterns in the M1 of the hemisphere ipsilateral to movement (Diedrichsen et al., 2013). Given these previous findings, it is possible that the weighted pre-activation of movement elements that we observe during the preparatory period may elicit a homologous pre-suppression of movement elements in the opposite hemisphere. The current research cannot definitively say whether this mechanism is due to active suppression or rather reversed pre-activation as there were fewer unused probe trials than used probe trials resulting in a lower expectancy rate, which could cause slower overall reaction times. Despite this, the interaction gradient effect that is currently observed cannot be explained by a reduced expectancy, and previous research where an unused effector, the thumb, had an equal likelihood to used effectors showed a similar reduction in availability relative to those used effectors (Mantziara et al., 2021). To confirm, future research should include all current unused effectors while ensuring that there are an even number of used and unused probes. Moreover, the correlation that we observe between the strength of the CQ and suppression gradients is positive, suggesting that stronger element pre-ordering actually results in an identical, rather than mirrored, suppression gradient on the unused hand on the individual level. Findings from fMRI show that those voxel groups in the contralateral motor cortex which show the highest activation during movements of each finger also show the greatest activation when movements are produced with the homologous ipsilateral finger (Diedrichsen et al., 2013), providing support for the results that we observe here. Future

studies should investigate can be observed on the individual level, or whether it is a group level phenomenon.

4.4.2 CQ gradient, but not suppression gradient, correlates with behaviour

Previous findings indicate a correlation between CQ gradient and performance (Mantziara et al., 2021). Here we attempted to replicate this finding, however the correlations were not as strong as found previously, especially with regards to e.g. reaction time. While the tasks differed in that the previous research employed a set timing structure to target sequences, the cause of this is unclear. The addition of extra effectors to be probed in the form of the unused hand may have caused participants to perform slower overall on probe trials, although further research is required to investigate this. The current study also reveals that there is no link between the CQ suppression gradient and performance. This seems to be logical, as despite the hemisphere ipsilateral to movement possessing similar neural patterns to those in the contralateral hemisphere (Diedrichsen et al., 2013), the ipsilateral hemisphere does not possess spinal projections to the sequence's target effector.

4.4.3 Video game expertise and performance metrics predict greater CQ gradient separation

We investigated whether CQ and suppression gradient processes were impacted in individuals who had extensive training in music, dance, sports, and video gaming. Of these forms of expertise, the number of hours per week playing video games predicted a greater CQ gradient during this task. While motor (Bickmann et al., 2021; Romano Bergstrom et al., 2012) and cognitive (Choi et al., 2020; Kowal et al., 2018) differences have been between reported between gamers and non-gaming control participants (Granic et al., 2014), there has been little investigation into whether this form of expertise changes or enhances the movement planning processes, despite enhanced movement sequence execution being related to the quality of movement plans (Ariani & Diedrichsen, 2019). Our findings suggest more hours spent per week playing video games leads to benefits in movement planning processes, which in turn is associated with faster sequence initiation. The extent of this benefit should be explored in greater detail by using participants who are involved with competitive eSports and often play video games full time (Sousa et al., 2020). Moreover, the current study investigated expertise using a relatively brief questionnaire, which may have

caused other forms of expertise which might be less common than video gaming to be underrepresented. Future findings should again recruit participants with greater levels of expertise, such as from music, dance, and sports clubs.

Additionally, we found that a greater CQ gradient was predicted by slower movement times, greater error rates, and faster initiation. While faster initiation time replicates previous research, it is unclear why slower and more erroneous movements predict greater CQ processes when previous findings associated greater CQ with higher quality of movements (Kornysheva et al., 2019b; Mantziara et al., 2021). Moreover, faster movement time predicted a greater suppression gradient in the Unused hand. Evidence suggests that competing movements in unused effectors is selectively suppressed to resolve competitive processes (Bestmann & Duque, 2016; Labruna et al., 2014), thus our findings seem to suggest that the more effective such inhibition of unrelated effectors, the quicker sequential movements can be executed.

4.5 Materials and methods

4.5.1 Participants

47 University students (39 Female, *M* = 21.23 years, *SD* = 5.10) achieved an error rate of < 20% during production trials in the test phase, a criterion defined to allow comparison with established findings (Yewbrey et al., 2023). Additionally, we broadened the inclusion criteria so that we could analyse a greater range of performance; 58 participants (47 Female, *M* = 21.00 years, *SD* = 4.70) reached this new criteria of an error rate < 100% and evidence of the following: no extended periods of random key presses, no periods of single key repetitions, no random responses to probe trials, no periods of inactivity, no extended periods of repeating a single sequence, evidence that they were not producing target sequences at random without notice of the sequence cue, and limited numbers of general press errors including mechanical errors. Data from an additional 40 participants did not achieve these broader criteria, so were excluded. All participants were recruited through an online participation panel and were awarded module credits after the completion of each day. Of the skilled group, 45 participants were right-handed and 2 were left-handed (*M* = 77.87 laterality index, *SD* = 37.38, Adapted from Oldfield (1971),

https://www.brainmapping.org/shared/Edinburgh.php). Of the broader group, 55 participants were right-handed and 3 were left-handed (*M* = 77.60 laterality index, *SD* = 39.14). All participants were between the ages of 18 and 65, possessed normal hearing, had normal or corrected-to-normal vision, and had no history of psychiatric or neurological disorders. All participants provided informed consent prior to their participation through an online questionnaire hosted by Qualtrics (Qualtrics, Provo, UT). This experiment and its procedures were approved by the Bangor University School of Psychology Ethics Committee (Ethics approval number 2017-16100-A14905).

4.5.2 Apparatus

All data for this study were collected online using PsychoPy version 2020.2.10 (Peirce et al., 2019), hosted on Pavlovia (https://pavlovia.org/) using the University of Birmingham's site license. The task required participants to use their own hardware including a physical keyboard, and were recommended to launch the experiment using the Chrome browser (https://www.google.com/intl/en_uk/chrome/) which has been verified to produce sub-millisecond timing precision (Bridges et al., 2020). Upon sign-up, participants were each assigned a unique numeric ID that determined which sequence set they would encounter with odd ID numbers assigned sequence set one, and even ID numbers assigned sequence set two.

4.5.3 Experimental design

Participants were trained to produce two four-element movement sequences from memory as fast and accurately as possible in a delayed sequence production paradigm, adapted from previous studies (Kornysheva et al., 2019b; Mantziara et al., 2021; Yewbrey et al., 2023). Each Go trial began with an abstract image (Sequence Cue) that appeared for 500ms, which was associated with a sequence. Sequence Cues were greyscale radial stimuli and generated by varying their curvature and frequency (Hélie & Cousineau, 1998). A short preparatory period followed where a fixation cross was presented for 500ms. Next, two black hands (right and left) appeared against a green background to signify that the participant should execute the target sequence from memory. These Memory trials would end if a participant didn't make a press within two seconds, and within four seconds if a press was made. During training and refresher blocks (see Procedure), a proportion of Go

trials would be Instructed, where a red dot on the tip of the finger on the target hand indicated the target digit and moved to the next target finger after each press. Instructed trials ended after four seconds if no presses were made, and after five seconds if the participant had made a press. After the production period, feedback would appear for 1,000ms displaying how many points were earned that trial (See Feedback) with a visual schematic depicting each press as either correct ('X') or incorrect (indicated by '–'). Alternatively, in Probe trials, only one button press would be cued. The cue could indicate a press that was or was not a member of the target sequence (left or right hand), and the trial would end after one second if no press was made. The overall structure of Probe trials was otherwise the same as Go trials.

In Go trials, participants were awarded up to ten points: five points for initial reaction time, and a further five points for total execution time. For reaction time, points were awarded at thresholds: 0-500ms, 500-700ms, 700-1,000ms, 1,000-2,000ms, 2,000-3,000ms, and >3,000ms, for five, four, three, two, one, and zero points respectively. Furthermore, an additional five points were awarded for total execution time at thresholds: 0-2,000ms, 2,000-3,000ms, 3,000-4,000ms, 4,000-5,000ms, 5,000-6,000, and >6,000 seconds, for five, four, three, two, one, and zero points respectively. In Probe trials, up to five points would be awarded depending on reaction time at thresholds matching those of the Go trials. Additionally, zero points were awarded for all trials in which an incorrect press was made. Auditory feedback accompanied the visual schematic with successive rising tones corresponding to the number of points being played.

Two sets of sequences were distributed across participants based on assigned ID number (see Apparatus). In the skilled group, 27 participants were assigned sequence set one and 20 sequence set two, whereas in the broad group 31 were assigned set one and 27 set two. Within each set, one sequence was produced by the four fingers (index to little) on the right hand and the other on the left hand, and the sequences were manually generated to avoid ascending/descending digit triplets whilst also avoiding biasing extrinsic or intrinsic reference frames (Wiestler et al., 2014).

4.5.4 Procedure

During the first day of training, participants first completed an example block to get familiarised with all three trial types: Instructed, Memory, and Probe. They then proceeded to complete 8 blocks of 16 Instructed trials, five Probe trials where the target press was on the same hand as the cued sequence, and one probe trial where the target was on the opposite hand (unused hand probe). Following a break, they were then informed that the next blocks would feature visually guided trials intermixed with trials from memory. These four blocks contained 8 Instructed, 8 Memory, five Probe, and one unused hand probe, and completion of these blocks marked the end of the first day of training. The second day started with four blocks which matched the makeup of those at the end of the first day. For the final eight blocks of training, they completed 16 Memory trials, five Probes, and one unused Probe. On the third and final day, they completed one refresher block which matched the makeup of the final section of day one. During the test phase, they completed 12 blocks, each consisting of 10 Memory trials, 8 Probe trials, and 2 unused Probe trials. Probe and sequence exposure was pseudorandomised within train and test sections.

Chapter 5 - Discussion

This thesis investigated both the mechanisms and the anatomical regions underlying movement planning and execution, including how such mechanisms might allow the motor system to transition from the former to the latter. The following chapter will begin with an overview of the results obtained from *Chapters 2*, *3*, and *4*. The findings are then discussed with respect to the wider motor learning literature, bridging the gap between the cognitive and strictly motoric aspects of the motor hierarchy and planning literature. The functions and interactions of individual anatomical regions are speculated to form a systems level framework for hierarchical motor function across planning and execution. The implications of such a model are then discussed with respect to clinical examples and future research avenues.

5.1 Overview

Movement sequences are often referred to as hierarchical structures, consisting of high- and low-level process including action selection, intermediate, and execution layers (Diedrichsen & Kornysheva, 2015a). This structure allows the motor system to flexibly recombine known features, such as the order and timing of movements, to facilitate the learning of new sequences (Kornysheva et al., 2013; Ullén & Bengtsson, 2003). Moreover, recent advancements in neuroimaging and multivariate analysis have allowed for anatomical localisation of hierarchical layers, with high-level elements thought to occupy secondary motor regions (Kornysheva & Diedrichsen, 2014; Russo et al., 2020; Yokoi & Diedrichsen, 2019a) and low-level elements occupying primary motor and somatosensory cortices (Ariani et al., 2022; Berlot et al., 2020; Yokoi et al., 2018). Yet, with a rapidly growing field of research investigating movement preparation (Haith & Bestmann, 2020), it is not clear whether such rigid separation persists across both planning and execution. Research from neurophysiology suggests that for single movements, informative activity during the planning period occupies a subspace in which the output is null to downstream connections (Kaufman et al., 2014), where the cortex receives an indiscriminate signal to move from subcortical structures which marks the point of initiation and causes transition of maintained activity into an orthogonal potent subspace (Inagaki et al., 2018, 2022; Kaufman et al., 2016). These mechanisms are thought to act alongside interhemispheric and

corticospinal inhibition (Duque et al., 2017) to allow the motor system to effectively prepare upcoming movements whilst avoiding unintentional readout by downstream motor neurons and subsequently muscles. These findings in single movements have intriguing implications for the planning and execution of movement sequences; are holistic sequences also planned by a transition into orthogonal subspace? What role does inhibition play in the planning of multiple upcoming movements?

This thesis identified a high- to low-level hierarchical shift from planning to execution in the cortex, represented by a shift from order and timing control to integration alongside online timing. Additionally, the hippocampus specified the order of upcoming movements prior to initiation. Moreover, it identified shifts in the occupied subspace of basal ganglia, thalamus, and hippocampus across movement phases, in addition to a selective finger-specific gradient of inhibition in the effector contralateral to movement during planning. The implications of these findings and how they relate to the current literature are discussed in the subsequent sections of this chapter.

5.2 A Systems-Level Hierarchical Shift from Planning to Execution

Chapters 2 and *3* used multivariate pattern analysis and principal component analysis to investigate the presence of order, timing, and integration (sequence features) during planning and execution, in addition to changes in the low dimensional distance between the neural patterns of each movement phase for each given sequence. Firstly, of note is the minimal presence of sequence features during planning in the cortex; order and marginal timing only seemed to be present within superior parietal and ventral premotor cortices. By far the strongest effect, however, was the pre-ordering of movements in hippocampus, an effect that has been also shown by findings in the context of episodic memory (Davachi & DuBrow, 2015).

The mechanism observed may be related to CQ, as findings from multivariate analysis of MEG signals suggest that the CQ signal originates in parahippocampal regions (Kornysheva et al., 2019a). Further, the hippocampus has extensive connections to the cortex, of which the connections to the parietal lobe make up the extensive ‘where’ pathway in the dual stream model of memory (Huang et al., 2021). The superior parietal cortex has been implicated in the planning of movement (Gallivan et al., 2013) and represents movement

intentions in absence of exact motoric requirements (Henderson et al., 2022; Shushruth et al., 2022), thus may work in tandem with the hippocampus to retrieve and order upcoming movements associated with the sequence cue, then maintain motor goals during the delay period prior to movement. Moreover, these regions have been found to interact closely during navigation tasks, where hippocampal grid cells encode world-centered coordinates that the parietal cortex converts into body-based coordinates, allowing for effective locomotion and guidance (Rolls, 2020; Whitlock et al., 2008). In a similar manner, it could be that sequential movement tasks may require the superior parietal lobule to map the abstract order of movements generated by the hippocampus CQ onto intrinsic, body-centered reference frames (Wiestler et al., 2014). However, future research should use electrophysiology, or non-invasive neural recordings with a high temporal resolution such as MEG and EEG, to investigate whether such mapping occurs during planning, initiation, or execution.

With a potential CQ source identified through a hippocampal-parietal interaction, *Chapter 4* identified a traditional CQ gradient using behavioural methods (Mantziara et al., 2021) but additionally a mirrored gradient of suppression on the hand contralateral to the one to be used in the upcoming movement, where fingers become less available the more that their contralateral counterpart in intrinsic space is prepared. General interhemispheric inhibition has been shown previously during motor tasks with respect to M1 (Perez & Cohen, 2009), with functional inhibition being discussed in the introduction of this thesis (see 1.2.1 Planning as a distinct neural state to execution; Duque et al., 2017), however based on the findings from *Chapter 2* and *Chapter 3* the observed gradient inhibition is likely to originate from hippocampal or parietal regions. There is limited evidence for such a phenomenon, although findings from TMS suggest that stimulation of the anterior intraparietal sulcus results in inhibition of the contralateral primary motor cortex (Koch et al., 2009) so this mechanism is not unlikely, yet further research is required to determine whether this effect is entirely functionally mediated. Having identified a potential mechanism of inhibition, we can now propose an update to the established CQ model (Bullock, 2004; Bullock & Rhodes, 2002) where the nodes contained in the competitive choice layer don't just actively inhibit competing movements on the target hand, but also the homologous finger on the contralateral hand. This would provide us with a solid

framework to explain the phenomenon that we observed in the results of *Chapter 4* and allow computational modelling studies a foundation to further investigate the proposed mechanism.

Despite a clear system for the definition and mapping of movement order preceding movement, the planning of independent timing was seemingly absent. Contemporary research into the planning of movement timing suggests that the representation of a timing structure is volatile and cannot be prepared a priori to be stored for later use (Maslovat & Klapp, 2022). More specifically, the authors propose that a temporary neural network is generated just prior to response initiation, which utilizes neural transmission delays to generate different lengths of temporal intervals between elements of movement sequences (Klapp & Maslovat, 2020), providing a potential explanation for why we do not observe timing during the lengthy period preceding movement in the current task. Only while the movement is being executed do we see extensive control of independent timing across bilateral motor and prefrontal cortices. Curiously, despite heavy links to timing processes, neither cerebellum nor basal ganglia show significant sequential timing control (Kunimatsu et al., 2018; Narain et al., 2018; Tanaka et al., 2021). This may be due to the way we kept the inter-press intervals consistent yet rearranged across timing conditions; these subcortical regions may simply be tuned towards control of individual timing intervals which would cause sequences to become identical at the temporal scale of fMRI given the relatively sluggish BOLD response (Logothetis, 2003). Coincidentally, this null finding may provide more evidence that the timing control that occurs in the cortex is related to the entire timing structure across a sequence.

So, despite timing not being planned a priori, the order of movements in an upcoming sequence is planned by complementary processes in hippocampal and parietal regions. Upon initiation, evidence from rodent electrophysiology suggests that the transition from planning to execution begins with a signal to move which ascends, from the pons through the thalamus, into the cortex (Inagaki et al., 2018, 2022). While we did not attempt to identify such a signal directly using fMRI, we showed that multivariate distance in the thalamus, alongside basal ganglia and hippocampus, between neural patterns for sequential planning and execution was significantly greater than carefully controlled simulations with no distance. Moreover, we observed a cluster of integration in the thalamus that, although

not significant after Bonferroni correction across regions, could indicate that it processed information that was unique to each sequence. Our results do not provide direct evidence in support of the ascending signal theory, but suggest it remains a strong possibility and provide evidence against the aged idea that the thalamus is solely a relay station for sensory inputs to the cortex (Shine et al., 2023). What is clear is that neural patterns become rearranged, best represented by the state shift from high- to low-level control that occurs across motor cortical regions. This state shift also appears to happen trial by trial, indicating that processing the order initially during planning to later combine with timing provides some kind of benefit to the system or to performance. We hypothesise that such a mechanism allows the system to remain flexible, should task demands change shortly prior to initiation. Results from neurophysiology in rodents indeed suggest that a task which requires flexibility can induce in greater cortical involvement during sequence learning tasks, rather than the movement kinematics being stored directly within the basal ganglia such as in previous studies of over-learnt repetitive sequence tasks (Harpaz et al., 2022; Mizes et al., 2023b). Thus, our event-related design results in a contextual interference training regime (Heald et al., 2021; Magill & Hall, 1990), requiring flexibility which might bias the motor system into the primarily cortical control we observed during execution (Cross et al., 2007; Wymbs & Grafton, 2013). It would be valuable for future research to train participants using an overly repetitive training regimen to see if alternative brain regions, including subcortical structures, are employed under such conditions. However, it is important to note that these findings were drawn from neurophysiological recordings in rodents, and there are several major differences in the anatomy of the corticospinal tract between primates and rodents (Lemon, 2008). Research tracing synaptic connections in non-human primates using retrograde rabies virus revealed unique cortico-motoneuronal (CM) cells in M1 with monosynaptic connections to motoneurons which directly innervate the finger muscles (Rathelot & Strick, 2009). As such, the lack of these CM cells in rodents may cause a greater reliance on storage of movement kinematics in the basal ganglia as opposed to the cortex.

The highlighted results of this thesis clearly indicate that the planning and execution of movement sequences is a systems-level process that requires a plethora of brain regions, both cortical and subcortical, performing distinct roles at specific stages of movement. The

order of movements, belonging to the more cognitive-related 'What' category of motor planning (Haith & Bestmann, 2020; Wong et al., 2015), is planned a priori by a hippocampal-parietal network and causes inhibition of competing effectors through the motor system ipsilateral to the upcoming movement. Timing, however, another feature belonging to 'What', shows some albeit limited planning a priori while being implemented heavily during execution across the cortex. 'How', the category related to the definition of movement kinematics and thought of as purely motor generation, occurs during execution across the premotor to parietal cortex. As such, these results provide evidence for a systems-level hierarchical shift from high- to low-level hierarchical sequence features.

An analogy could be made between the hierarchical shift we observe and the populations of neurons that operate within output-null and output-potent dimensions (Kaufman et al., 2014). In the research carried out in this thesis, particularly in parietal cortex, overlapping neuronal populations seem to control for order and timing during planning, which transition to integration during execution. This is similar to previously observed findings in electrophysiology where neuronal activity is informative of movement parameters such as velocity (Churchland et al., 2006), direction (Messier & Kalaska, 2000; Riehle & Requin, 1989), and movement order (Tanji & Shima, 1994) during the planning period but shifts in multidimensional representations during execution to a format that drives downstream neurons to produce movement (Inagaki et al., 2018; Kaufman et al., 2016).

5.3 Future Research Directions and limitations

Questions remain which require future research using alternate methodology to gain further insight and build a clearer understanding of how the system interacts. Firstly, while we investigated the neural distance between planning and execution in subcortical regions, we did not investigate whether this mechanism was also present in the cortex. Due to the observed shift in sequence feature control it would be easy to assume such distances would also be present in cortical regions, yet recent findings, posted as a preprint after the publication of *Chapter 2*, suggest that sequence-specific representations in secondary motor regions such as dorsal premotor and anterior superior parietal cortex were maintained across planning and execution, as opposed to primary motor cortex whose representations switched (Ariani et al., 2023). These opposing findings warrant further investigation but could be caused by some differences in design choices: this research used a similar Go No-

Go design to *Chapters 2* and *3*, sequences were executed as fast as possible with no timing structure and consisted of repeated presses of three fingers. Moreover, this research used single versus multi-finger sequences to produce evidence of planning during execution across several regions, which our experiment was unable to detect as all sequences contained the same movement elements. As such, it is currently not clear what role planning during execution plays in our task specifically, and in the systems-level hypothesis, warranting further research using methods with greater temporal resolution such as MEG to attempt to detect the planning of upcoming presses while the prior is being executed.

Regarding *Chapter 4*, we show that the availability of fingers on the hand contralateral to the cued movement was generally lower than the availability of those on the cued hand, alongside the mirrored gradient. While the differentiation between unused fingers is solid, it is unclear whether the general effect of non-finger specific reduced availability in the unused relative to used hand is due to interhemispheric suppression, or just lowered expectancy given these trials were much less common than trials that cued the upcoming hand. The latter is unlikely, however, as previous research showed a similar effect where the unused effector was suppressed despite an equal number of used and unused effector probe trials (Mantziara et al., 2021). There is a need for neural recordings to identify whether this is active suppression, and whether or not a competitive suppression gradient can be identified based on pattern probabilities using linear decoding (Kornysheva et al., 2019a). Furthermore, investigating the nature of this inhibition mechanism may lead to models which explain how certain disorders, such as Parkinson's disease, have trouble initiating movements (Rubin et al., 2012), as there is reduced suppression of competing movements.

5.4 Implications for Neurological Disorders

As discussed in *Chapter 1* (see 1.1 Neural control of movement sequences), neurological disorders that cause motor deficits can cause malfunction in various regions and mechanisms across the brain. Parkinson's disease results in a loss of dopaminergic neurons in the substantia nigra, resulting in misfunction of the basal ganglia (Rubin et al., 2012). Based on results from this thesis, the BG do not seem to show a tuning to sequence features, or their integration, but increase in activity and shift their neural patterns from planning to execution. This suggests that their role may be more related to the execution of

single movements, which we would not be able to detect using the current paradigm as sequences consisted of the same constituent presses in different orders. As such, the basal ganglia may be more concerned with lower-level 'How' processes, as opposed to higher-level 'What' (Haith & Bestmann, 2020; Wong et al., 2015). Contrastingly, Alzheimer's disease, which stereotypically causes significant degeneration of the hippocampus (Dubois et al., 2016; Förstl & Kurz, 1999), might result in a breakdown of 'What', due to the hippocampus primarily processing higher-level order during planning. Such breakdown of sequential order in Alzheimer's patients has been observed in spatial navigation tasks, where the order of reaches was impaired but the location of targets remained intact (Kalová et al., 2005); this breakdown of order has been proposed to underly key deficits in working memory observed in patients (De Belder et al., 2017). Given how crucial the order of movements is when executing a sequence, an intriguing avenue for future research would be to observe the definition of movement order during movement planning in the parietal cortex in Alzheimer's patients, which would reveal whether the hippocampus is necessary for the parietal cortex to be able to define the upcoming order. If not, it would suggest some distinct mechanism in parietal cortex allowing long-term storage of movement sequences in an abstract form. Moreover, if the degeneration in hippocampus prevents it from planning the movement order, the hemisphere ipsilateral to movement may not become selectively inhibited, as was observed in *Chapter 4*, leading to greater levels of cross-callosal competition in the competitive choice layer and causing difficulty inhibiting competing plans, resulting in greater difficulty initiating movement or producing movement in the correct order, leading to transposition errors.

5.5 Closing Remarks

The order and timing of movement sequences are crucial elements that must be combined efficiently and precisely to produce effective and flexible movements. These sequence features also exist at different levels of a conceptual motor hierarchy which allows for flexible selection and recombination when task demands vary. This thesis investigated the neural basis of sequence features during the planning period and incorporated such findings with established literature, showing that order is planned by a hippocampal-parietal network, and that this causes inhibition of competing effectors, even in the contralateral hemisphere. Upon initiation, representations across the cortex shift from high-level abstract

plans into lower-level execution-related control, mirroring similar findings of orthogonal subspaces from neuronal population recordings only on a larger scale. This systems-level hypothesis of a hierarchical shift allows clear pathways for research to investigate functional deficits in Parkinson's and Alzheimer's patients, while providing a solid foundation and predictions for future basic science to investigate.

References

Abrahamse, E. L., Ruitenberg, M. F. L., de Kleine, E., & Verwey, W. B. (2013). Control of automated behavior: Insights from the discrete sequence production task. *Frontiers in Human Neuroscience*, *7*(MAR), 82. https://doi.org/10.3389/fnhum.2013.00082

Acuna, D. E., Wymbs, N. F., Reynolds, C. A., Picard, N., Turner, R. S., Strick, P. L., Grafton, S. T., & Kording, K. P. (2014). Multifaceted aspects of chunking enable robust algorithms. *Journal of Neurophysiology*, *112*(8), 1849–1856. https://doi.org/10.1152/jn.00028.2014

Adams, P., Guillery, R. W., Sherman, S. M., Sillito, A. M., Sherman, S. M., & Guillery, R. W. (2002). The role of the thalamus in the flow of information to the cortex. *Philosophical Transactions of the Royal Society of London. Series B: Biological Sciences*, *357*(1428), 1695–1708. https://doi.org/10.1098/rstb.2002.1161

Albanese, A., Bhatia, K., Bressman, S. B., DeLong, M. R., Fahn, S., Fung, V. S. C., Hallett, M., Jankovic, J., Jinnah, H. A., Klein, C., Lang, A. E., Mink, J. W., & Teller, J. K. (2013). Phenomenology and classification of dystonia: A consensus update. *Movement Disorders*, *28*(7), 863–873. https://doi.org/10.1002/mds.25475

Albouy, G., Fogel, S., King, B. R., Laventure, S., Benali, H., Karni, A., Carrier, J., Robertson, E. M., & Doyon, J. (2015). Maintaining vs. Enhancing motor sequence memories: Respective roles of striatal and hippocampal systems. *NeuroImage*, *108*, 423–434. https://doi.org/10.1016/j.neuroimage.2014.12.049

Albouy, G., King, B. R., Maquet, P., & Doyon, J. (2013). Hippocampus and striatum: Dynamics and interaction during acquisition and sleep-related motor sequence memory consolidation. *Hippocampus*, *23*(11), 985–1004. https://doi.org/10.1002/hipo.22183

Albouy, G., Sterpenich, V., Balteau, E., Vandewalle, G., Desseilles, M., Dang-Vu, T., Darsaud, A., Ruby, P., Luppi, P.-H., Degueldre, C., Peigneux, P., Luxen, A., & Maquet, P. (2008). Both the hippocampus and striatum are involved in consolidation of motor sequence memory. *Neuron*, *58*(2), 261–272. https://doi.org/10.1016/j.neuron.2008.02.008

Ames, K. C., Ryu, S. I., & Shenoy, K. V. (2014). Neural Dynamics of Reaching following Incorrect or Absent Motor Preparation. *Neuron*, *81*(2), 438–451. https://doi.org/10.1016/j.neuron.2013.11.003

Ariani, G., & Diedrichsen, J. (2019). Sequence learning is driven by improvements in motor planning. *Journal of Neurophysiology*, *121*(6), 2088–2100. https://doi.org/10.1152/jn.00041.2019

Ariani, G., Kordjazi, N., Pruszynski, J. A., & Diedrichsen, J. (2021). The Planning Horizon for Movement Sequences. *eNeuro*, *8*(2), ENEURO.0085-21.2021. https://doi.org/10.1523/ENEURO.0085-21.2021

Ariani, G., Pruszynski, J. A., & Diedrichsen, J. (2022). Motor planning brings human primary somatosensory cortex into action-specific preparatory states. *eLife*, *11*. https://doi.org/10.7554/elife.69517

Ariani, G., Shahbazi, M., & Diedrichsen, J. (2023). *Cortical areas for planning sequences before and during movement* (p. 2023.11.05.565682). bioRxiv. https://doi.org/10.1101/2023.11.05.565682

Ariani, G., Wurm, M. F., & Lingnau, A. (2015). Decoding internally and externally driven movement plans. *Journal of Neuroscience*, *35*(42), 14160–14171. https://doi.org/10.1523/JNEUROSCI.0596-15.2015

Averbeck, B. B., Chafee, M. V., Crowe, D. A., & Georgopoulos, A. P. (2002). Parallel processing of serial movements in prefrontal cortex. *Proceedings of the National*

Academy of Sciences of the United States of America, *99*(20), 13172–13177. https://doi.org/10.1073/pnas.162485599

Averbeck, B. B., Chafee, M. V., Crowe, D. A., & Georgopoulos, A. P. (2003). Neural activity in prefrontal cortex during copying geometrical shapes. I. Single cells encode shape, sequence, and metric parameters. *Experimental Brain Research*, *150*(2), 127–141. https://doi.org/10.1007/s00221-003-1416-6

Bednark, J. G., Campbell, M. E. J., & Cunnington, R. (2015). Basal ganglia and cortical networks for sequential ordering and rhythm of complex movements. *Frontiers in Human Neuroscience*, *9*(JULY), 1–13. https://doi.org/10.3389/fnhum.2015.00421

Bengtsson, S. L., Ehrsson, H. H., Forssberg, H., & Ullén, F. (2004). Dissociating brain regions controlling the temporal and ordinal structure of learned movement sequences. *European Journal of Neuroscience*, *19*(9), 2591–2602. https://doi.org/10.1111/j.0953-816X.2004.03269.x

Benjamin, P., Staras, K., & Kemenes, G. (2010). What roles do tonic inhibition and disinhibition play in the control of motor programs? *Frontiers in Behavioral Neuroscience*, *4*. https://www.frontiersin.org/articles/10.3389/fnbeh.2010.00030

Benz, S., Sellaro, R., Hommel, B., & Colzato, L. S. (2016). Music Makes the World Go Round: The Impact of Musical Training on Non-musical Cognitive Functions—A Review. *Frontiers in Psychology*, *6*. https://www.frontiersin.org/articles/10.3389/fpsyg.2015.02023

Berlot, E., Popp, N. J., & Diedrichsen, J. (2020). A critical re-evaluation of fmri signatures of motor sequence learning. *eLife*, *9*, 1–24. https://doi.org/10.7554/eLife.55241

Berlot, E., Popp, N. J., Grafton, S. T., & Diedrichsen, J. (2021a). Combining Repetition Suppression and Pattern Analysis Provides New Insights into the Role of M1 and

Parietal Areas in Skilled Sequential Actions. *The Journal of Neuroscience*, *41*(36), 7649–7661. https://doi.org/10.1523/jneurosci.0863-21.2021

Berlot, E., Popp, N. J., Grafton, S. T., & Diedrichsen, J. (2021b). Combining Repetition Suppression and Pattern Analysis Provides New Insights into the Role of M1 and Parietal Areas in Skilled Sequential Actions. *The Journal of Neuroscience*, *41*(36), 7649–7661. https://doi.org/10.1523/jneurosci.0863-21.2021

Bestmann, S., & Duque, J. (2016). Transcranial Magnetic Stimulation: Decomposing the Processes Underlying Action Preparation. *The Neuroscientist*, *22*(4), 392–405. https://doi.org/10.1177/1073858415592594

Bianco, R., Novembre, G., Keller, P. E., Villringer, A., & Sammler, D. (2018). Musical genre-dependent behavioural and EEG signatures of action planning. A comparison between classical and jazz pianists. *NeuroImage*, *169*, 383–394. https://doi.org/10.1016/j.neuroimage.2017.12.058

Bickmann, P., Wechsler, K., Rudolf, K., Tholl, C., Froböse, I., & Grieben, C. (2021). Comparison of Reaction Time Between eSports Players of Different Genres and Sportsmen. *International Journal of eSports Research (IJER)*, *1*(1), 1–16. https://doi.org/10.4018/IJER.20210101.oa1

Biotteau, M., Chaix, Y., & Albaret, J.-M. (2016). What Do We Really Know About Motor Learning in Children with Developmental Coordination Disorder? *Current Developmental Disorders Reports*, *3*(2), 152–160. https://doi.org/10.1007/s40474-016-0084-8

Bosch-Bouju, C., Hyland, B. I., & Parr-Brownlie, L. C. (2013). Motor thalamus integration of cortical, cerebellar and basal ganglia information: Implications for normal and

parkinsonian conditions. *Frontiers in Computational Neuroscience*, *0*(NOV), 163. https://doi.org/10.3389/fncom.2013.00163

Bostan, A. C., & Strick, P. L. (2018). The basal ganglia and the cerebellum: Nodes in an integrated network. *Nature Reviews Neuroscience*, *19*(6), 338–350. https://doi.org/10.1038/s41583-018-0002-7

Bridges, D., Pitiot, A., MacAskill, M. R., & Peirce, J. W. (2020). The timing mega-study: Comparing a range of experiment generators, both lab-based and online. *PeerJ*, *8*, e9414. https://doi.org/10.7717/peerj.9414

Brooks, D. N., & Baddeley, A. D. (1976). What can amnesic patients learn? *Neuropsychologia*, *14*(1), 111–122. https://doi.org/10.1016/0028-3932(76)90012-9

Buch, E. R., Claudino, L., Quentin, R., Bönstrup, M., & Cohen, L. G. (2021). Consolidation of human skill linked to waking hippocampo-neocortical replay. *Cell Reports*, *35*(10), 109193. https://doi.org/10.1016/j.celrep.2021.109193

Buckner, R. L. (2013). The Cerebellum and Cognitive Function: 25 Years of Insight from Anatomy and Neuroimaging. *Neuron*, *80*(3), 807–815. https://doi.org/10.1016/j.neuron.2013.10.044

Buhusi, C. V., & Meck, W. H. (2005). What makes us tick? Functional and neural mechanisms of interval timing. *Nature Reviews Neuroscience*, *6*(10), Article 10. https://doi.org/10.1038/nrn1764

Bullock, D. (2004). Adaptive neural models of queuing and timing in fluent action. *Trends in Cognitive Sciences*, *8*(9), 426–433. https://doi.org/10.1016/j.tics.2004.07.003

Bullock, D., & Rhodes, B. (2002). *Competitive queing for planning and serial performance*. Boston University Center for Adaptive Systems and Department of Cognitive …. https://open.bu.edu/handle/2144/2291

Byl, N. N., Merzenich, M. M., & Jenkins, W. M. (1996). A primate genesis model of focal dystonia and repetitive strain injury: I. Learning-induced dedifferentiation of the representation of the hand in the primary somatosensory cortex in adult monkeys. *Neurology*, *47*(2), 508–520. https://doi.org/10.1212/WNL.47.2.508

Calderon, C. B., Verguts, T., & Frank, M. J. (2022). Thunderstruck: The ACDC model of flexible sequences and rhythms in recurrent neural circuits. *PLoS Computational Biology*, *18*(2 February 2022), 1–33. https://doi.org/10.1371/journal.pcbi.1009854

Chabrol, F. P., Blot, A., & Mrsic-Flogel, T. D. (2019). Cerebellar Contribution to Preparatory Activity in Motor Neocortex. *Neuron*, *103*(3), 506-519.e4. https://doi.org/10.1016/j.neuron.2019.05.022

Chettouf, S., Rueda-Delgado, L. M., De Vries, R., Ritter, P., & Daffertshofer, A. (2020). Are unimanual movements bilateral? *Neuroscience & Biobehavioral Reviews*, *113*, 39–50. https://doi.org/10.1016/j.neubiorev.2020.03.002

Choi, E., Shin, S.-H., Ryu, J.-K., Jung, K.-I., Kim, S.-Y., & Park, M.-H. (2020). Commercial video games and cognitive functions: Video game genres and modulating factors of cognitive enhancement. *Behavioral and Brain Functions*, *16*(1), 2. https://doi.org/10.1186/s12993-020-0165-z

Christian, K. M., & Thompson, R. F. (2003). Neural Substrates of Eyeblink Conditioning: Acquisition and Retention. *Learning & Memory*, *10*(6), 427–455. https://doi.org/10.1101/lm.59603

Churchland, M. M., Cunningham, J. P., Kaufman, M. T., Ryu, S. I., & Shenoy, K. V. (2010). Cortical Preparatory Activity: Representation of Movement or First Cog in a Dynamical Machine? *Neuron*, *68*(3), 387–400. https://doi.org/10.1016/j.neuron.2010.09.015

Churchland, M. M., Santhanam, G., & Shenoy, K. V. (2006). Preparatory Activity in Premotor and Motor Cortex Reflects the Speed of the Upcoming Reach. *Journal of Neurophysiology*, *96*(6), 3130–3146. https://doi.org/10.1152/jn.00307.2006

Cisek, P., & Kalaska, J. F. (2005). Neural correlates of reaching decisions in dorsal premotor cortex: Specification of multiple direction choices and final selection of action. *Neuron*, *45*(5), 801–814. https://doi.org/10.1016/j.neuron.2005.01.027

Clower, W. T. (1998). Early Contributions to the Reflex Chain Hypothesis. *Journal of the History of the Neurosciences*, *7*(1), 32–42. https://doi.org/10.1076/jhin.7.1.32.13099

Cohen, N. J., & Squire, L. R. (1980). Preserved Learning and Retention of Pattern-Analyzing Skill in Amnesia: Dissociation of Knowing How and Knowing That. *Science*, *210*(4466), 207–210. https://doi.org/10.1126/science.7414331

Conditt, M. A., & Mussa-Ivaldi, F. A. (1999). Central representation of time during motor learning. *Proceedings of the National Academy of Sciences of the United States of America*, *96*(20), 11625–11630. https://doi.org/10.1073/pnas.96.20.11625

Cox, D. D., & Savoy, R. L. (2003). Functional magnetic resonance imaging (fMRI) "brain reading": Detecting and classifying distributed patterns of fMRI activity in human visual cortex. *NeuroImage*, *19*(2), 261–270. https://doi.org/10.1016/S1053-8119(03)00049-1

Cross, E. S., Schmitt, P. J., & Grafton, S. T. (2007). Neural Substrates of Contextual Interference during Motor Learning Support a Model of Active Preparation. *Journal of Cognitive Neuroscience*, *19*(11), 1854–1871. https://doi.org/10.1162/jocn.2007.19.11.1854

Crowe, D. A., Zarco, W., Bartolo, R., & Merchant, H. (2014). Dynamic representation of the temporal and sequential structure of rhythmic movements in the primate medial

premotor cortex. *Journal of Neuroscience*, *34*(36), 11972–11983. https://doi.org/10.1523/JNEUROSCI.2177-14.2014

Culham, J. C., & Valyear, K. F. (2006). Human parietal cortex in action. *Current Opinion in Neurobiology*, *16*(2), 205–212. https://doi.org/10.1016/j.conb.2006.03.005

Dale, A. M., Fischl, B., & Sereno, M. I. (1999). Cortical surface-based analysis: I. Segmentation and surface reconstruction. *NeuroImage*, *9*(2), 179–194. https://doi.org/10.1006/nimg.1998.0395

Davachi, L., & DuBrow, S. (2015). How the hippocampus preserves order: The role of prediction and context. *Trends in Cognitive Sciences*, *19*(2), 92–99. https://doi.org/10.1016/j.tics.2014.12.004

D'Avella, A., Saltiel, P., & Bizzi, E. (2003). Combinations of muscle synergies in the construction of a natural motor behavior. *Nature Neuroscience*, *6*(3), 300–308. https://doi.org/10.1038/nn1010

Dayan, E., & Cohen, L. G. (2011). Neuroplasticity subserving motor skill learning. *Neuron*, *72*(3), 443–454. https://doi.org/10.1016/j.neuron.2011.10.008

De Belder, M., Santens, P., Sieben, A., & Fias, W. (2017). Impaired processing of serial order determines working memory impairments in Alzheimer's disease. *Journal of Alzheimer's Disease*, *59*(4), 1171–1186.

Desrochers, T. M., Chatham, C. H., & Badre, D. (2015). The Necessity of Rostrolateral Prefrontal Cortex for Higher-Level Sequential Behavior. *Neuron*, *87*(6), 1357–1368. https://doi.org/10.1016/j.neuron.2015.08.026

Dhawale, A. K., Wolff, S. B. E., Ko, R., & Ölveczky, B. P. (2021). The basal ganglia control the detailed kinematics of learned motor skills. *Nature Neuroscience*, *24*(9), 1256–1269. https://doi.org/10.1038/s41593-021-00889-3

Diedrichsen, J. (2006). A spatially unbiased atlas template of the human cerebellum. *NeuroImage*, *33*(1), 127–138. https://doi.org/10.1016/j.neuroimage.2006.05.056

Diedrichsen, J., Balsters, J. H., Flavell, J., Cussans, E., & Ramnani, N. (2009). A probabilistic MR atlas of the human cerebellum. *NeuroImage*, *46*(1), 39–46. https://doi.org/10.1016/j.neuroimage.2009.01.045

Diedrichsen, J., Criscimagna-Hemminger, S. E., & Shadmehr, R. (2007). Dissociating timing and coordination as functions of the cerebellum. *Journal of Neuroscience*, *27*(23), 6291–6301. https://doi.org/10.1523/JNEUROSCI.0061-07.2007

Diedrichsen, J., & Kornysheva, K. (2015a). Motor skill learning between selection and execution. *Trends in Cognitive Sciences*, *19*(4), 227–233. https://doi.org/10.1016/j.tics.2015.02.003

Diedrichsen, J., & Kornysheva, K. (2015b). Motor skill learning between selection and execution. *Trends in Cognitive Sciences*, *19*(4). https://doi.org/10.1016/j.tics.2015.02.003

Diedrichsen, J., & Kriegeskorte, N. (2017). Representational models: A common framework for understanding encoding, pattern-component, and representational-similarity analysis. *PLoS Computational Biology*, *13*(4). https://doi.org/10.1371/journal.pcbi.1005508

Diedrichsen, J., Ridgway, G. R., Friston, K. J., & Wiestler, T. (2011). Comparing the similarity and spatial structure of neural representations: A pattern-component model. *NeuroImage*, *55*(4), 1665–1678. https://doi.org/10.1016/j.neuroimage.2011.01.044

Diedrichsen, J., & Shadmehr, R. (2005). Detecting and adjusting for artifacts in fMRI time series data. *NeuroImage*, *27*(3), 624–634. https://doi.org/10.1016/j.neuroimage.2005.04.039

Diedrichsen, J., Wiestler, T., & Krakauer, J. W. (2013). Two distinct ipsilateral cortical representations for individuated finger movements. *Cerebral Cortex*, *23*(6), 1362–1377. https://doi.org/10.1093/cercor/bhs120

Diedrichsen, J., Yokoi, A., & Arbuckle, S. A. (2018). Pattern component modeling: A flexible approach for understanding the representational structure of brain activity patterns. *NeuroImage*, *180*, 119–133. https://doi.org/10.1016/j.neuroimage.2017.08.051

Diedrichsen, J., & Zotow, E. (2015). Surface-based display of volume-averaged cerebellar imaging data. *PLoS ONE*, *10*(7). https://doi.org/10.1371/journal.pone.0133402

Diener, H.-C., & Dichgans, J. (1992). Pathophysiology of cerebellar ataxia. *Movement Disorders*, *7*(2), 95–109. https://doi.org/10.1002/mds.870070202

Dolfen, N., Reverberi, S., Beeck, H. O. de, King, B. R., & Albouy, G. (2023). *The hippocampus binds movements to their temporal position in a motor sequence* (p. 2022.12.20.521084). bioRxiv. https://doi.org/10.1101/2022.12.20.521084

Doyon, J., Bellec, P., Amsel, R., Penhune, V., Monchi, O., Carrier, J., Lehéricy, S., & Benali, H. (2009). Contributions of the basal ganglia and functionally related brain structures to motor learning. *Behavioural Brain Research*, *199*(1), 61–75. https://doi.org/10.1016/j.bbr.2008.11.012

Doyon, J., Gaudreau, D., Jr., R. L., Castonguay, M., Bédard, P. J., Bédard, F., & Bouchard, J.-P. (1997). Role of the Striatum, Cerebellum, and Frontal Lobes in the Learning of a Visuomotor Sequence. *Brain and Cognition*, *34*(2), 218–245. https://doi.org/10.1006/brcg.1997.0899

Dubois, B., Hampel, H., Feldman, H. H., Scheltens, P., Aisen, P., Andrieu, S., Bakardjian, H., Benali, H., Bertram, L., Blennow, K., Broich, K., Cavedo, E., Crutch, S., Dartigues, J.-F., Duyckaerts, C., Epelbaum, S., Frisoni, G. B., Gauthier, S., Genthon, R., … Jack, C. R.

(2016). Preclinical Alzheimer's disease: Definition, natural history, and diagnostic criteria. *Alzheimer's & Dementia : The Journal of the Alzheimer's Association*, *12*(3), 292–323. https://doi.org/10.1016/j.jalz.2016.02.002

Duque, J., Greenhouse, I., Labruna, L., & Ivry, R. B. (2017). Physiological Markers of Motor Inhibition during Human Behavior. *Trends in Neurosciences*, *40*(4), 219–236. https://doi.org/10.1016/j.tins.2017.02.006

Duque, J., & Ivry, R. B. (2009a). Role of corticospinal suppression during motor preparation. *Cerebral Cortex*, *19*(9), 2013–2024. https://doi.org/10.1093/cercor/bhn230

Duque, J., & Ivry, R. B. (2009b). Role of corticospinal suppression during motor preparation. *Cerebral Cortex*, *19*(9), 2013–2024. https://doi.org/10.1093/cercor/bhn230

Duque, J., Labruna, L., Cazares, C., & Ivry, R. B. (2014). Dissociating the influence of response selection and task anticipation on corticospinal suppression during response preparation. *Neuropsychologia*, *65*, 287–296. https://doi.org/10.1016/j.neuropsychologia.2014.08.006

Duque, J., Mazzocchio, R., Dambrosia, J., Murase, N., Olivier, E., & Cohen, L. G. (2005). Kinematically specific interhemispheric inhibition operating in the process of generation of a voluntary movement. *Cerebral Cortex (New York, N.Y.: 1991)*, *15*(5), 588–593. https://doi.org/10.1093/cercor/bhh160

Ebbinghaus, H. (2013). Memory: A Contribution to Experimental Psychology. *Annals of Neurosciences*, *20*(4), 155–156. https://doi.org/10.5214/ans.0972.7531.200408

Eichenbaum, H. (2014). Time cells in the hippocampus: A new dimension for mapping memories. *Nature Reviews Neuroscience*, *15*(11), Article 11. https://doi.org/10.1038/nrn3827

Elsayed, G. F., Lara, A. H., Kaufman, M. T., Churchland, M. M., & Cunningham, J. P. (2016). Reorganization between preparatory and movement population responses in motor cortex. *Nature Communications*, *7*(1), 1–15. https://doi.org/10.1038/ncomms13239

Emmons, E. B., De Corte, B. J., Kim, Y., Parker, K. L., Matell, M. S., & Narayanan, N. S. (2017). Rodent Medial Frontal Control of Temporal Processing in the Dorsomedial Striatum. *The Journal of Neuroscience: The Official Journal of the Society for Neuroscience*, *37*(36), 8718–8733. https://doi.org/10.1523/JNEUROSCI.1376-17.2017

Evinger, C., Kaneko, C. R., & Fuchs, A. F. (1982). Activity of omnipause neurons in alert cats during saccadic eye movements and visual stimuli. *Journal of Neurophysiology*, *47*(5), 827–844. https://doi.org/10.1152/jn.1982.47.5.827

Ferbert, A., Priori, A., Rothwell, J. C., Day, B. L., Colebatch, J. G., & Marsden, C. D. (1992). Interhemispheric inhibition of the human motor cortex. *The Journal of Physiology*, *453*(1), 525–546. https://doi.org/10.1113/jphysiol.1992.sp019243

Fiori, F., Chiappini, E., Candidi, M., Romei, V., Borgomaneri, S., & Avenanti, A. (2017). Long-latency interhemispheric interactions between motor-related areas and the primary motor cortex: A dual site TMS study. *Scientific Reports*, *7*(1), Article 1. https://doi.org/10.1038/s41598-017-13708-2

Fischl, B., Sereno, M. I., Tootell, R. B. H., & Dale, A. M. (1999). High-resolution intersubject averaging and a coordinate system for the cortical surface. *Human Brain Mapping*, *8*(4), 272–284. https://doi.org/10.1002/(SICI)1097-0193(1999)8:4<272::AID-HBM10>3.0.CO;2-4

Fitzpatrick, A. M., Dundon, N. M., & Valyear, K. F. (2019). The neural basis of hand choice: An fMRI investigation of the Posterior Parietal Interhemispheric Competition model. *NeuroImage*, *185*, 208–221. https://doi.org/10.1016/j.neuroimage.2018.10.039

Flash, T., & Hochner, B. (2005). Motor primitives in vertebrates and invertebrates. *Current Opinion in Neurobiology*, *15*(6), 660–666. https://doi.org/10.1016/j.conb.2005.10.011

Flash, T., & Hogan, N. (1985). The coordination of arm movements: An experimentally confirmed mathematical model. *Journal of Neuroscience*, *5*(7), 1688–1703. https://doi.org/10.1523/JNEUROSCI.05-07-01688.1985

Förstl, H., & Kurz, A. (1999). Clinical features of Alzheimer's disease. *European Archives of Psychiatry and Clinical Neuroscience*, *249*(6), 288–290. https://doi.org/10.1007/s004060050101

Frank, M. J. (2011). Computational models of motivated action selection in corticostriatal circuits. *Current Opinion in Neurobiology*, *21*(3), 381–386. https://doi.org/10.1016/j.conb.2011.02.013

Friend, D. M., & Kravitz, A. V. (2014). Working together: Basal ganglia pathways in action selection. *Trends in Neurosciences*, *37*(6), 301–303. https://doi.org/10.1016/j.tins.2014.04.004

Gale, D. J., Flanagan, J. R., & Gallivan, J. P. (2021). Human Somatosensory Cortex Is Modulated during Motor Planning. *Journal of Neuroscience*, *41*(27), 5909–5922. https://doi.org/10.1523/JNEUROSCI.0342-21.2021

Gallivan, J. P., McLean, D. A., Flanagan, J. R., & Culham, J. C. (2013). Where One Hand Meets the Other: Limb-Specific and Action-Dependent Movement Plans Decoded from Preparatory Signals in Single Human Frontoparietal Brain Areas. *Journal of Neuroscience*, *33*(5), 1991–2008. https://doi.org/10.1523/JNEUROSCI.0541-12.2013

Gallivan, J. P., McLean, D. A., Valyear, K. F., Pettypiece, C. E., & Culham, J. C. (2011). Decoding Action Intentions from Preparatory Brain Activity in Human Parieto-Frontal

Networks. *Journal of Neuroscience*, *31*(26), 9599–9610. https://doi.org/10.1523/JNEUROSCI.0080-11.2011

Gao, Z., Davis, C., Thomas, A. M., Economo, M. N., Abrego, A. M., Svoboda, K., De Zeeuw, C. I., & Li, N. (2018). A cortico-cerebellar loop for motor planning. *Nature*, *563*(7729), 113–116. https://doi.org/10.1038/s41586-018-0633-x

Gaser, C., & Schlaug, G. (2003). Brain Structures Differ between Musicians and Non-Musicians. *Journal of Neuroscience*, *23*(27), 9240–9245. https://doi.org/10.1523/JNEUROSCI.23-27-09240.2003

Gentner, R., Gorges, S., Weise, D., Aufm Kampe, K., Buttmann, M., & Classen, J. (2010). Encoding of motor skill in the corticomuscular system of musicians. *Current Biology*, *20*(20), 1869–1874. https://doi.org/10.1016/j.cub.2010.09.045

Georgopoulos, A. P., Kalaska, J. F., Caminiti, R., & Massey, J. T. (1982). On the relations between the direction of two-dimensional arm movements and cell discharge in primate motor cortex. *Journal of Neuroscience*, *2*(11), 1527–1537. https://doi.org/10.1523/JNEUROSCI.02-11-01527.1982

Georgopoulos, A. P., Merchant, H., Naselaris, T., & Amirikian, B. (2007). Mapping of the preferred direction in the motor cortex. *Proceedings of the National Academy of Sciences*, *104*(26), 11068–11072. https://doi.org/10.1073/pnas.0611597104

Gerloff, C., Corwell, B., Chen, R., Hallett, M., & Cohen, L. G. (1997). Stimulation over the human supplementary motor area interferes with the organization of future elements in complex motor sequences. *Brain*, *120*(9), 1587–1602. https://doi.org/10.1093/brain/120.9.1587

Gobel, E. W., Sanchez, D. J., & Reber, P. J. (2011). Integration of Temporal and Ordinal Information During Serial Interception Sequence Learning. *Journal of Experimental*

Psychology: Learning Memory and Cognition, *37*(4), 994–1000. https://doi.org/10.1037/a0022959

Goodman, D., & Kelso, J. S. (1980). Are movements prepared in parts? Not under compatible (naturalized) conditions. *Journal of Experimental Psychology: General*, *109*(4), 475.

Grafton, S. T., & Hamilton, A. F. D. C. (2007). Evidence for a distributed hierarchy of action representation in the brain. *Human Movement Science*, *26*(4), 590–616. https://doi.org/10.1016/j.humov.2007.05.009

Granic, I., Lobel, A., & Engels, R. C. M. E. (2014). The benefits of playing video games. *American Psychologist*, *69*(1), 66–78. https://doi.org/10.1037/a0034857

Graybiel, A. M. (1998). The basal ganglia and chunking of action repertoires. *Neurobiology of Learning and Memory*, *70*(1–2), 119–136. https://doi.org/10.1006/nlme.1998.3843

Graziano, M. S. A. (2016). Ethological Action Maps: A Paradigm Shift for the Motor Cortex. *Trends in Cognitive Sciences*, *20*(2), 121–132. https://doi.org/10.1016/j.tics.2015.10.008

Graziano, M. S. A., Taylor, C. S. R., & Moore, T. (2002). Complex Movements Evoked by Microstimulation of Precentral Cortex. *Neuron*, *34*(5), 841–851. https://doi.org/10.1016/S0896-6273(02)00698-0

Graziano, M. S. A., Taylor, C. S. R., Moore, T., & Cooke, D. F. (2002). The Cortical Control of Movement Revisited. *Neuron*, *36*(3), 349–362. https://doi.org/10.1016/S0896-6273(02)01003-6

Green, A. M., & Kalaska, J. F. (2011). Learning to move machines with the mind. *Trends in Neurosciences*, *34*(2), 61–75. https://doi.org/10.1016/j.tins.2010.11.003

Guo, Z. V., Inagaki, H. K., Daie, K., Druckmann, S., Gerfen, C. R., & Svoboda, K. (2017). Maintenance of persistent activity in a frontal thalamocortical loop. *Nature*, *545*(7653), 181–186. https://doi.org/10.1038/nature22324

Gurney, K., Prescott, T. J., & Redgrave, P. (2001). A computational model of action selection in the basal ganglia. I. A new functional anatomy. *Biological Cybernetics*, *84*(6), 401–410. https://doi.org/10.1007/PL00007984

Haith, A. M., & Bestmann, S. (2020). Preparation of Movement. In D. Poeppel, G. R. Mangun, & M. S. Gazzaniga (Eds.), *The Cognitive Neurosciences* (6th ed., pp. 541–548). The MIT Press. https://doi.org/10.7551/mitpress/11442.003.0059

Haith, A. M., Pakpoor, J., & Krakauer, J. W. (2016). Independence of movement preparation and movement initiation. *Journal of Neuroscience*, *36*(10), 3007–3015. Scopus. https://doi.org/10.1523/JNEUROSCI.3245-15.2016

Hallett, M. (1994). Movement-related cortical potentials. *Electromyography and Clinical Neurophysiology*, *34*(1), 5–13.

Harpaz, N. K., Hardcastle, K., & Ölveczky, B. P. (2022). Learning-induced changes in the neural circuits underlying motor sequence execution. *Current Opinion in Neurobiology*, *76*, 102624.

Haynes, J.-D., & Rees, G. (2006). Decoding mental states from brain activity in humans. *Nature Reviews Neuroscience*, *7*(7), Article 7. https://doi.org/10.1038/nrn1931

Heald, J. B., Lengyel, M., & Wolpert, D. M. (2021). Contextual inference underlies the learning of sensorimotor repertoires. *Nature*, *600*(7889), 489–493. https://doi.org/10.1038/s41586-021-04129-3

Hélie, S., & Cousineau, D. (1998). *Mixed effects of training on transfer*. Citeseer.

Henderson, M. M., Rademaker, R. L., & Serences, J. T. (2022). Flexible utilization of spatial- and motor-based codes for the storage of visuo-spatial information. *eLife*, *11*, e75688. https://doi.org/10.7554/eLife.75688

Hick, W. E. (1952). On the Rate of Gain of Information. *Quarterly Journal of Experimental Psychology*, *4*(1), 11–26. https://doi.org/10.1080/17470215208416600

Hikosaka, O., Nakamura, K., Sakai, K., & Nakahara, H. (2002a). Central mechanisms of motor skill learning. *Current Opinion in Neurobiology*, *12*(2), 217–222. https://doi.org/10.1016/S0959-4388(02)00307-0

Hikosaka, O., Nakamura, K., Sakai, K., & Nakahara, H. (2002b). Central mechanisms of motor skill learning. *Current Opinion in Neurobiology*, *12*(2), 217–222. https://doi.org/10.1016/S0959-4388(02)00307-0

Houghton, G. (1990). The problem of serial order: A neural network model of sequence learning and recall. In *Current research in natural language generation* (pp. 287–319).

Houghton, G., & Hartley, T. (1995). Parallel models of serial behavior: Lashley revisited. *Psyche*, *2*(25), 2–25.

Huang, C.-C., Rolls, E. T., Hsu, C.-C. H., Feng, J., & Lin, C.-P. (2021). Extensive Cortical Connectivity of the Human Hippocampal Memory System: Beyond the "What" and "Where" Dual Stream Model. *Cerebral Cortex (New York, NY)*, *31*(10), 4652–4669. https://doi.org/10.1093/cercor/bhab113

Hubel, D. H., & Wiesel, T. N. (1962). Receptive fields, binocular interaction and functional architecture in the cat's visual cortex. *The Journal of Physiology*, *160*(1), 106-154.2.

Inagaki, H. K., Chen, S., Ridder, M. C., Sah, P., Li, N., Yang, Z., Hasanbegovic, H., Gao, Z., Gerfen, C. R., & Svoboda, K. (2022). A midbrain-thalamus-cortex circuit reorganizes

cortical dynamics to initiate movement. *Cell*, *185*(6), 1065-1081.e23. https://doi.org/10.1016/j.cell.2022.02.006

Inagaki, H. K., Inagaki, M., Romani, S., & Svoboda, K. (2018). Low-Dimensional and Monotonic Preparatory Activity in Mouse Anterior Lateral Motor Cortex. *Journal of Neuroscience*, *38*(17), 4163–4185. https://doi.org/10.1523/JNEUROSCI.3152-17.2018

Itskov, V., Curto, C., Pastalkova, E., & Buzsáki, G. (2011). Cell Assembly Sequences Arising from Spike Threshold Adaptation Keep Track of Time in the Hippocampus. *Journal of Neuroscience*, *31*(8), 2828–2834. https://doi.org/10.1523/JNEUROSCI.3773-10.2011

Ivry, R. (1997). Cerebellar Timing Systems. In *International Review of Neurobiology* (Vol. 41, pp. 555–573). Elsevier. https://doi.org/10.1016/S0074-7742(08)60370-0

Ivry, R. B., & Schlerf, J. E. (2008). Dedicated and intrinsic models of time perception. *Trends in Cognitive Sciences*, *12*(7), 273–280. https://doi.org/10.1016/j.tics.2008.04.002

Ivry, R. B., & Spencer, R. M. C. (2004). The neural representation of time. *Current Opinion in Neurobiology*, *14*(2), 225–232. https://doi.org/10.1016/j.conb.2004.03.013

Jazayeri, M., & Shadlen, M. N. (2015). A Neural Mechanism for Sensing and Reproducing a Time Interval. *Current Biology*, *25*(20), 2599–2609. https://doi.org/10.1016/j.cub.2015.08.038

Johansson, F., Hesslow, G., & Medina, J. F. (2016). Mechanisms for motor timing in the cerebellar cortex. *Current Opinion in Behavioral Sciences*, *8*, 53–59. https://doi.org/10.1016/j.cobeha.2016.01.013

Jones, E. G., Coulter, J. D., & Wise, S. P. (1979). Commissural columns in the sensory-motor cortex of monkeys. *Journal of Comparative Neurology*, *188*(1), 113–135. https://doi.org/10.1002/cne.901880110

Kalová, E., Vlček, K., Jarolímová, E., & Bureš, J. (2005). Allothetic orientation and sequential ordering of places is impaired in early stages of Alzheimer's disease: Corresponding results in real space tests and computer tests. *Behavioural Brain Research*, *159*(2), 175–186. https://doi.org/10.1016/j.bbr.2004.10.016

Karniel, A., & Mussa-Ivaldi, F. A. (2003). Sequence, time, or state representation: How does the motor control system adapt to variable environments? *Biological Cybernetics*, *89*(1), 10–21. https://doi.org/10.1007/s00422-003-0397-7

Kaufman, M. T., Churchland, M. M., Ryu, S. I., & Shenoy, K. V. (2014). Cortical activity in the null space: Permitting preparation without movement. *Nature Neuroscience*, *17*(3), 440–448. https://doi.org/10.1038/nn.3643

Kaufman, M. T., Seely, J. S., Sussillo, D., Ryu, S. I., Shenoy, K. V., & Churchland, M. M. (2016). The largest response component in the motor cortex reflects movement timing but not movement type. *eNeuro*, *3*(4). https://doi.org/10.1523/ENEURO.0085-16.2016

Kawai, R., Markman, T., Poddar, R., Ko, R., Fantana, A. L., Dhawale, A. K., Kampff, A. R., & Ölveczky, B. P. (2015). Motor Cortex Is Required for Learning but Not for Executing a Motor Skill. *Neuron*, *86*(3), 800–812. https://doi.org/10.1016/j.neuron.2015.03.024

Kennerley, S. W., Sakai, K., & Rushworth, M. F. S. (2004). Organization of Action Sequences and the Role of the Pre-SMA. *Journal of Neurophysiology*, *91*(2), 978–993. https://doi.org/10.1152/jn.00651.2003

Khilkevich, A., Zambrano, J., Richards, M.-M., & Mauk, M. D. (2018). Cerebellar implementation of movement sequences through feedback. *eLife*, *7*, e37443. https://doi.org/10.7554/eLife.37443

Khushu, S., Kumaran, S. S., Tripathi, R. P., Gupta, A., Jain, P. C., & Jain, V. (2001). Functional magnetic resonance imaging of the primary motor cortex in humans: Response to

increased functional demands. *Journal of Biosciences*, *26*(2), 205–215. https://doi.org/10.1007/BF02703644

Kincaid, A. E., Duncan, S., & Scott, S. A. (2002). Assessment of Fine Motor Skill in Musicians and Nonmusicians: Differences in Timing versus Sequence Accuracy in a Bimanual Fingering Task. *Perceptual and Motor Skills*, *95*(1), 245–257. https://doi.org/10.2466/pms.2002.95.1.245

King, B. R., Mareike A. Gann, Dante Mantini, Julien Doyon, & Albouy, G. (2022). Persistence of hippocampal and striatal multivoxel patterns during awake rest after motor sequence learning. *iScience*. https://doi.org/10.1016/j.isci.2022.105498

King, M., Hernandez-Castillo, C. R., Poldrack, R. A., Ivry, R. B., & Diedrichsen, J. (2019). Functional boundaries in the human cerebellum revealed by a multi-domain task battery. *Nature Neuroscience*, *22*(8), 1371–1378. https://doi.org/10.1038/s41593-019-0436-x

Klapp, S. T., & Maslovat, D. (2020). Programming of action timing cannot be completed until immediately prior to initiation of the response to be controlled. *Psychonomic Bulletin & Review*, *27*(5), 821–832. https://doi.org/10.3758/s13423-020-01740-9

Klein, P.-A., Duque, J., Labruna, L., & Ivry, R. B. (2016). Comparison of the two cerebral hemispheres in inhibitory processes operative during movement preparation. *NeuroImage*, *125*, 220–232. https://doi.org/10.1016/j.neuroimage.2015.10.007

Knierim, J. J. (2015). The hippocampus. *Current Biology*, *25*(23), R1116–R1121. https://doi.org/10.1016/j.cub.2015.10.049

Koch, G., Ruge, D., Cheeran, B., Fernandez Del Olmo, M., Pecchioli, C., Marconi, B., Versace, V., Lo Gerfo, E., Torriero, S., Oliveri, M., Caltagirone, C., & Rothwell, J. C. (2009). TMS activation of interhemispheric pathways between the posterior parietal cortex and

the contralateral motor cortex. *The Journal of Physiology*, *587*(Pt 17), 4281–4292. https://doi.org/10.1113/jphysiol.2009.174086

Kornysheva, K. (2016). Encoding temporal features of skilled movements-what, whether and how? In *Advances in Experimental Medicine and Biology* (Vol. 957, pp. 35–54). Springer New York LLC. https://doi.org/10.1007/978-3-319-47313-0_3

Kornysheva, K., Bush, D., Meyer, S. S., Sadnicka, A., Barnes, G., & Burgess, N. (2019a). Neural Competitive Queuing of Ordinal Structure Underlies Skilled Sequential Action. *Neuron*, *101*(6), 1166-1180.e3. https://doi.org/10.1016/j.neuron.2019.01.018

Kornysheva, K., Bush, D., Meyer, S. S., Sadnicka, A., Barnes, G., & Burgess, N. (2019b). Neural Competitive Queuing of Ordinal Structure Underlies Skilled Sequential Action. *Neuron*, *101*(6), 1166-1180.e3. https://doi.org/10.1016/j.neuron.2019.01.018

Kornysheva, K., & Diedrichsen, J. (2014). Human premotor areas parse sequences into their spatial and temporal features. *eLife*, *3*, e03043. https://doi.org/10.7554/eLife.03043

Kornysheva, K., Sierk, A., & Diedrichsen, J. (2013). Interaction of temporal and ordinal representations in movement sequences. *Journal of Neurophysiology*, *109*(5), 1416–1424. https://doi.org/10.1152/jn.00509.2012

Kowal, M., Toth, A. J., Exton, C., & Campbell, M. J. (2018). Different cognitive abilities displayed by action video gamers and non-gamers. *Computers in Human Behavior*, *88*, 255–262. https://doi.org/10.1016/j.chb.2018.07.010

Kriegeskorte, N. (2008). Representational similarity analysis – connecting the branches of systems neuroscience. *Frontiers in Systems Neuroscience*. https://doi.org/10.3389/neuro.06.004.2008

Kumar, V. J., van Oort, E., Scheffler, K., Beckmann, C. F., & Grodd, W. (2017). Functional anatomy of the human thalamus at rest. *NeuroImage*, *147*, 678–691. https://doi.org/10.1016/j.neuroimage.2016.12.071

Kunimatsu, J., Suzuki, T. W., Ohmae, S., & Tanaka, M. (2018). Different contributions of preparatory activity in the basal ganglia and cerebellum for self-timing. *eLife*, *7*. https://doi.org/10.7554/eLife.35676

Labruna, L., Lebon, F., Duque, J., Klein, P.-A., Cazares, C., & Ivry, R. B. (2014). Generic Inhibition of the Selected Movement and Constrained Inhibition of Nonselected Movements during Response Preparation. *Journal of Cognitive Neuroscience*, *26*(2), 269–278. https://doi.org/10.1162/jocn_a_00492

Lafuente, V. de, Jazayeri, M., Merchant, H., Gracía-Garibay, O., Cadena-Valencia, J., & Malagón, A. M. (2022). Keeping time and rhythm by replaying a sensory-motor engram. *bioRxiv*, *52*(July), 1–23. https://doi.org/10.1101/2022.01.03.474812

Landry, S. P., & Champoux, F. (2017). Musicians react faster and are better multisensory integrators. *Brain and Cognition*, *111*, 156–162. https://doi.org/10.1016/j.bandc.2016.12.001

Lara, A. H., Elsayed, G. F., Zimnik, A. J., Cunningham, J. P., & Churchland, M. M. (2018). Conservation of preparatory neural events in monkey motor cortex regardless of how movement is initiated. *eLife*, *7*, e31826. https://doi.org/10.7554/eLife.31826

Lashley, K. S. (1951). *The problem of serial order in behavior* (Vol. 21). Bobbs-Merrill Oxford.

Lemon, R. N. (2008). Descending Pathways in Motor Control. *Annual Review of Neuroscience*, *31*(1), 195–218. https://doi.org/10.1146/annurev.neuro.31.060407.125547

Leocani, L., Cohen, L. G., Wassermann, E. M., Ikoma, K., & Hallett, M. (2000). Human corticospinal excitability evaluated with transcranial magnetic stimulation during different reaction time paradigms. *Brain*, *123*(6), 1161–1173. https://doi.org/10.1093/brain/123.6.1161

Lewis, P. A., & Miall, R. C. (2003). Distinct systems for automatic and cognitively controlled time measurement: Evidence from neuroimaging. *Current Opinion in Neurobiology*, *13*(2), 250–255. https://doi.org/10.1016/S0959-4388(03)00036-9

Li, N., Daie, K., Svoboda, K., & Druckmann, S. (2016). Robust neuronal dynamics in premotor cortex during motor planning. *Nature*, *532*(7600), 459–464. https://doi.org/10.1038/nature17643

Li, N., & Mrsic-Flogel, T. D. (2020). Cortico-cerebellar interactions during goal-directed behavior. *Current Opinion in Neurobiology*, *65*, 27–37. https://doi.org/10.1016/j.conb.2020.08.010

Lindner, A., Iyer, A., Kagan, I., & Andersen, R. A. (2010). Human Posterior Parietal Cortex Plans Where to Reach and What to Avoid. *Journal of Neuroscience*, *30*(35), 11715–11725. https://doi.org/10.1523/JNEUROSCI.2849-09.2010

Logothetis, N. K. (2003). The underpinnings of the BOLD functional magnetic resonance imaging signal. *Journal of Neuroscience*, *23*(10), 3963–3971. https://doi.org/10.1523/jneurosci.23-10-03963.2003

Lungu, O., Monchi, O., Albouy, G., Jubault, T., Ballarin, E., Burnod, Y., & Doyon, J. (2014). Striatal and Hippocampal Involvement in Motor Sequence Chunking Depends on the Learning Strategy. *PLoS ONE*, *9*(8), e103885. https://doi.org/10.1371/journal.pone.0103885

Magill, R. A., & Hall, K. G. (1990). A review of the contextual interference effect in motor skill acquisition. *Human Movement Science*, *9*(3), 241–289. https://doi.org/10.1016/0167-9457(90)90005-X

Mantziara, M., Ivanov, T., Houghton, G., & Kornysheva, K. (2021). Competitive state of movements during planning predicts sequence performance. *Journal of Neurophysiology*, *125*(4), 1251–1268. https://doi.org/10.1152/jn.00645.2020

Maris, E., & Oostenveld, R. (2007). Nonparametric statistical testing of EEG- and MEG-data. *Journal of Neuroscience Methods*, *164*(1), 177–190. https://doi.org/10.1016/j.jneumeth.2007.03.024

Maslovat, D., & Klapp, S. T. (2022). Trouble doing two differently timed actions at once: What is the problem? *Psychological Review*. https://doi.org/10.1037/rev0000383

Matsuzaka, Y., Picard, N., & Strick, P. L. (2007). Skill representation in the primary motor cortex after long-term practice. *Journal of Neurophysiology*, *97*(2), 1819–1832. https://doi.org/10.1152/jn.00784.2006

Maudrich, T., Kenville, R., Schempp, C., Noack, E., & Ragert, P. (2021). Comparison of whole-body sensorimotor skill learning between strength athletes, endurance athletes and healthy sedentary adults. *Heliyon*, *7*(8), e07723. https://doi.org/10.1016/j.heliyon.2021.e07723

Mauk, M. D., & Buonomano, D. V. (2004). The Neural Basis of Temporal Processing. *Annual Review of Neuroscience*, *27*(1), 307–340. https://doi.org/10.1146/annurev.neuro.27.070203.144247

Medina, J. F., Carey, M. R., & Lisberger, S. G. (2005). The Representation of Time for Motor Learning. *Neuron*, *45*(1), 157–167. https://doi.org/10.1016/j.neuron.2004.12.017

Merchant, H., Harrington, D. L., & Meck, W. H. (2013). Neural basis of the perception and estimation of time. *Annual Review of Neuroscience*, *36*, 313–336. https://doi.org/10.1146/annurev-neuro-062012-170349

Merchant, H., Pérez, O., Zarco, W., & Gámez, J. (2013). Interval tuning in the primate medial premotor cortex as a general timing mechanism. *Journal of Neuroscience*, *33*(21), 9082–9096. https://doi.org/10.1523/JNEUROSCI.5513-12.2013

Messier, J., & Kalaska, J. F. (2000). Covariation of Primate Dorsal Premotor Cell Activity With Direction and Amplitude During a Memorized-Delay Reaching Task. *Journal of Neurophysiology*, *84*(1), 152–165. https://doi.org/10.1152/jn.2000.84.1.152

Meyer, B.-U., Röricht, S., von Einsiedel, H. G., Kruggel, F., & Weindl, A. (1995). Inhibitory and excitatory interhemispheric transfers between motor cortical areas in normal humans and patients with abnormalities of the corpus callosum. *Brain*, *118*(2), 429–440. https://doi.org/10.1093/brain/118.2.429

Meyer, M., Lamers, D., Kayhan, E., Hunnius, S., & Oostenveld, R. (2021). Enhancing reproducibility in developmental EEG research: BIDS, cluster-based permutation tests, and effect sizes. *Developmental Cognitive Neuroscience*, *52*, 101036. https://doi.org/10.1016/j.dcn.2021.101036

Miall, R. C., Christensen, L. O. D., Cain, O., & Stanley, J. (2007). Disruption of State Estimation in the Human Lateral Cerebellum. *PLoS Biology*, *5*(11), e316. https://doi.org/10.1371/journal.pbio.0050316

Mink, J. W. (1996). THE BASAL GANGLIA: FOCUSED SELECTION AND INHIBITION OF COMPETING MOTOR PROGRAMS. *Progress in Neurobiology*, *50*(4), 381–425. https://doi.org/10.1016/S0301-0082(96)00042-1

Mizes, K. G. C., Lindsey, J., Escola, G. S., & Ölveczky, B. P. (2023a). Dissociating the contributions of sensorimotor striatum to automatic and visually guided motor sequences. *Nature Neuroscience*, *26*(10), Article 10. https://doi.org/10.1038/s41593-023-01431-3

Mizes, K. G. C., Lindsey, J., Escola, G. S., & Ölveczky, B. P. (2023b). *Motor cortex is required for flexible but not automatic motor sequences* (p. 2023.09.05.556348). bioRxiv. https://doi.org/10.1101/2023.09.05.556348

Mondok, C., & Wiener, M. (2023). Selectivity of timing: A meta-analysis of temporal processing in neuroimaging studies using activation likelihood estimation and reverse inference. *Frontiers in Human Neuroscience*, *16*. https://www.frontiersin.org/articles/10.3389/fnhum.2022.1000995

Moser, M.-B., Rowland, D. C., & Moser, E. I. (2015). Place Cells, Grid Cells, and Memory. *Cold Spring Harbor Perspectives in Biology*, *7*(2), a021808. https://doi.org/10.1101/cshperspect.a021808

Mushiake, H., Saito, N., Sakamoto, K., Itoyama, Y., & Tanji, J. (2006). Activity in the Lateral Prefrontal Cortex Reflects Multiple Steps of Future Events in Action Plans. *Neuron*, *50*(4), 631–641. https://doi.org/10.1016/j.neuron.2006.03.045

Nambu, I., Hagura, N., Hirose, S., Wada, Y., Kawato, M., & Naito, E. (2015). Decoding sequential finger movements from preparatory activity in higher-order motor regions: A functional magnetic resonance imaging multi-voxel pattern analysis. *European Journal of Neuroscience*, *42*(10), 2851–2859. https://doi.org/10.1111/ejn.13063

Narain, D., Remington, E. D., Zeeuw, C. I. D., & Jazayeri, M. (2018). A cerebellar mechanism for learning prior distributions of time intervals. *Nature Communications*, *9*(1), Article 1. https://doi.org/10.1038/s41467-017-02516-x

Ni, Z., Gunraj, C., Nelson, A. J., Yeh, I.-J., Castillo, G., Hoque, T., & Chen, R. (2009). Two Phases of Interhemispheric Inhibition between Motor Related Cortical Areas and the Primary Motor Cortex in Human. *Cerebral Cortex*, *19*(7), 1654–1665. https://doi.org/10.1093/cercor/bhn201

Norman, K. A., Polyn, S. M., Detre, G. J., & Haxby, J. V. (2006). Beyond mind-reading: Multi-voxel pattern analysis of fMRI data. *Trends in Cognitive Sciences*, *10*(9), 424–430. https://doi.org/10.1016/j.tics.2006.07.005

Oldfield, R. C. (1971). The assessment and analysis of handedness: The Edinburgh inventory. *Neuropsychologia*, *9*(1), 97–113. https://doi.org/10.1016/0028-3932(71)90067-4

Oosterhof, N. N., Wiestler, T., Downing, P. E., & Diedrichsen, J. (2011). A comparison of volume-based and surface-based multi-voxel pattern analysis. *NeuroImage*, *56*(2), 593–600. https://doi.org/10.1016/j.neuroimage.2010.04.270

Opitz, B., Brady, D., & Leonard, H. C. (2020). Motor and non-motor sequence prediction is equally affected in children with developmental coordination disorder. *PLOS ONE*, *15*(11), e0232562. https://doi.org/10.1371/journal.pone.0232562

O'Reilly, J. X., McCarthy, K. J., Capizzi, M., & Nobre, A. C. (2008). Acquisition of the temporal and ordinal structure of movement sequences in incidental learning. *Journal of Neurophysiology*, *99*(5), 2731–2735. https://doi.org/10.1152/jn.01141.2007

O'Shea, D. J., & Shenoy, K. V. (2016). The Importance of Planning in Motor Learning. *Neuron*, *92*(4), 669–671. https://doi.org/10.1016/j.neuron.2016.11.003

Overduin, S. A., D'Avella, A., Carmena, J. M., & Bizzi, E. (2012). Microstimulation Activates a Handful of Muscle Synergies. *Neuron*, *76*(6), 1071–1077. https://doi.org/10.1016/j.neuron.2012.10.018

Overduin, S. A., D'Avella, A., Roh, J., Carmena, J. M., & Bizzi, E. (2015). Representation of muscle synergies in the primate brain. *Journal of Neuroscience*, *35*(37), 12615–12624. https://doi.org/10.1523/JNEUROSCI.4302-14.2015

Paton, J. J., & Buonomano, D. V. (2018). The Neural Basis of Timing: Distributed Mechanisms for Diverse Functions. *Neuron*, *98*(4), 687–705. https://doi.org/10.1016/j.neuron.2018.03.045

Pearce, T. M., & Moran, D. W. (2012). Strategy-dependent encoding of planned arm movements in the dorsal premotor cortex. *Science*, *337*(6097), 984–988. https://doi.org/10.1126/science.1220642

Peigneux, P., Laureys, S., Fuchs, S., Collette, F., Perrin, F., Reggers, J., Phillips, C., Degueldre, C., Del Fiore, G., & Aerts, J. (2004). Are spatial memories strengthened in the human hippocampus during slow wave sleep? *Neuron*, *44*(3), 535–545.

Peirce, J., Gray, J. R., Simpson, S., MacAskill, M., Höchenberger, R., Sogo, H., Kastman, E., & Lindeløv, J. K. (2019). PsychoPy2: Experiments in behavior made easy. *Behavior Research Methods*, *51*(1), 195–203. https://doi.org/10.3758/s13428-018-01193-y

Perez, M. A., & Cohen, L. G. (2009). Interhemispheric inhibition between primary motor cortices: What have we learned? *The Journal of Physiology*, *587*(Pt 4), 725–726. https://doi.org/10.1113/jphysiol.2008.166926

Picard, N., Matsuzaka, Y., & Strick, P. L. (2013). Extended practice of a motor skill is associated with reduced metabolic activity in M1. *Nature Neuroscience*, *16*(9), 1340–1347. https://doi.org/10.1038/nn.3477

Rakitin, B. C., Penney, T. B., Gibbon, J., Malapani, C., Hinton, S. C., & Meck, W. H. (1998). Scalar expectancy theory and peak-interval timing in humans. *Journal of Experimental Psychology: Animal Behavior Processes*, *24*(1), 15–33. https://doi.org/10.1037/0097-7403.24.1.15

Ramkumar, P., Acuna, D. E., Berniker, M., Grafton, S. T., Turner, R. S., & Kording, K. P. (2016). Chunking as the result of an efficiency computation trade-off. *Nature Communications*, *7*(1), 1–11. https://doi.org/10.1038/ncomms12176

Ramnani, N., & Passingham, R. E. (2001). Changes in the human brain during rhythm learning. *Journal of Cognitive Neuroscience*, *13*(7), 952–966. https://doi.org/10.1162/089892901753165863

Rathelot, J.-A., & Strick, P. L. (2009). Subdivisions of primary motor cortex based on cortico-motoneuronal cells. *Proceedings of the National Academy of Sciences*, *106*(3), 918–923. https://doi.org/10.1073/pnas.0808362106

Redgrave, P., Prescott, T. J., & Gurney, K. (1999). The basal ganglia: A vertebrate solution to the selection problem? *Neuroscience*, *89*(4), 1009–1023.

Remington, E. D., Egger, S. W., Narain, D., Wang, J., & Jazayeri, M. (2018). A Dynamical Systems Perspective on Flexible Motor Timing. *Trends in Cognitive Sciences*, *22*(10), 938–952. https://doi.org/10.1016/j.tics.2018.07.010

Ridding, M. C., Brouwer, B., & Nordstrom, M. A. (2000). Reduced interhemispheric inhibition in musicians. *Experimental Brain Research*, *133*(2), 249–253. https://doi.org/10.1007/s002210000428

Riehle, A., & Requin, J. (1989). Monkey primary motor and premotor cortex: Single-cell activity related to prior information about direction and extent of an intended

movement. *Journal of Neurophysiology*, *61*(3), 534–549. https://doi.org/10.1152/jn.1989.61.3.534

Rolls, E. T. (2020). Spatial coordinate transforms linking the allocentric hippocampal and egocentric parietal primate brain systems for memory, action in space, and navigation. *Hippocampus*, *30*(4), 332–353. https://doi.org/10.1002/hipo.23171

Romano Bergstrom, J. C., Howard Jr., J. H., & Howard, D. V. (2012). Enhanced Implicit Sequence Learning in College-age Video Game Players and Musicians. *Applied Cognitive Psychology*, *26*(1), 91–96. https://doi.org/10.1002/acp.1800

Rosenbaum, D. A. (1980). Human movement initiation: Specification of arm, direction, and extent. *Journal of Experimental Psychology: General*, *109*(4), 444–474. https://doi.org/10.1037/0096-3445.109.4.444

Rosenbaum, D. A., Barnes, H. J., & Slotta, J. D. (1988). In defense of the advance specification hypothesis for motor control. *Psychological Research*, *50*(1), 58–62. https://doi.org/10.1007/BF00309412

Rosenbaum, D. A., Cohen, R. G., Jax, S. A., Weiss, D. J., & van der Wel, R. (2007). The problem of serial order in behavior: Lashley's legacy. *Human Movement Science*, *26*(4), 525–554. https://doi.org/10.1016/j.humov.2007.04.001

Rosenbaum, D. A., Kenny, S. B., & Derr, M. A. (1983). Hierarchical control of rapid movement sequences. *Journal of Experimental Psychology: Human Perception and Performance*, *9*(1), 86–102. https://doi.org/10.1037/0096-1523.9.1.86

Rubin, J. E., McIntyre, C. C., Turner, R. S., & Wichmann, T. (2012). Basal ganglia activity patterns in parkinsonism and computational modeling of their downstream effects. *The European Journal of Neuroscience*, *36*(2), 2213–2228. https://doi.org/10.1111/j.1460-9568.2012.08108.x

Russo, A. A., Khajeh, R., Bittner, S. R., Perkins, S. M., Cunningham, J. P., Abbott, L. F., & Churchland, M. M. (2020). Neural Trajectories in the Supplementary Motor Area and Motor Cortex Exhibit Distinct Geometries, Compatible with Different Classes of Computation. *Neuron*, *107*(4), 745-758.e6. https://doi.org/10.1016/j.neuron.2020.05.020

Sadnicka, A., Kornysheva, K., Rothwell, J. C., & Edwards, M. J. (2018). A unifying motor control framework for task-specific dystonia. *Nature Reviews Neurology*, *14*(2), 116–124. https://doi.org/10.1038/nrneurol.2017.146

Sadnicka, A., Wiestler, T., Butler, K., Altenmüller, E., Edwards, M. J., Ejaz, N., & Diedrichsen, J. (2023). Intact finger representation within primary sensorimotor cortex of musician's dystonia. *Brain*, *146*(4), 1511–1522. https://doi.org/10.1093/brain/awac356

Sakai, K., Kitaguchi, K., & Hikosaka, O. (2003). Chunking during human visuomotor sequence learning. *Experimental Brain Research*, *152*(2), 229–242. https://doi.org/10.1007/s00221-003-1548-8

Schendan, H. E., Searl, M. M., Melrose, R. J., & Stern, C. E. (2003). An FMRI study of the role of the medial temporal lobe in implicit and explicit sequence learning. *Neuron*, *37*(6), 1013–1025. https://doi.org/10.1016/s0896-6273(03)00123-5

Schlaug, G., Jäncke, L., Huang, Y., Staiger, J. F., & Steinmetz, H. (1995). Increased corpus callosum size in musicians. *Neuropsychologia*, *33*(8), 1047–1055. https://doi.org/10.1016/0028-3932(95)00045-5

Schneider, B. A., & Ghose, G. M. (2012). Temporal Production Signals in Parietal Cortex. *PLOS Biology*, *10*(10), e1001413. https://doi.org/10.1371/journal.pbio.1001413

Serences, J. T. (2004). A comparison of methods for characterizing the event-related BOLD timeseries in rapid fMRI. *NeuroImage*, *21*(4), 1690–1700. https://doi.org/10.1016/j.neuroimage.2003.12.021

Shenoy, K. V., Sahani, M., & Churchland, M. M. (2013). Cortical control of arm movements: A dynamical systems perspective. *Annual Review of Neuroscience*, *36*, 337–359. https://doi.org/10.1146/annurev-neuro-062111-150509

Sherman, S. M. (2007). The thalamus is more than just a relay. *Current Opinion in Neurobiology*, *17*(4), 417–422. https://doi.org/10.1016/j.conb.2007.07.003

Shima, K., & Tanji, J. (1998a). Both supplementary and presupplementary motor areas are crucial for the temporal organization of multiple movements. *Journal of Neurophysiology*, *80*(6), 3247–3260. https://doi.org/10.1152/jn.1998.80.6.3247

Shima, K., & Tanji, J. (1998b). Both supplementary and presupplementary motor areas are crucial for the temporal organization of multiple movements. *Journal of Neurophysiology*, *80*(6), 3247–3260.

Shima, K., & Tanji, J. (2000). Neuronal activity in the supplementary and presupplementary motor areas for temporal organization of multiple movements. *Journal of Neurophysiology*, *84*(4), 2148–2160.

Shin, J. C., & Ivry, R. B. (2002). Concurrent Learning of Temporal and Spatial Sequences. *Journal of Experimental Psychology: Learning Memory and Cognition*, *28*(3), 445–457. https://doi.org/10.1037/0278-7393.28.3.445

Shin, J. C., & Ivry, R. B. (2003). Spatial and temporal sequence learning in patients with Parkinson's disease or cerebellar lesions. *Journal of Cognitive Neuroscience*, *15*(8), 1232–1243.

Shine, J. M. (2021). The thalamus integrates the macrosystems of the brain to facilitate complex, adaptive brain network dynamics. *Progress in Neurobiology*, *199*, 101951. https://doi.org/10.1016/j.pneurobio.2020.101951

Shine, J. M., Lewis, L. D., Garrett, D. D., & Hwang, K. (2023). The impact of the human thalamus on brain-wide information processing. *Nature Reviews Neuroscience*, 1–15. https://doi.org/10.1038/s41583-023-00701-0

Shushruth, S., Zylberberg, A., & Shadlen, M. N. (2022). Sequential sampling from memory underlies action selection during abstract decision-making. *Current Biology*, *32*(9), 1949-1960.e5. https://doi.org/10.1016/j.cub.2022.03.014

Sobierajewicz, J., Naskręcki, R., Jaśkowski, W., & Van der Lubbe, R. H. J. (2018). Do musicians learn a fine sequential hand motor skill differently than non-musicians? *PLoS ONE*, *13*(11), e0207449. https://doi.org/10.1371/journal.pone.0207449

Sohn, Y. H., Jung, H. Y., Kaelin-Lang, A., & Hallett, M. (2003). Excitability of the ipsilateral motor cortex during phasic voluntary hand movement. *Experimental Brain Research*, *148*(2), 176–185. https://doi.org/10.1007/s00221-002-1292-5

Sousa, A., Ahmad, S. L., Hassan, T., Yuen, K., Douris, P., Zwibel, H., & DiFrancisco-Donoghue, J. (2020). Physiological and Cognitive Functions Following a Discrete Session of Competitive Esports Gaming. *Frontiers in Psychology*, *11*. https://www.frontiersin.org/articles/10.3389/fpsyg.2020.01030

Sporn, S., Chen, X., & Galea, J. M. (2022). The dissociable effects of reward on sequential motor behavior. *Journal of Neurophysiology*, *128*(1), 86–104. https://doi.org/10.1152/jn.00467.2021

Steele, C. J., & Penhune, V. B. (2010). Specific Increases within Global Decreases: A Functional Magnetic Resonance Imaging Investigation of Five Days of Motor

Sequence Learning. *Journal of Neuroscience*, *30*(24), 8332–8341. https://doi.org/10.1523/JNEUROSCI.5569-09.2010

Sveinbjornsdottir, S. (2016). The clinical symptoms of Parkinson's disease. *Journal of Neurochemistry*, *139*(S1), 318–324. https://doi.org/10.1111/jnc.13691

Tanaka, M., Kunimatsu, J., Suzuki, T. W., Kameda, M., Ohmae, S., Uematsu, A., & Takeya, R. (2021). Roles of the Cerebellum in Motor Preparation and Prediction of Timing. *Neuroscience*, *462*, 220–234. https://doi.org/10.1016/j.neuroscience.2020.04.039

Tanji, J., & Evarts, E. V. (1976). Anticipatory activity of motor cortex neurons in relation to direction of an intended movement. *Journal of Neurophysiology*, *39*(5), 1062–1068. https://doi.org/10.1152/jn.1976.39.5.1062

Tanji, J., & Shima, K. (1994). Role for supplementary motor area cells in planning several movements ahead. *Nature*, *371*(6496), 413–416. https://doi.org/10.1038/371413a0

Teixeira-Machado, L., Arida, R. M., & de Jesus Mari, J. (2019). Dance for neuroplasticity: A descriptive systematic review. *Neuroscience & Biobehavioral Reviews*, *96*, 232–240. https://doi.org/10.1016/j.neubiorev.2018.12.010

Thalmann, M., Souza, A. S., & Oberauer, K. (2019). How does chunking help working memory? *Journal of Experimental Psychology. Learning, Memory, and Cognition*, *45*(1), 37–55. https://doi.org/10.1037/xlm0000578

Thompson, R. F., & Kim, J. J. (1996). Memory systems in the brain and localization of a memory. *Proceedings of the National Academy of Sciences*, *93*(24), 13438–13444. https://doi.org/10.1073/pnas.93.24.13438

Todorov, E., & Jordan, M. I. (1998). Smoothness Maximization Along a Predefined Path Accurately Predicts the Speed Profiles of Complex Arm Movements. *Journal of Neurophysiology*, *80*(2), 696–714. https://doi.org/10.1152/jn.1998.80.2.696

Ullén, F., & Bengtsson, S. L. (2003). Independent Processing of the Temporal and Ordinal Structure of Movement Sequences. *Journal of Neurophysiology*, *90*(6), 3725–3735. https://doi.org/10.1152/jn.00458.2003

Van Essen, D. C., Drury, H. A., Dickson, J., Harwell, J., Hanlon, D., & Anderson, C. H. (2001). An integrated software suite for surface-based analyses of cerebral cortex. *Journal of the American Medical Informatics Association*, *8*(5), 443–459. https://doi.org/10.1136/jamia.2001.0080443

van Halteren-van Tilborg, I. A. D. A., Scherder, E. J. A., & Hulstijn, W. (2007). Motor-Skill Learning in Alzheimer's Disease: A Review with an Eye to the Clinical Practice. *Neuropsychology Review*, *17*(3), 203–212. https://doi.org/10.1007/s11065-007-9030-1

Verwey, W. B. (2023a). C-SMB 2.0: Integrating over 25 years of motor sequencing research with the Discrete Sequence Production task. *Psychonomic Bulletin & Review*, 1–48. https://doi.org/10.3758/s13423-023-02377-0

Verwey, W. B. (2023b). C-SMB 2.0: Integrating over 25 years of motor sequencing research with the Discrete Sequence Production task. *Psychonomic Bulletin & Review*. https://doi.org/10.3758/s13423-023-02377-0

Verwey, W. B., & Abrahamse, E. L. (2012). Distinct modes of executing movement sequences: Reacting, associating, and chunking. *Acta Psychologica*, *140*(3), 274–282. https://doi.org/10.1016/j.actpsy.2012.05.007

Verwey, W. B., & Eikelboom, T. (2003). Evidence for Lasting Sequence Segmentation in the Discrete Sequence-Production Task. *Journal of Motor Behavior*, *35*(2), 171–181. https://doi.org/10.1080/00222890309602131

Vyas, S., Golub, M. D., Sussillo, D., & Shenoy, K. V. (2020). Computation Through Neural Population Dynamics. *Annual Review of Neuroscience*, *43*(1), 249–275. https://doi.org/10.1146/annurev-neuro-092619-094115

Walther, A., Nili, H., Ejaz, N., Alink, A., Kriegeskorte, N., & Diedrichsen, J. (2016). Reliability of dissimilarity measures for multi-voxel pattern analysis. *NeuroImage*, *137*, 188–200. https://doi.org/10.1016/j.neuroimage.2015.12.012

Wang, J., Narain, D., Hosseini, E. A., & Jazayeri, M. (2018). Flexible timing by temporal scaling of cortical responses. *Nature Neuroscience*, *21*(1), 102–112. https://doi.org/10.1038/s41593-017-0028-6

Washburn, M. F. (1916). *Movement and mental imagery: Outlines of a motor theory of the complexer mental processes* (pp. xv, 252). Houghton Mifflin Company. https://doi.org/10.1037/11575-000

Watson, J. B. (1920). Is thinking merely the action of language mechanisms? *British Journal of Psychology*, *11*, 87–104.

Whitlock, J. R., Sutherland, R. J., Witter, M. P., Moser, M.-B., & Moser, E. I. (2008). Navigating from hippocampus to parietal cortex. *Proceedings of the National Academy of Sciences*, *105*(39), 14755–14762. https://doi.org/10.1073/pnas.0804216105

Wiestler, T., & Diedrichsen, J. (2013). Skill learning strengthens cortical representations of motor sequences. *eLife*, *2013*(2), 801. https://doi.org/10.7554/eLife.00801

Wiestler, T., McGonigle, D. J., & Diedrichsen, J. (2011). Integration of sensory and motor representations of single fingers in the human cerebellum. *Journal of Neurophysiology*, *105*(6), 3042–3053. https://doi.org/10.1152/jn.00106.2011

Wiestler, T., Waters-Metenier, S., & Diedrichsen, J. (2014). Effector-independent motor sequence representations exist in extrinsic and intrinsic reference frames. *Journal of Neuroscience*, *34*(14), 5054–5064. https://doi.org/10.1523/JNEUROSCI.5363-13.2014

Wilkinson, L., Khan, Z., & Jahanshahi, M. (2009). The role of the basal ganglia and its cortical connections in sequence learning: Evidence from implicit and explicit sequence learning in Parkinson's disease. *Neuropsychologia*, *47*(12), 2564–2573. https://doi.org/10.1016/j.neuropsychologia.2009.05.003

Wilson, P. H., Ruddock, S., Smits-Engelsman, B., Polatajko, H., & Blank, R. (2013). Understanding performance deficits in developmental coordination disorder: A meta-analysis of recent research. *Developmental Medicine and Child Neurology*, *55*(3), 217–228. https://doi.org/10.1111/j.1469-8749.2012.04436.x

Wong, A. L., Goldsmith, J., & Krakauer, J. W. (2016). A motor planning stage represents the shape of upcoming movement trajectories. *Journal of Neurophysiology*, *116*(2), 296–305. https://doi.org/10.1152/jn.01064.2015

Wong, A. L., Haith, A. M., & Krakauer, J. W. (2015). Motor planning. *Neuroscientist*, *21*(4), 385–398. https://doi.org/10.1177/1073858414541484

Worsley, K. J., Marrett, S., Neelin, P., Vandal, A. C., Friston, K. J., & Evans, A. C. (1996). A unified statistical approach for determining significant signals in images of cerebral activation. *Human Brain Mapping*, *4*(1), 58–73. https://doi.org/10.1002/(SICI)1097-0193(1996)4:1<58::AID-HBM4>3.0.CO;2-O

Wright, D. J., Holmes, P. S., Di Russo, F., Loporto, M., & Smith, D. (2012a). Differences in cortical activity related to motor planning between experienced guitarists and non-musicians during guitar playing. *Human Movement Science*, *31*(3), 567–577. https://doi.org/10.1016/j.humov.2011.07.001

Wright, D. J., Holmes, P. S., Di Russo, F., Loporto, M., & Smith, D. (2012b). Reduced Motor Cortex Activity during Movement Preparation following a Period of Motor Skill Practice. *PLOS ONE*, *7*(12), e51886. https://doi.org/10.1371/journal.pone.0051886

Wymbs, N. F., Bassett, D. S., Mucha, P. J., Porter, M. A., & Grafton, S. T. (2012). Differential Recruitment of the Sensorimotor Putamen and Frontoparietal Cortex during Motor Chunking in Humans. *Neuron*, *74*(5), 936–946. https://doi.org/10.1016/j.neuron.2012.03.038

Wymbs, N. F., & Grafton, S. T. (2013). Contributions from the left PMd and the SMA during sequence retrieval as determined by depth of training. *Experimental Brain Research. Experimentelle Hirnforschung. Experimentation Cerebrale*, *224*(1), 49–58. https://doi.org/10.1007/s00221-012-3287-1

Wymbs, N. F., & Grafton, S. T. (2015). The human motor system supports sequence-specific representations over multiple training-dependent timescales. *Cerebral Cortex*, *25*(11), 4213–4225. https://doi.org/10.1093/cercor/bhu144

Yang, L., Leung, H., Plank, M., Snider, J., & Poizner, H. (2015). EEG activity during movement planning encodes upcoming peak speed and acceleration and improves the accuracy in predicting hand kinematics. *IEEE Journal of Biomedical and Health Informatics*, *19*(1), 22–28. https://doi.org/10.1109/JBHI.2014.2327635

Yewbrey, R., Mantziara, M., & Kornysheva, K. (2023). Cortical Patterns Shift from Sequence Feature Separation during Planning to Integration during Motor Execution. *Journal of Neuroscience*, *43*(10), 1742–1756. https://doi.org/10.1523/JNEUROSCI.1628-22.2023

Yokoi, A., Arbuckle, S. A., & Diedrichsen, J. (2018). The role of human primary motor cortex in the production of skilled finger sequences. *Journal of Neuroscience*, *38*(6), 1430–1442. https://doi.org/10.1523/JNEUROSCI.2798-17.2017

Yokoi, A., & Diedrichsen, J. (2019a). Neural Organization of Hierarchical Motor Sequence Representations in the Human Neocortex. *Neuron*, *103*(6), 1178-1190.e7. https://doi.org/10.1016/j.neuron.2019.06.017

Yokoi, A., & Diedrichsen, J. (2019b). Neural Organization of Hierarchical Motor Sequence Representations in the Human Neocortex. *Neuron*, *103*(6), 1178-1190.e7. https://doi.org/10.1016/j.neuron.2019.06.017

Zeid, O., & Bullock, D. (2019). Moving in time: Simulating how neural circuits enable rhythmic enactment of planned sequences. *Neural Networks*, *120*, 86–107. https://doi.org/10.1016/j.neunet.2019.08.006

Zhou, S., Masmanidis, S. C., & Buonomano, D. V. (2020). Neural Sequences as an Optimal Dynamical Regime for the Readout of Time. *Neuron*, *108*(4), 651-658.e5. https://doi.org/10.1016/j.neuron.2020.08.020

Zimmermann, J. B., Seki, K., & Jackson, A. (2011). Reanimating the arm and hand with intraspinal microstimulation. *Journal of Neural Engineering*, *8*(5), 054001. https://doi.org/10.1088/1741-2560/8/5/054001

Zimnik, A. J., & Churchland, M. M. (2021a). Independent generation of sequence elements by motor cortex. *Nature Neuroscience*, *24*(3), 412–424. https://doi.org/10.1038/s41593-021-00798-5

Zimnik, A. J., & Churchland, M. M. (2021b). Independent generation of sequence elements by motor cortex. *Nature Neuroscience*, *24*(3), 412–424. https://doi.org/10.1038/s41593-021-00798-5